# Final Report:

# Dump Truck Hoist Redesign

December 5, 2011


| Team Four Members: | | Team Advisor: |
| --- | --- | --- |
| Fajar Adri Putro | | Qingjin Peng; E1-386; University of Manitoba |
| Sharleen Jhajj | | Industry Sponsor: |
| Matt Grafeneder | | Cancade Company Ltd.; 1651-12$^{th}$ St, Brandon, MB |
| Jason Fehr | | Contact: Michael Rosumowitsch |

Quattro Consulting
University of Manitoba
Winnipeg, MB, R3T 2N2
(204) 880 – 8522

December 5th 2011

Michael Rosumowitsch
Engineering Manager
Cancade Company Ltd.
1651 - 12th Street
Brandon, MB, R7A7L1

Dear Mr. Rosumowitsch,

We are submitting to you the report titled "Dump Truck Hoist Redesign," due on December 5th 2011, in agreement with the course Engineering Design (MECH 4860) administered by Dr. Paul Labossiere.

The report entails the final redesigns of the hoist as created by Quattro Consulting in accordance to the criteria and target specification presented by Cancade Company Ltd. In the report you will also find assembly drawings of the final redesigns, finite element analysis, cost analysis and stress analysis which will further enhance your understanding of the designs demonstrated.

We would like to express our gratitude and appreciation to Professor Qingjin Peng for providing the team with his expertise and advice throughout the course of the project.

Quattro consulting would like to thank you for your time and hope the report not only meets but exceeds your expectations. Should you have any questions regarding the report, please do not hesitate to contact us by either phone or email.

With Best Regards,

Fajar Adri Putro
Team Manager

umadripu@cc.umanitoba.ca

Quattro Consulting
University of Manitoba
Winnipeg, MB, R3T 2N2
(204) 880 – 8522

December 5th 2011

Professor Qingjin Peng
Office E1-386
Faculty of Engineering
University of Manitoba
Winnipeg, MB, R3T 2N2

Dear Dr. Peng,

We are submitting to you the report titled "Dump Truck Hoist Redesign," due on December 5th 2011, in agreement with the course Engineering Design (MECH 4860) administered by Dr. Paul Labossiere.

The report entails the final redesigns of the hoist as created by Quattro Consulting in accordance to the criteria and target specification presented by Cancade Company Ltd. In the report you will also find assembly drawings of the final redesigns, finite element analysis, preliminary cost analysis and stress analysis which will further enhance your understanding of the designs demonstrated.

We would like to express our gratitude and appreciation to for providing the team with your expertise and advice throughout the course of the project.

Quattro consulting would like to thank you for your time and hope the report not only meets but exceeds your expectations. Should you have any questions regarding the report, please do not hesitate to contact us by either phone or email.

With Best Regards,

Fajar Adri Putro
Team Manager

umadripu@cc.umanitoba.ca

All figures and tables contained in this report are property of Quattro Consulting for the exception of Figure 2 and Figure 3.

Figure 2, Figure 3 and the Cancade Company Ltd. logo are property of Cancade Company Ltd. and permission to use in this report has been obtained.

# Executive Summary

Quattro Consulting's final design report discusses the new hoist designs for Cancade Company Ltd. Cancade is a manufacturing company which produces heavy hauling equipment for agriculture, construction and oil and gas applications. Quattro Consulting was responsible for the redesign of Cancade's current hoist. Cancade requested that the new hoist design reduce the amount of both parts and welds by 30% or more. Improvement in lifting capacity from 50,000lbs to 60,000lbs and higher dumping angle of 50° from previously 36.5° are also desirable. The new design must maintain the safety factor of 1.5 at any given situation.

Quattro Consulting produced two independent designs for this project by following different approaches. Design 1 is based on the current hoist's design parameters. Alternatively, design 2 incorporates major redesign of hoist components.

Design 1 is able to achieve the dumping angle of 46.5° with a 60,000lbs load. Design 1 reduces the amount of welds by 51% and parts by 55%. The second design is capable of lifting a 60,000lbs load with the maximum dumping angle of 50°. The weld reduction achieved by Design 2 is 44% while the amount the parts are reduced by 33%.

To achieve such a high dumping angle, both designs must slightly exceed the space constraint when the hoist is fully collapsed. Exceeding the space constraint can be tolerated as long as the hoist does not interfere with the truck frame or cross members. In the case of interference, the truck frame may need to be modified.

Both designs meet the required target specifications requested by Cancade. Therefore, both hoist designs can be implemented at the clients' discretion.

# Table of Contents

## List of Figures

## List of Tables

# 1 Introduction

Quattro Consulting in partnership with Cancade Company Ltd. has been working for the past three months to redesign Cancade's dump truck hoist. Cancade is a Brandon based multi-dimensional manufacturing company producing agricultural, construction and oilfield equipment. Cancade has been serving the Canadian and American market for over 90 years. [1] The company's truck division provides solutions to customers' heavy hauling needs. The company manufactures, including but not limited to, a wide variety of boxes and trailers for hauling gravel, grain, or other industrial equipment and an optional hoist that is universal to allow any of their box designs to be dumped with ease.[1] Cancade also retrofits their products onto customers' existing trucks.[2]

Cancade has been utilizing the same hoist design the past for fifteen years. [2] Once manufactured, the hoist is installed between the box and the truck or trailer frame. Figure 1 illustrates Cancade's current hoist design. The hoist mechanism allows the box to be tipped to unload the contents. However, Cancade's fifteen year old hoist design contains too many individual parts, making it labor intensive to construct. The current design's lifting capacity and dumping angle are deemed insufficient to compete with other manufacturers' hoists. Quattro consulting was approached to help Cancade redesign their current hoist to meet or exceed competitors' specifications.

Figure 1: Cancade's Current Hoist

The final report discusses Quattro Consulting's final hoist designs. The report encompasses the key aspects of the design, stress analysis, preliminary cost analysis and manufacturability assessment. Other elements of the design, such as previous concepts and concept selection, can be found in the appendices.

## 1.1 Target Specifications

Cancade provided Quattro Consulting with a list of target specifications for the redesigned hoist. First and foremost, the new hoist must be safe. Cancade requested that the design utilize a factor of safety of 1.5. The new design must be simpler. To accomplish a simpler design, the number of individual parts must be kept to a minimum which will ultimately reduce the manufacturing time. In order to simplify the design, Cancade requested a 30% reduction in individual parts. With 30% fewer parts, the amount of welds is expected to also be reduced by 30%.

The new hoist must be compatible with Cancade's existing box designs. It must be able to handle the biggest box size with a length of 22'. The box is mounted to the frame at a fixed location with a box side pin-to-pin distance of 155", and an overhang of 18". The box side pin-to-pin distance is defined as the center-to-center distance between the box hinge and hoist's box mount. Overhang is the distance from the hinges to the end of the box hanging outside the truck frame. Figure 2 illustrates the installation and location of the hoist relative to the box and the frame.

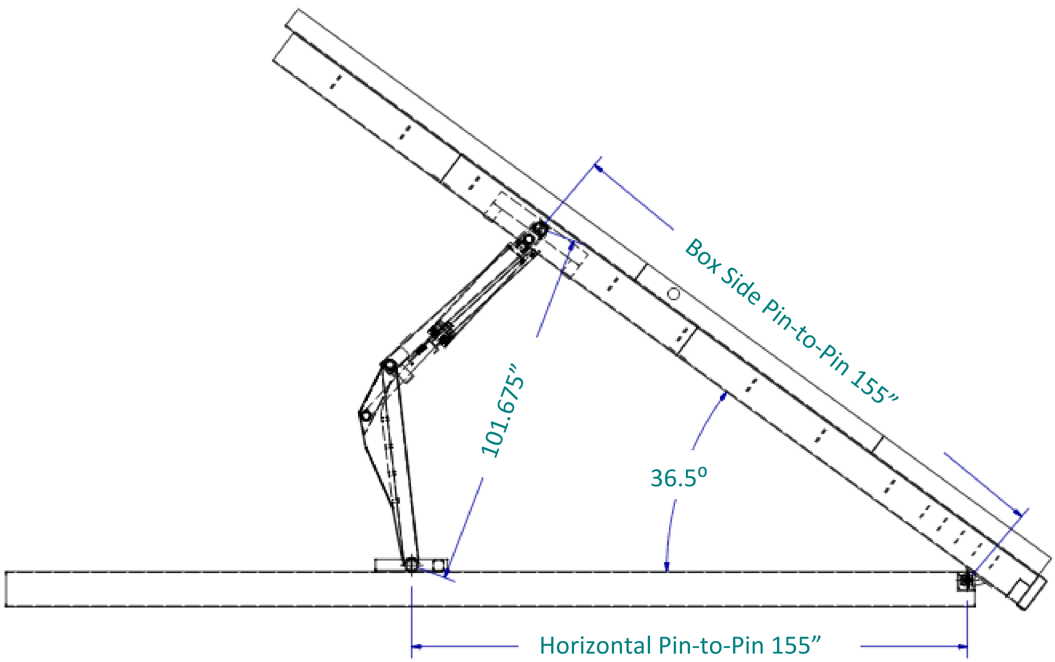


Figure 2: Hoist Lifted Position & Installation Configuration

To be compatible with different truck frames, when compacted, the hoist should ideally be contained within in a space approximately 4" deep by 33" long under the truck frame, as seen in Figure 3.

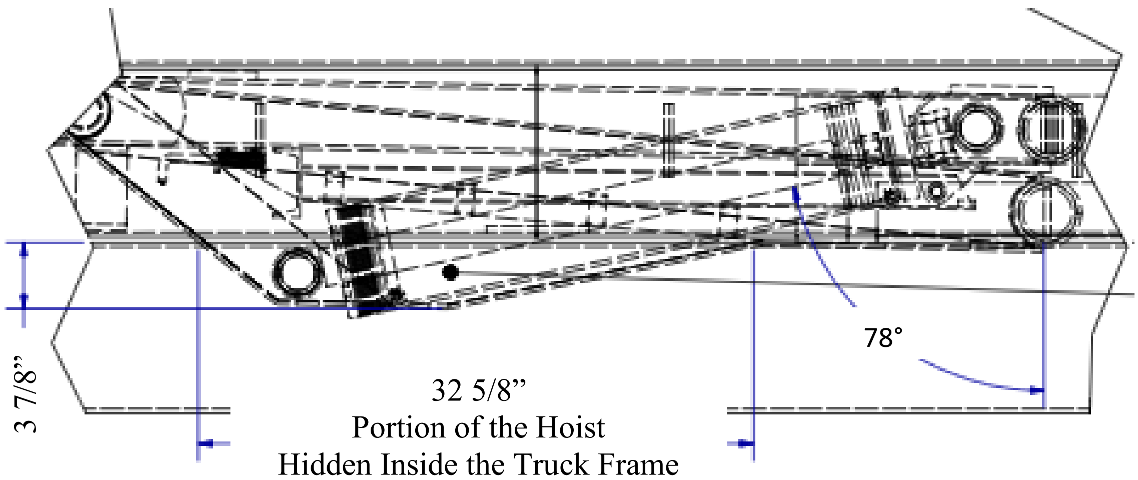


Figure 3: Hoist Compacted Configuration

As a part of the hoist improvement, Cancade requested that the new hoist improve the lifting capacity from 50,000lbs to 60,000lbs, and increase the maximum dumping angle to 50°, from the previous 36°. This information is summarized in Table I.

TABLE I: TARGET SPECIFICATION

| | |
|---|---|
| Factor of Safety | 1.5 |
| Individual Parts Reduction | 30% |
| Welds Reduction | 30% |
| Maximum Box Size | 22' |
| Pin-to-Pin Distance | 155" |
| Compacted size | 4" x 33" |
| Maximum Lifting Capacity | 60,000lbs |
| Maximum Dumping Angle | 50° |

## 1.2 Project Objective

The main objective of this project is to redesign Cancade's current hoist. The newly designed hoist ideally meets all of the target specifications and improvements as stated in the previous section. The new concepts were generated through various brainstorming processes. The concepts were then developed through Computer Aided Design (CAD) models. Technical analysis, including force analysis and finite element analysis (FEA), was performed to ensure structural integrity. Manufacturability assessment and preliminary cost analysis of the new designs were also carried out.

## 2 Designs and Analysis

Quattro Consulting proposes two designs for this project. The reason for the two designs is to explore the possibilities of different solutions by taking two independent approaches. The two designs meet the same specification while maintaining different design parameters. Both designs have good potential to be implemented. Therefore, Quattro Consulting decided to pursue both designs. The detail of the designs will be discussed in the sections to follow.

Design 1 is based on Cancade's current design. Design parameters such as material type and overall structure are maintained. An improvement in the dumping angle was made by increasing the length of the members while the lifting capacity was improved by incorporating a more efficient and stronger design. The isometric view of Design 1 is shown in Figure 4.

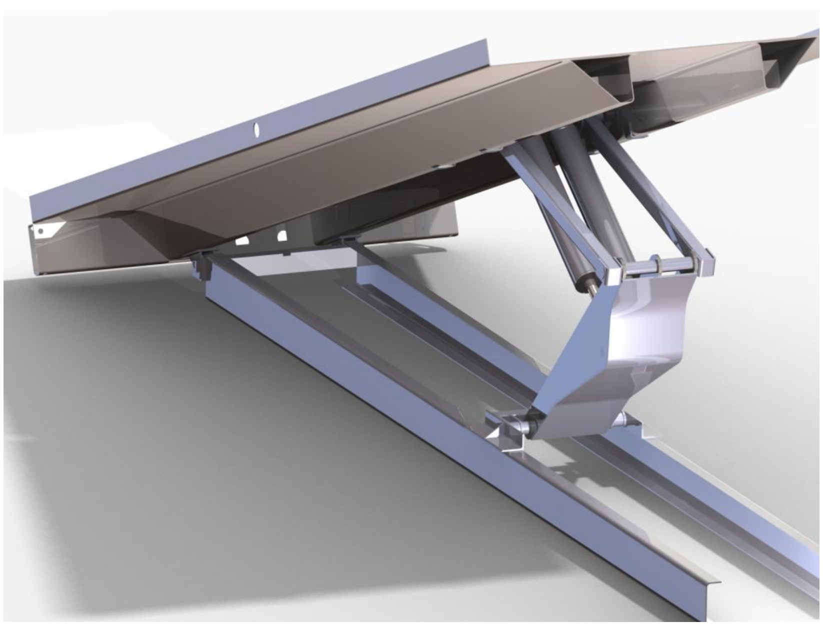

Figure 4: Isometric View of Design 1

Alternatively, design 2, shown in Figure 5, incorporates more radical changes. The material used for design 2 was initially changed to higher strength alloy steel. However, due to problems in material availability and high price, the material was reverted to the original A36 mild steel. [3]

To achieve a higher dumping angle, the length of the lower member was increased. The upper member was reduced to a single member to eliminate the amount of parts. Greaseless bushings were also incorporated to reduce maintenance costs.

Figure 5: Isometric View of Design 2

## 2.1 Force Analysis

Force analysis was required to determine the maximum forces and bending moment experienced by the members during operation. The determined forces were used to perform FEA on the individual members.

The force analysis, shown in Appendix B, concluded that the maximum forces experienced by the hoist members occur at a dumping angle of 0˚ for both hoists. In addition, the maximum bending moment occurred at 10˚ for both designs 1 and 2. These results were taken into consideration when sizing parts and assigning materials for both designs. The summary of the results are presented below:

TABLE II: FORCES EXPERIENCED AT A ZERO DEGREE DUMPING ANGLE - DESIGN 1 & DESIGN 2

| Design | Dumping Angle | Lower Member | | Cylinder | Top Member |
|---|---|---|---|---|---|
| | | *FDA [lbs]* | *FBD [lbs]* | *FCD [lbs]* | *FCB [lbs]* |
| 1 | 0 | -156,175.57 | -156,175.57 | -161,089.33 | 156,389.80 |
| 2 | 0 | -48585.57 | -59,817.80 | -183,706.80 | 177,891.07 |

Note: A negative value represents a member in compression.

TABLE III: MAXIMUM BENDING MOMENT RESULTS - DESIGN 1 & 2

| Design | Angle | Maximum Moment |
|---|---|---|
| 1 | 10˚ | 1,436,441 [lb-in] |
| 2 | 10˚ | 2,104,930 [lb-in] |

## 2.2 Details of Design 1

Design 1, shown in Figure 6, consists of two upper arms and one lower member as well as two hydraulic cylinders to power the hoist to raise and lower the box. The design uses ASTM A36 steel that has a yield stress of 36ksi. [4] Design 1 is able to lift 60,000lbs load to a maximum dumping angle of 46.5**°.**

The design process is mainly done in SolidWorks™ utilizing FEA to obtain the required size of each member. The detailed FEA study, including the convergence study, can be found in Appendix C-1. Exploded views and bill of materials of design 1 are available in Appendix C-2.

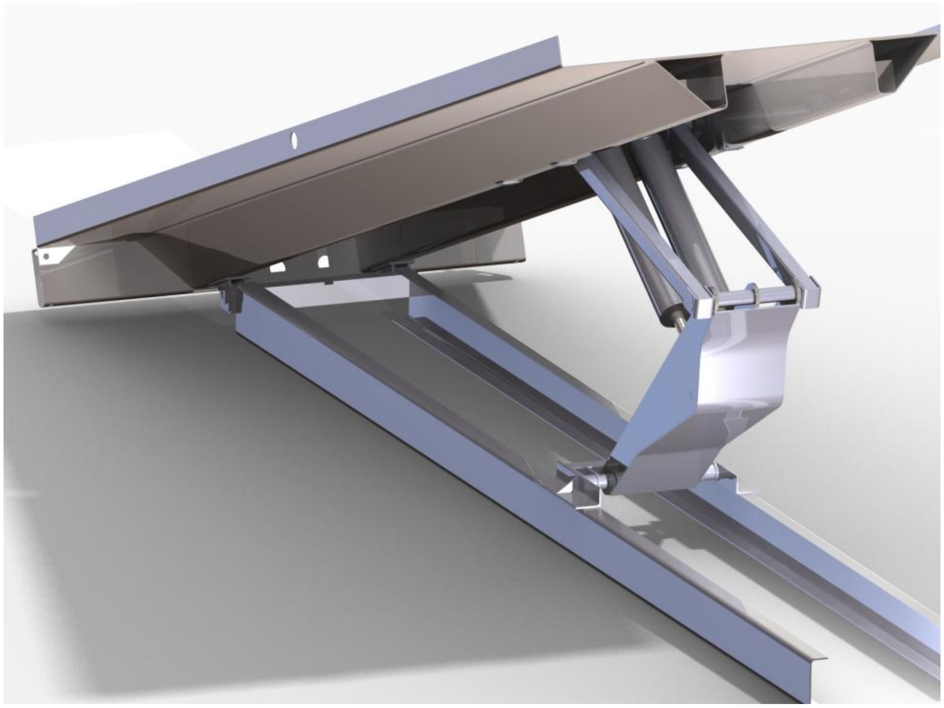

Figure 6: Hoist Design 1

### 2.2.1 Material Selection

The material chosen as mentioned earlier is ASTM A36 mild steel, as it is commonly used in industrial applications and is available in many different sizes. A36 steel also shows high strength while maintaining a low cost. Another advantage is that A36 is currently used by Cancade. [2]

### 2.2.2 Space Constraint

Design 1 is similar to the current design employed by Cancade. However, to attain a higher dumping angle, the members are lengthened. Having longer members causes the hoist to exceed the space that the current hoist occupies beneath the truck frame. This condition is illustrated in Figure 7, where the blue portion represents the new design that extends past the current design. This space was minimized, but in order to lift higher, a longer cylinder must be utilized thus pushing back the cylinder mounting point. The blue area extends below the space occupied by the current hoist to a maximum of 2” and protrudes to the rear 3” further. This protrusion may cause interference depending on the space available within the frame of the truck. This case will need to be further evaluated before implementation.

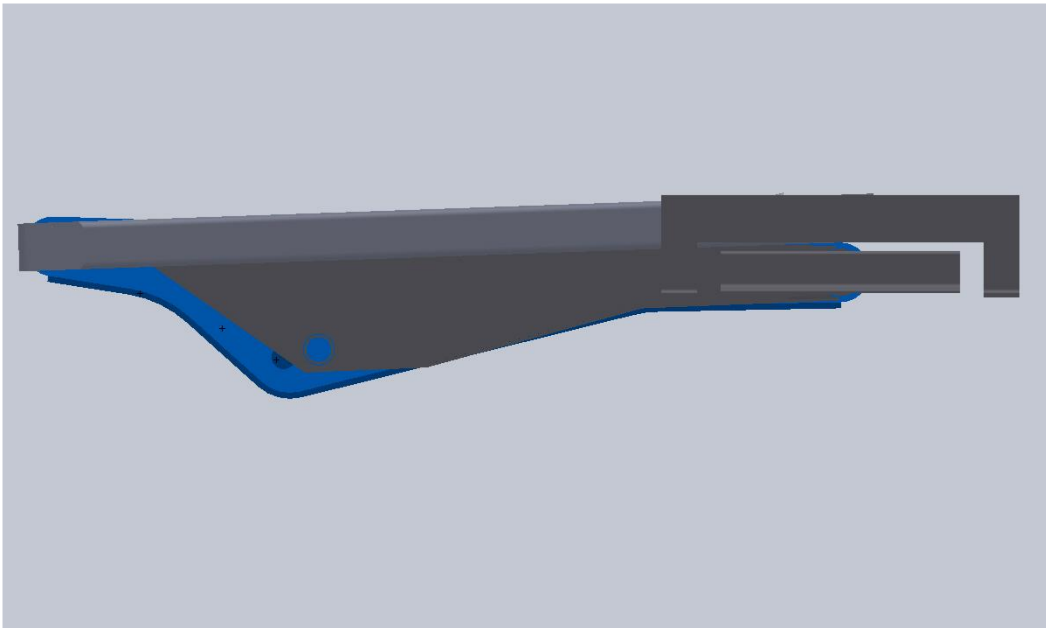

Figure 7: Comparison of Hoists

The maximum dumping angle of the 22' box is 46.5°. This angle is just short of the desired target of 50°. To lift to the desired target, the members would have to be lengthened further. The elongation would result in a larger space exceeding the current design as well as more stress in the members.

### 2.2.3 Assembly

An exploded view of the hoist assembly is shown in Figure 8. The assembly parts list is also shown in Figure 8. The exploded view shows the details of each component. The hoist is held together by four 2" pins of various lengths. The cylinders mount to the same pin as the upper members, which are then supported by the box mount. Another pin holds the upper members to the lower member which extends out of either side of the lower member for the upper members to connect to. There are two more pins on the lower member, one connects the hydraulic cylinders and the other connects the lower member to the frame mounts.

| ITEM NO. | PART NUMBER | DESCRIPTION | QTY. |
|---|---|---|---|
| 1 | | 6" Hydraulic Cylinder | 2 |
| 2 | 2003 | Box Mount | 2 |
| 3 | 2004 | Frame Mount | 1 |
| 4 | 2001 | Lower Hoist Member | 1 |
| 5 | 2002 | Upper Hoist Member | 2 |
| 6 | 1009 | 2" x 17" Round Bar | 1 |
| 7 | 1011 | 2" x 25" Round Bar | 1 |
| 8 | 1010 | 2" x 28 1/2" Round Bar | 1 |
| 9 | 1012 | 2" x 26 1/2" Round Bar | 1 |

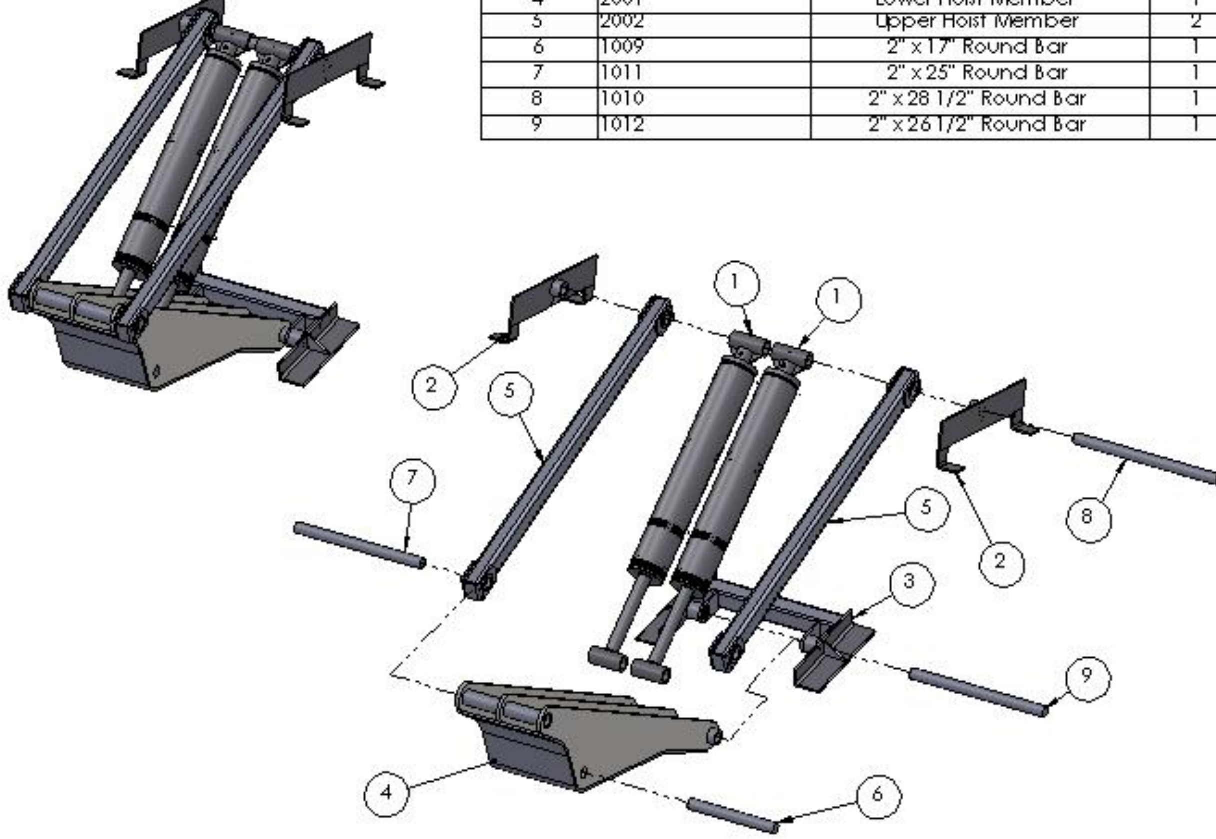

Figure 8: Hoist Assembly

The advantage of having the hoist pinned together is that it can be easily disassembled for servicing or replacement. The bearing surfaces on all members of the hoist should be kept well lubricated to reduce the friction, corrosion and erosion of the joints.

### 2.2.4 Lower Member

A drawing showing the assembly of the lower member, along with the bill of materials (BOM) with the dimensions of the parts, is shown in Figure 9.

| ITEM NO. | PART NUMBER | DESCRIPTION | QTY. |
|---|---|---|---|
| 1 | 1002 | 3/4" Plate | 3 |
| 2 | 1004 | 2 3/4" OD x 2" ID Round Tube, 20" Long | 1 |
| 3 | 1003 | 2 3/4" OD x 2" ID Round Tube, 17" Long | 1 |
| 4 | 1005 | 1/2" Plate | 1 |
| 5 | 1008 | 1/2" Plate | 4 |

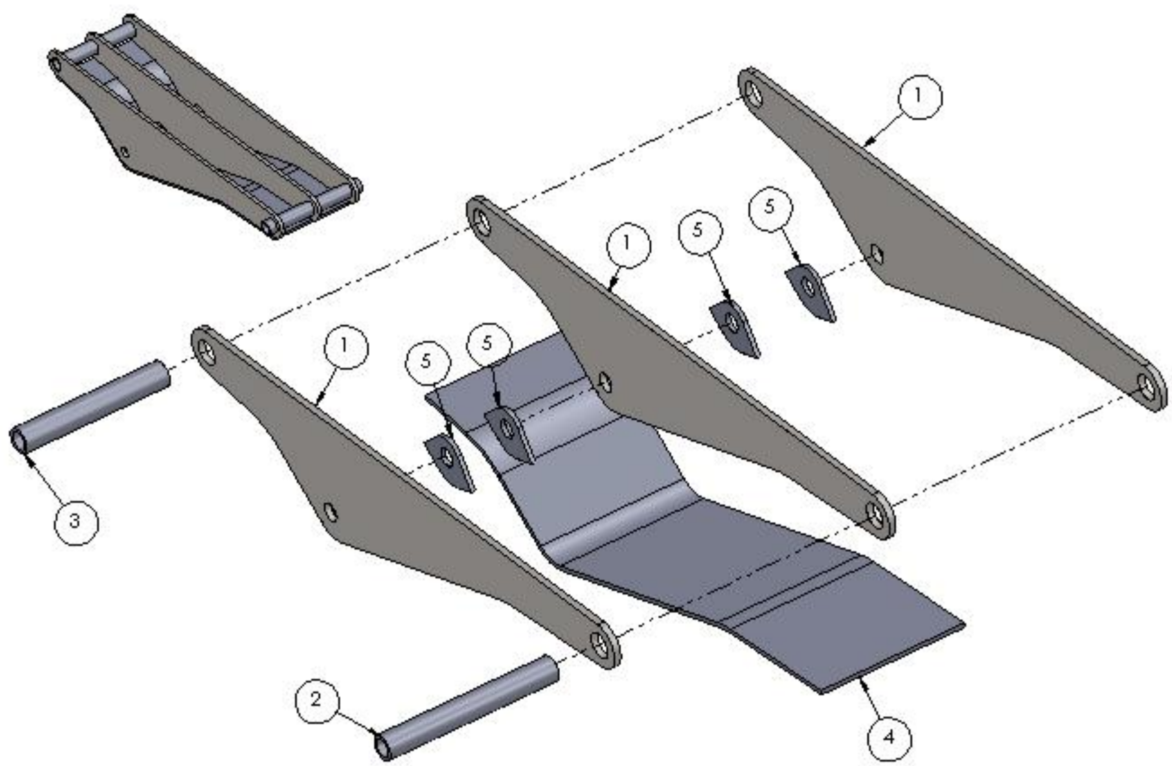


Figure 9: Lower Member Exploded View

The lower member consists of three main plates, item 1 in Figure 9, providing most of the structural support. The plates have three holes in them. The upper two holes are for attaching to the frame and upper member, while the lower hole is for the cylinder pin. These plates are supported by item 4 welded underneath, which also acts as a shield for the cylinders. This supporting plate was found to be necessary as it helps keep item 1 from buckling as well as provides strength in bending. The two round tubes, items 2 and 3, are welded into the holes on either end of item 1, acting as the pivot points for the hoist. Item 2 attaches to the truck frame mount and item 3 attaches to the upper members. Four smaller plates, item 5, are added at the bottom hole to provide support and a bearing surface for the pin that the cylinders attach to.

To ensure the structural integrity of the lower member FEA was performed, using the calculations in Appendix B, for the bearing forces. The FEA led to the final design shown in Figure 10. In the figure, the hoist is just starting to lift the box and is designed around the maximum force of the cylinder. The highest stress is just over 36ksi with a 1.5 factor of safety applied to the load. This stress can be seen by observing the areas around the holes where small red portions can be seen indicating the maximum stress. The maximum load when the hoist is compacted is 160,000lbs which, with a factor of safety of 1.5, equals 240,000lbs.

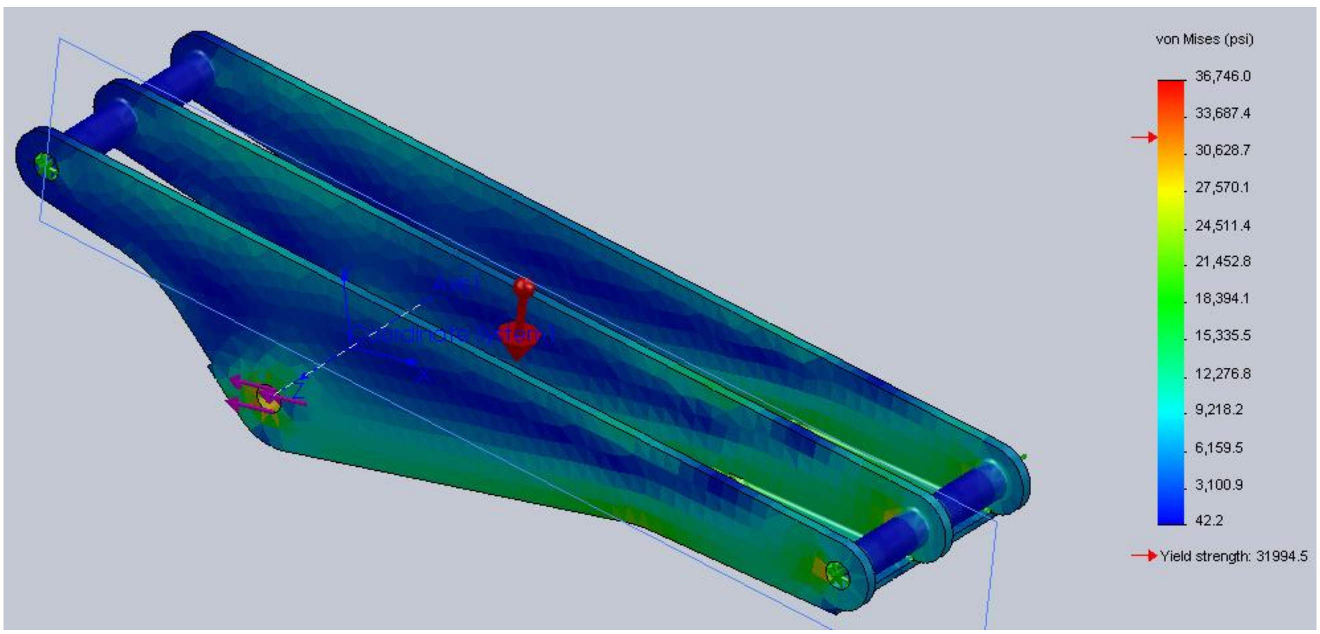


Figure 10: Lower Member FEA

Through calculations shown in Appendix B, the highest bending moment occurs when the hoist lifts the box to 10°. The corresponding load at 10° is 120,000lbs and with a factor of safety becomes 180,000lbs. The result shown in Figure 11 illustrates this situation. As a result, we can observe that the stress on the upper part has increased significantly. This stress is shown by the change in color in the upper part, while the stress in the other parts has not changed significantly. From the FEA von Mises plot, it can be concluded that the highest stress is still close to 36ksi in the same areas as Figure 10. Therefore, the lower member is sufficiently strong for the application.

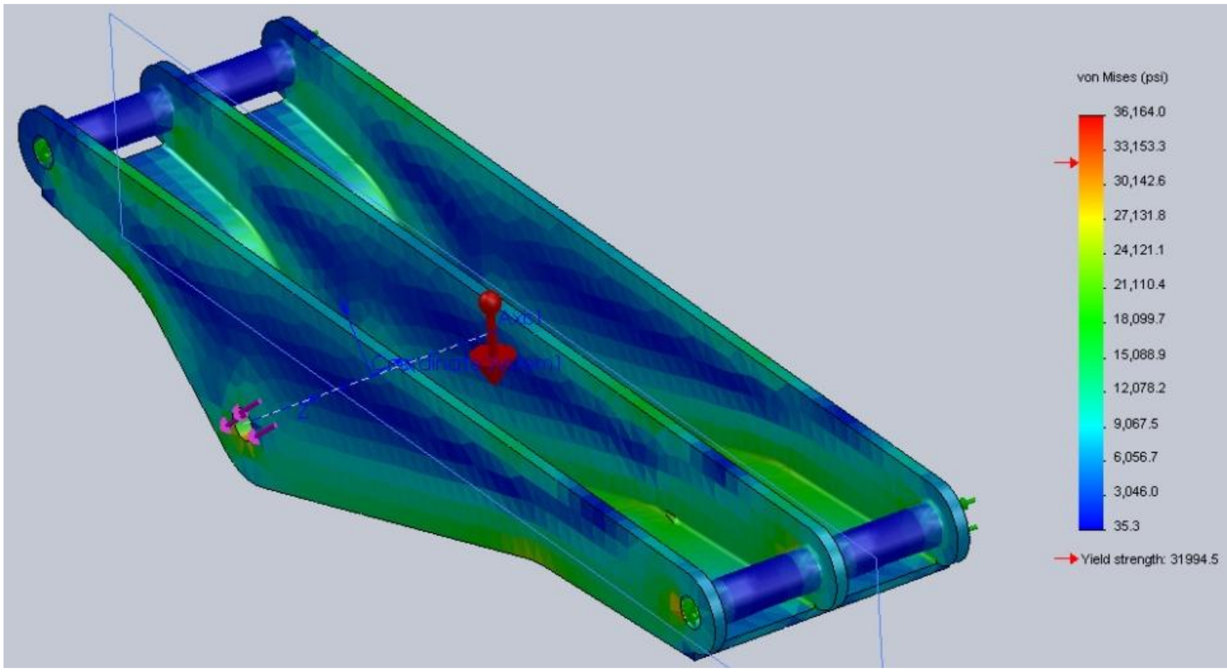

Figure 11: Lower Member FEA at 10°

The key areas to consider with high stress concentration are where the cylinders mount and the two points where the plates change angle. However, these two points cannot be eliminated as they were necessary to keep the hoist inside the space constraints as much as possible.

### 2.2.5 Upper Member

The upper member of the hoist consists of a rectangular tube, item 1 in Figure 12, with reinforcement plates, item 2, welded on each end. Item 3 is welded into a hole at either end of the rectangular tube to provide a mounting point to connect with the lower member and the upper box-mount. The reinforcement plates wrap around the ends of the tube and close it off. The plates ensure that there is no collection of dirt or water inside the members. The reinforcement plates also give strength to the round tube. This reinforcement allows the round tube to have a smaller outside diameter while maintaining the same strength.

| ITEM NO. | PART NUMBER | DESCRIPTION | QTY. |
|---|---|---|---|
| 1 | 1101 | 3x4x0.375Wall Rectangular Tube, 71" Long | 1 |
| 2 | 1007 | 3/8" Plate | 2 |
| 3 | 1006 | 3 1/4" OD x 2"ID Round Tube, 4" Long | 2 |

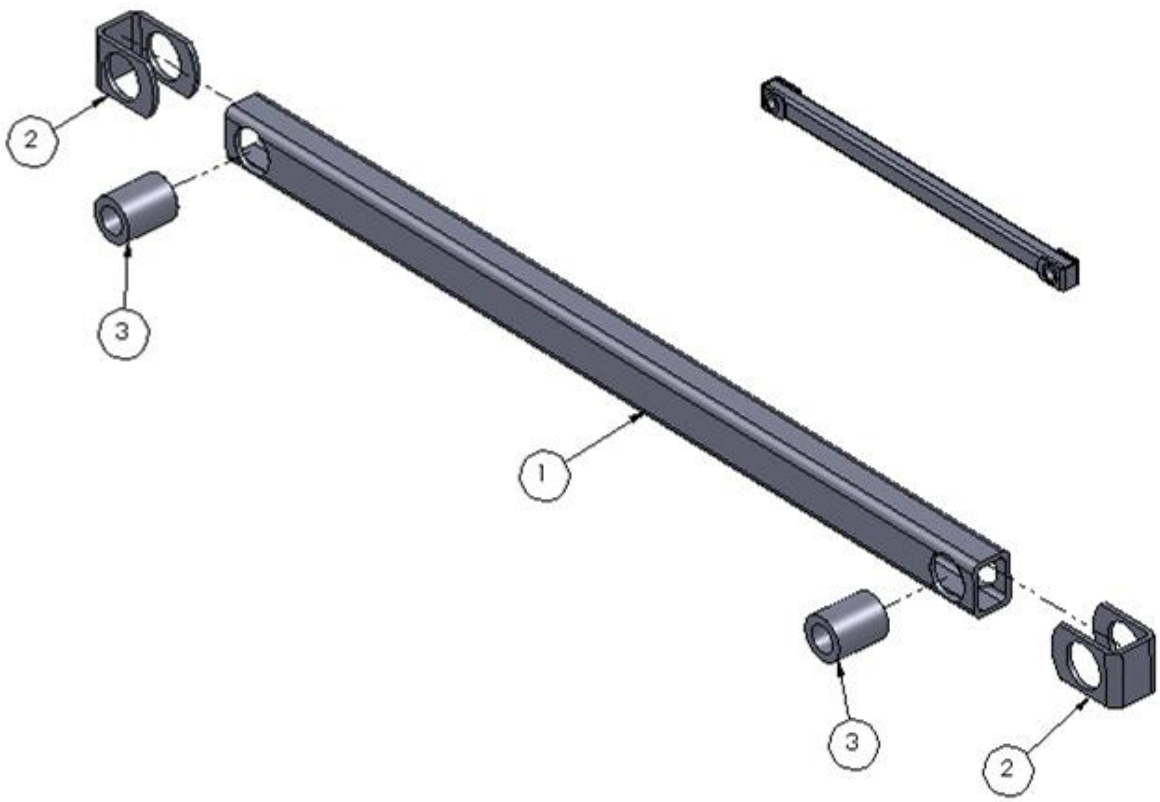


Figure 12: Lower Member Exploded View

There are two upper members in the hoist assembly, one on each side of the lower member, which means that each member is only required to support half the load the hoist experiences. As proven in Appendix B, the maximum load occurs during in the initial stage of the lift. Therefore, the initial lift will be the only scenario considered. The load occurring at this point is 160,000lbs and by incorporating the factor of safety, the load becomes 240,000lbs. Therefore, each member is designed to support 120,000lbs.

The FEA result shown in Figure 13 illustrates the condition during the application of the maximum load to the upper member. Since the upper member is symmetrical only half of it was considered in the analysis allowing the FEA to run faster. The results show that the critical area is in the round tube as the stresses everywhere else are lower. Therefore, the material around the critical area must be substantial enough to withstand the stress. The chosen round tube has a 3.25" outside diameter (OD) with a 2" internal diameter (ID). The reinforcement plate is 3/8" thick, giving the area enough strength to be able to withstand the maximum load it experiences. The selected rectangular tube is 3"x4" with 3/8" wall thickness. The chosen tube dimension is the smallest dimension that is capable of handling the load. The member needs to be as narrow as possible and must not exceed 4" in height or it would interfere with the truck box.

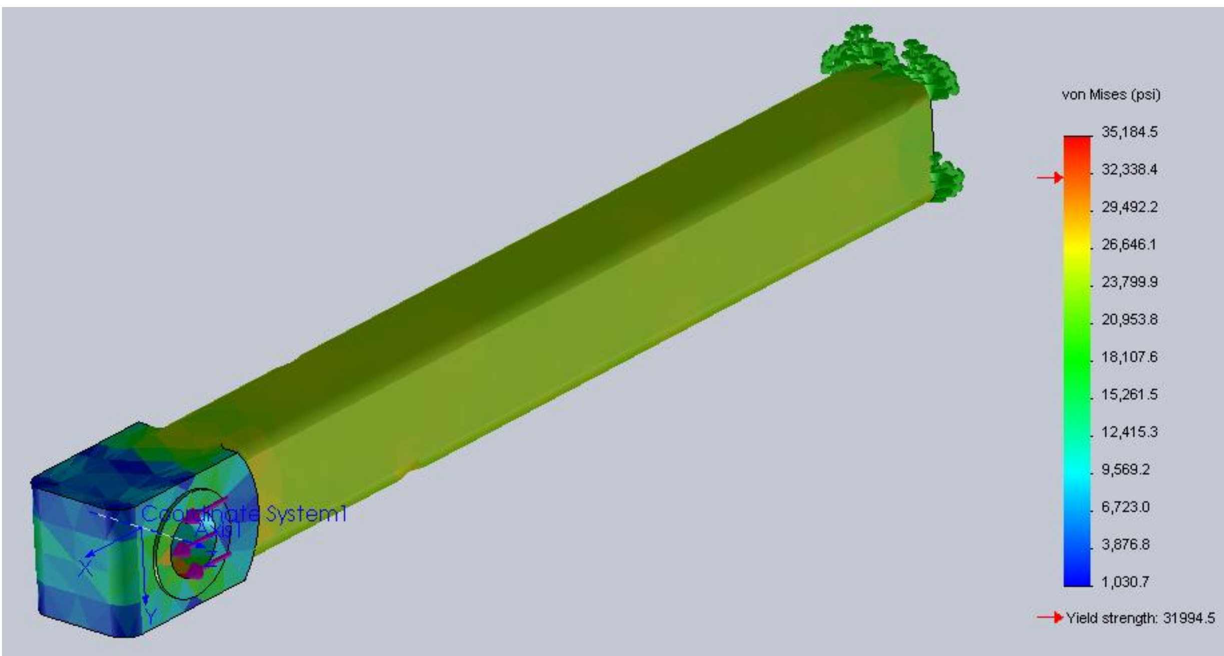


Figure 13: Lower Member FEA

### 2.2.6 Frame Mount

The frame mount connects the frame and the hoist. The frame mount is welded to the truck frame and acts as an attachment point for the lower member. The exploded view of the design is shown in Figure 14 along with the BOM.

| ITEM NO. | PART NUMBER | DESCRIPTION | QTY. |
|---|---|---|---|
| 1 | 3349114 | 5" x 3 1/2" x 3/8" Angle Iron | 2 |
| 2 | 1014 | 3 1/4" OD x 2" ID Round Tube | 2 |
| 3 | 1016 | 3 1/2" x 3 1/2" x 0.188 wall Tube | 1 |
| 4 | 1017 | 1/2" Plate | 4 |
| 5 | 1018 | 1/2" Plate | 2 |

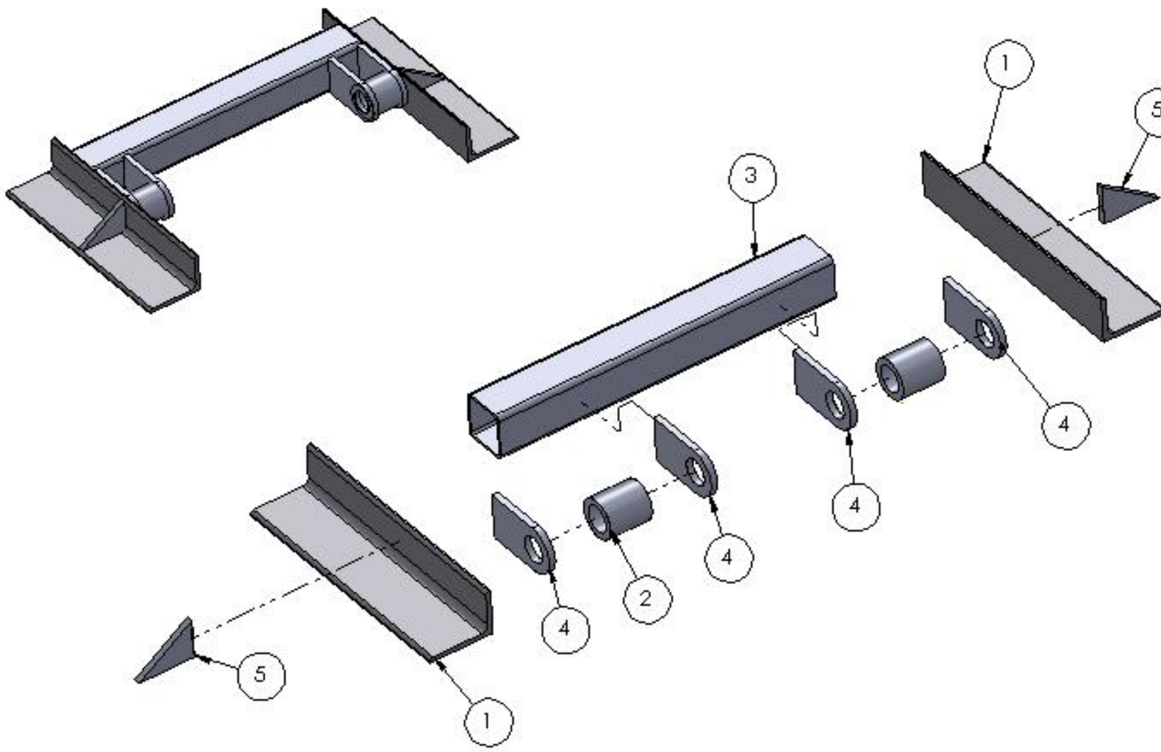


Figure 14: Frame Mount Exploded View

The frame mount consists of two angle irons welded to the truck frame with a square tube welded in between, giving it most of its' rigidity. The round tube is welded to the angle iron with the ½" plates, item 4, providing secondary support. The round tube has an internal diameter of 2" for the pin connection between the lower member and the frame mount.

The FEA done for the frame mount is shown in Figure 15. The mount is symmetrical so only half of it needs to be considered. From the FEA von Mises plot, it can be seen that the stresses are at an acceptable level throughout the structure. The highest stress is below 36ksi. Therefore, the frame mount will be able to handle the loads from the hoist.

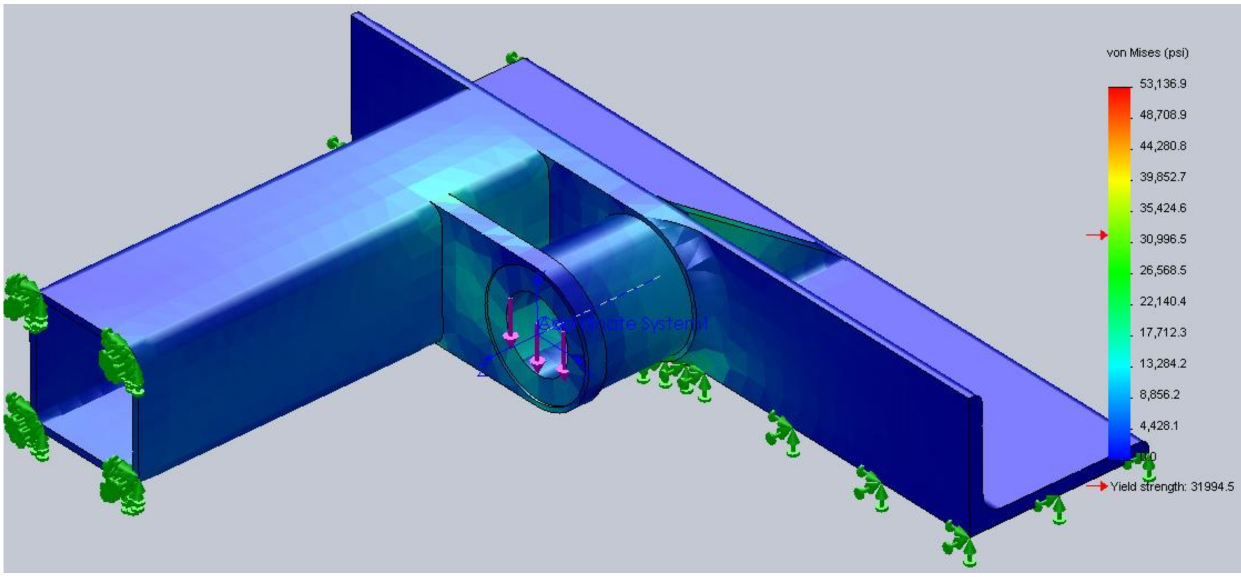


Figure 15: Frame Mount FEA

### 2.2.7 Box Mount

The box mount provides the connection between the upper member and the truck box. The box mount is similar to the current design. However, it has been slightly modified to work with Design 1. Item 1, the 3/8" plate, in Figure 16 is slightly taller so that the gusset could be added underneath the round tube. The two plates that wrap underneath the box frame were made slightly shorter to keep the mounting point the same. The round tube has a 2" ID for the pin that connects the upper member and the cylinders to the box.

| ITEM NO. | PART NUMBER | DESCRIPTION | QTY. |
| --- | --- | --- | --- |
| 1 | 3069871 | 3/8" Plate | 1 |
| 2 | T013 | 3" OD x 2" ID Round Tube | 1 |
| 3 | 3069872 | 3/8" Plate | 2 |
| 4 | T015 | 1/4" Plate | 1 |

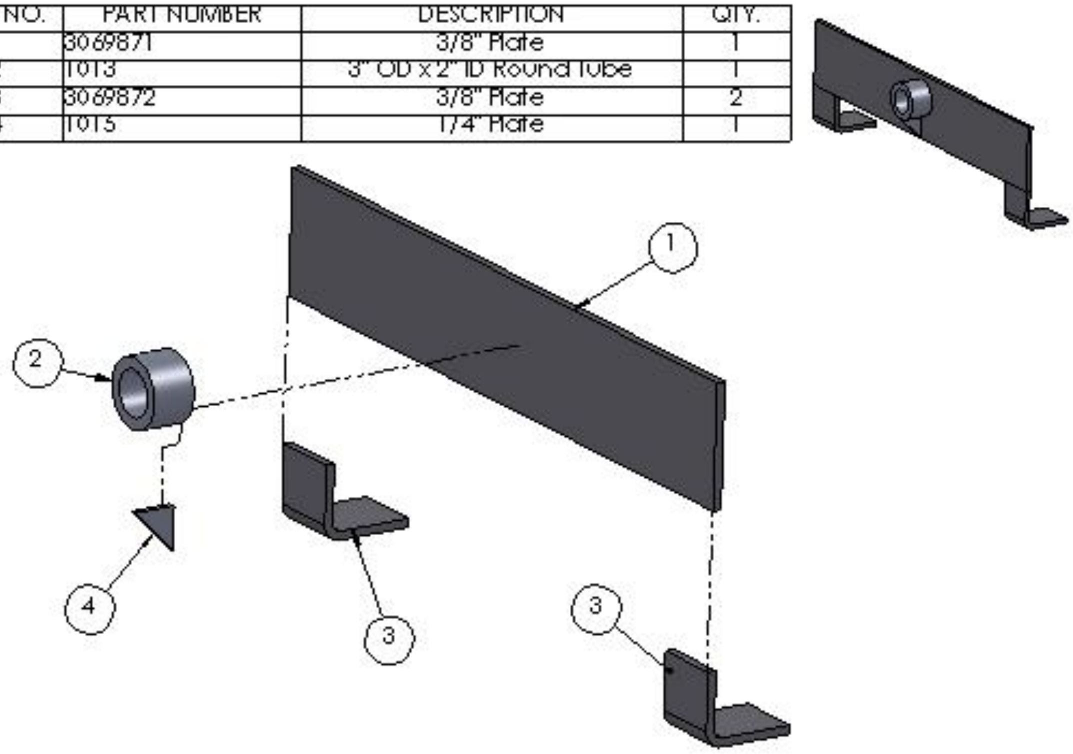


Figure 16: Box Mount Exploded View

The FEA done on the box mount is shown in Figure 17. Since the large plate is welded to the box, the only area of concern is in the round tube. A gusset underneath the tube was required to keep the stress below 36ksi. Once the gusset was added, the stress around the tube is well below acceptable level. After integrating a factor of safety to the applied load, the highest stress is less than 30ksi.

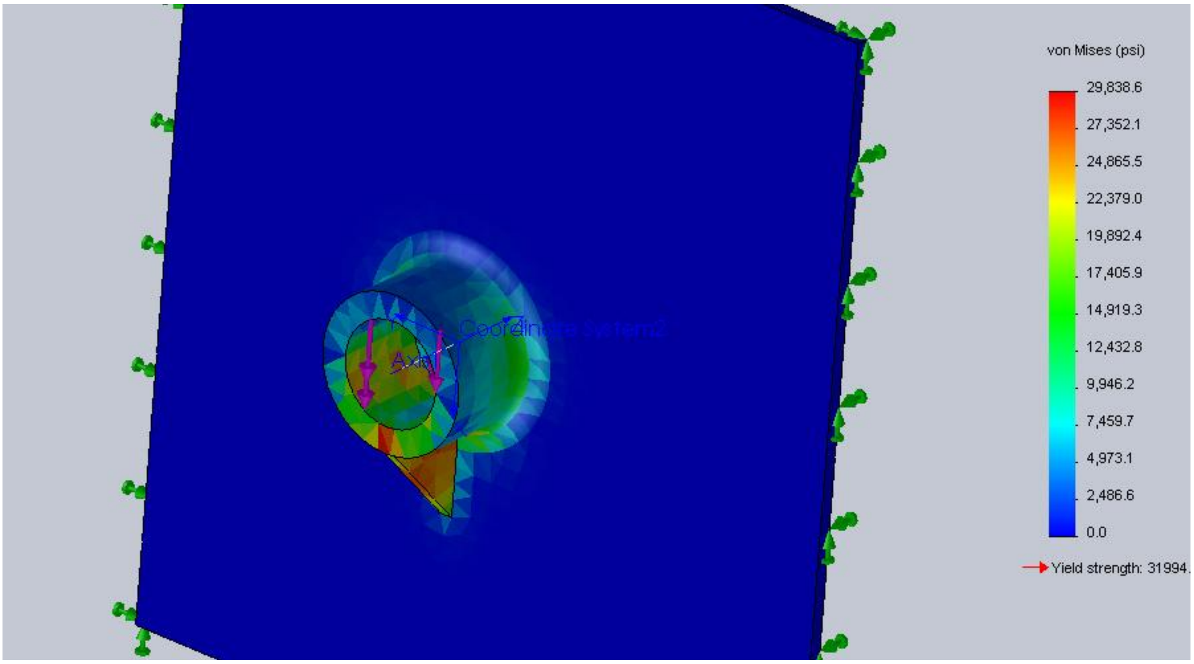


Figure 17: Box Mount FEA

### 2.2.8 Hydraulic Cylinders

In order to get the required lifting capacity, two six-inch cylinders are required. A two cylinder design occupies more space and requires more parts. However, a one cylinder design will require the cylinder diameter to be significantly larger. This leads to difficulty in sourcing material and potentially outsourcing the production of the cylinder. The chosen cylinder size has a 6" bore and requires 3,500psi to provide enough lifting power. When the hoist is fully collapsed, the center-to-center length of the cylinder reduces to 48". When extended, the cylinder must extend another 40" to reach the maximum dumping angle. This is the maximum amount of extension allowable in the cylinders. If the cylinders extend any further, they would then start to interfere with the hoist, causing damage.

## 2.3 Details of Design 2

Design 2 uses longer lower and upper members to be able to achieve the higher dumping angle as seen in Figure 18. However, the members in design 2 are not of equal length. The critical member in the redesign of the dumping hoist is the lower member which experiences the highest stresses. The length of the lower member was increased from an overall center to center length of 56.95" to a length of 81.91". The extra 24.96" causes a much larger bending moment on the lower member requiring either a thicker material, or a higher strength alloy.

Figure 18: Hoist design 2

The upper member of design 2 was increased from the original center distance of 56.91" to a length of 59.91" allowing for an overall dumping angle of 49.91° which is very close to the target dumping angle of 50°. Finally, the cylinders have a total length of 37.625" which is an overall increase of 5.125" from the original cylinders of 32.5".

### 2.3.1 Material Selection

Design 2 was first designed to be implemented using high strength ANSI 4340 alloy steel using rectangular tubing rather than welded plates. This design would allow for much lower manufacturing costs, but higher material costs. After much material research and cost analysis the conclusion is that using the high strength alloy steel would increase material costs exponentially and would become infeasible to manufacture. [3] The design is therefore modified to use the same ASTM A36 steel from design 1 with yield strength of 36ksi (250MPa). [4]

### 2.3.2 Space constraint

Some of the constraints the client gave were extremely strict which could not be met in order to attain the target specifications. One of the constraints given by the customer was to keep inside the same space constraint within the frame of the truck as the current design. In order to achieve a greater lifting capacity, a better attack angle of the cylinders was required. Therefore, the new design needed to sit deeper within the frame of the truck to achieve this angle as can be seen in Figure 19.

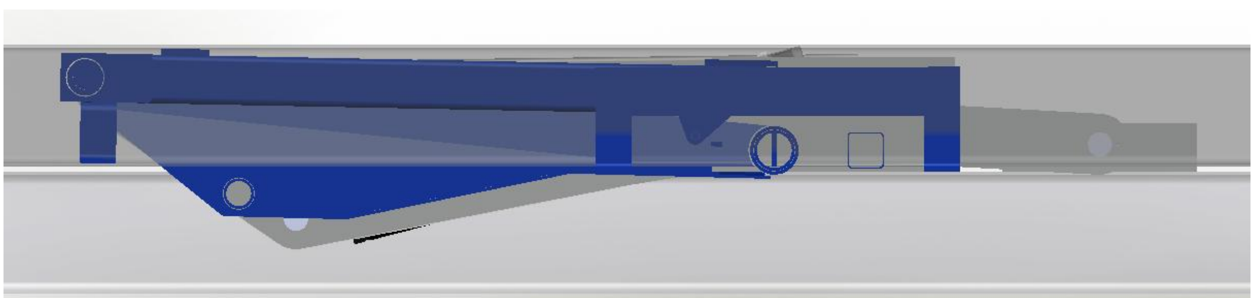

Figure 19: Comparison of space constraint

We see that the overall area beneath the frame has increased, the original design shown in blue, the new design shown in grey. The original design has a maximum depth of approximately 4" and overall length below the frame of 33". This space has increased to a maximum depth of 6.5" and an overall length below the frame of 44.5".

### 2.3.3 Assembly

The final assembly of design two can be found in Figure 20 showing the hoist in the fully upright position. All of the parts are held together by 2 x ½" bolts which are fastened through the holes in either side of the connecting pins.

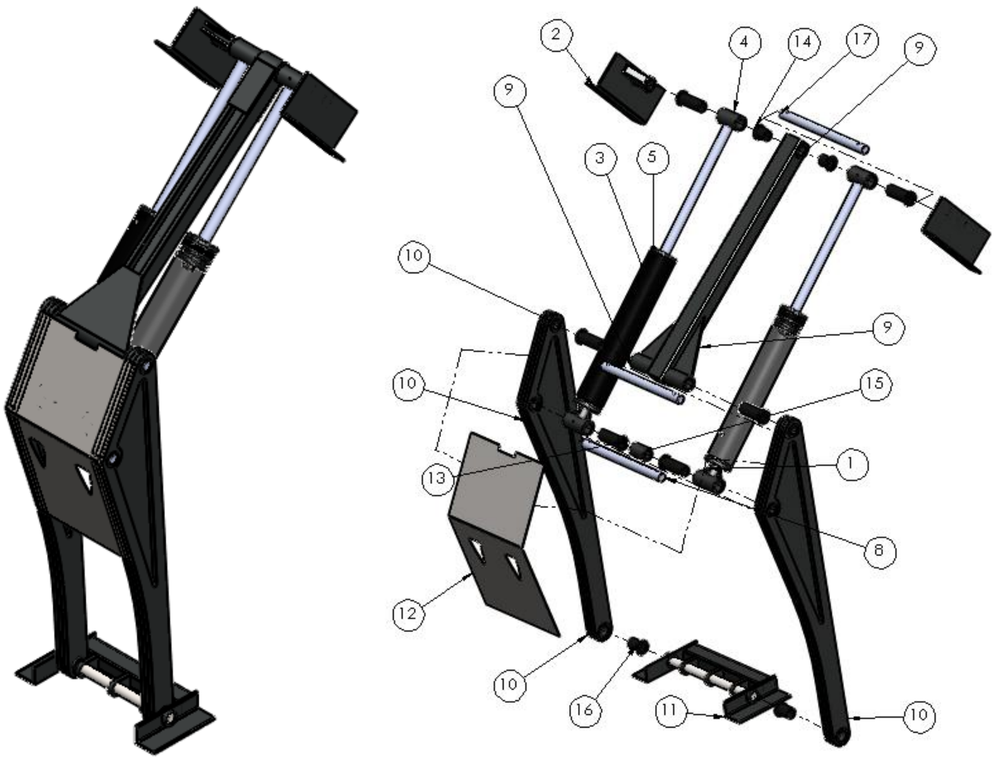


| ITEM NO. | PART NUMBER | DESCRIPTION | QTY. |
|---|---|---|---|
| 1 | 3347104 | cylinder part | 2 |
| 2 | upper box mount | see assembly drawing | 2 |
| 3 | 3117151 | cylinder part | 2 |
| 4 | 3117152 | cylinder part | 2 |
| 5 | 3119157 | cylinder part | 2 |
| 6 | 3119171 | cylinder part | 2 |
| 7 | NormalHexNut 1-1_4-12 UNF | cylinderpart | 2 |
| 8 | mid point pin | 2" bar stock | 2 |
| 9 | upper member | see assembly drawing | 1 |
| 10 | lower member | see assembly drawing | 2 |
| 11 | lower frame mount | see assembly drawing | 1 |
| 12 | Skid Plate | 1/4" chrome tread plate | 1 |
| 13 | greaseless cylinder bushing | polymer bushing | 6 |
| 14 | greaseless upper member bushing | polymer bushing | 2 |
| 15 | lower bushing spacer | 3.5" tubing 1/2" thick | 1 |
| 16 | greaseless lower member bushing | polymer bushing | 2 |
| 17 | mounting pin | 2" bar stock | 1 |

Figure 20: Final hoist assembly

### 2.3.4 Lower Member

As mentioned above, the lower member is redesigned to be made of plain carbon steel. The lower member is made up of three 1" plates welded together with ½" sleeves at each pin point as can be seen in Figure 21.

| ITEM NO. | PART NUMBER | DESCRIPTION | QTY. |
|---|---|---|---|
| 1 | lower member main | 1" plate | 1 |
| 2 | lower member material removed | 1" plate | 2 |
| 3 | lower member pin mount | 3" tubing 1/2" thick | 2 |
| 4 | lower member bushing mount | 3.5" tubing 1/2" thick | 1 |

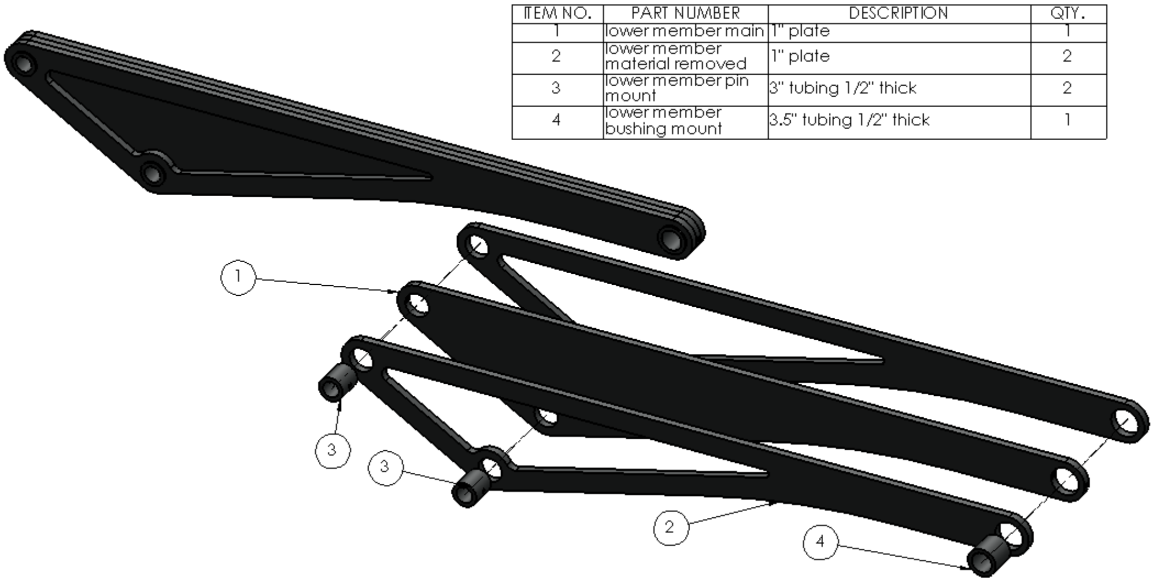


Figure 21: Lower member exploded view

The outer two plates are cut out for weight reduction, and these cutouts also allow for the three pieces to be welded together on the inside rather than all the way around the border. The member is then welded at the three sleeves as well.

FEA was used to then determine the amount of stress caused by the force of the cylinders. For this study we used the maximum allowable force of the cylinder on one member of 98,600lbs multiplied by a factor of safety of 1.5, rounded up to a force of 150,000lbs. This force was applied on the bottom sleeve where the cylinders mount. The top two sleeves were fixed with a hinge support allowing them to turn about their cylindrical axis, but not move otherwise. Figure 22 shows the results of the FEA, showing that the maximum stress in the member is well below the maximum of 36ksi. Figure 22 above is using a medium density mesh size, a further convergence evaluation of a coarse and fine mesh density can be found in Appendix D.

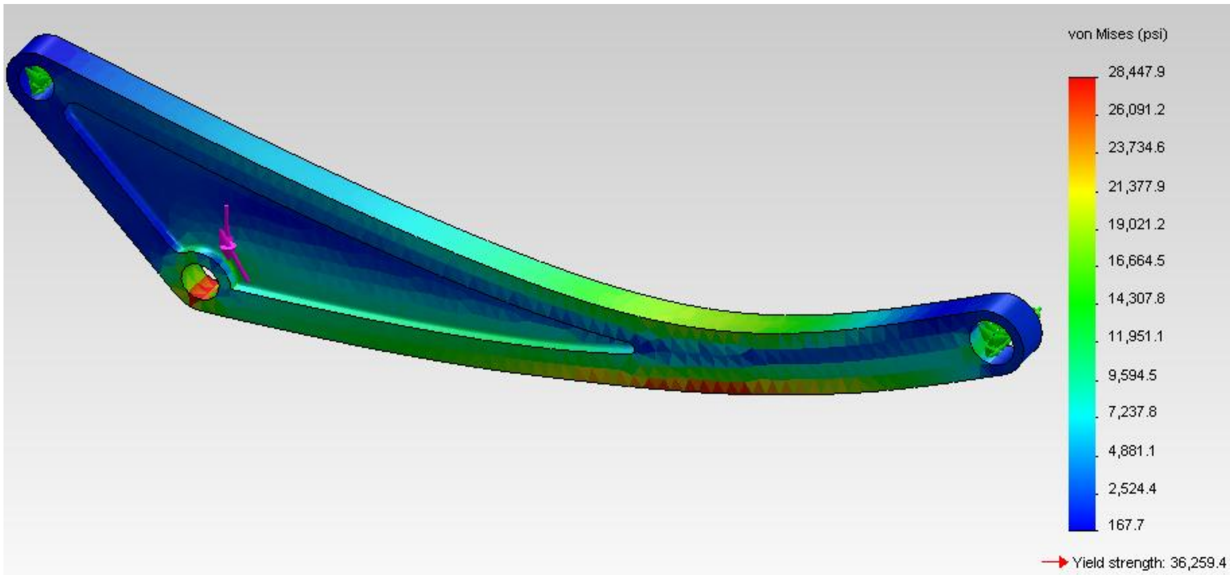


Figure 22: Lower member FEA medium mesh size

The lower member cannot be treated as a two force member. Therefore, the angle at which the maximum bending moment is applied is calculated in Appendix B. Maximum bending moment experienced by the lower member occurs when the dumping angle is at approximately 10°. At this angle the load in the cylinders is a total of 183,840 lbf which we multiply by the factor of safety of 1.5 and divide by two members to give a force of 137,880 lbf on each member at this angle. This data was applied to the FEA to see if it changes our results. Figure 23 shows the FEA at the angle of maximum bending moment on the lower member with the corresponding force.

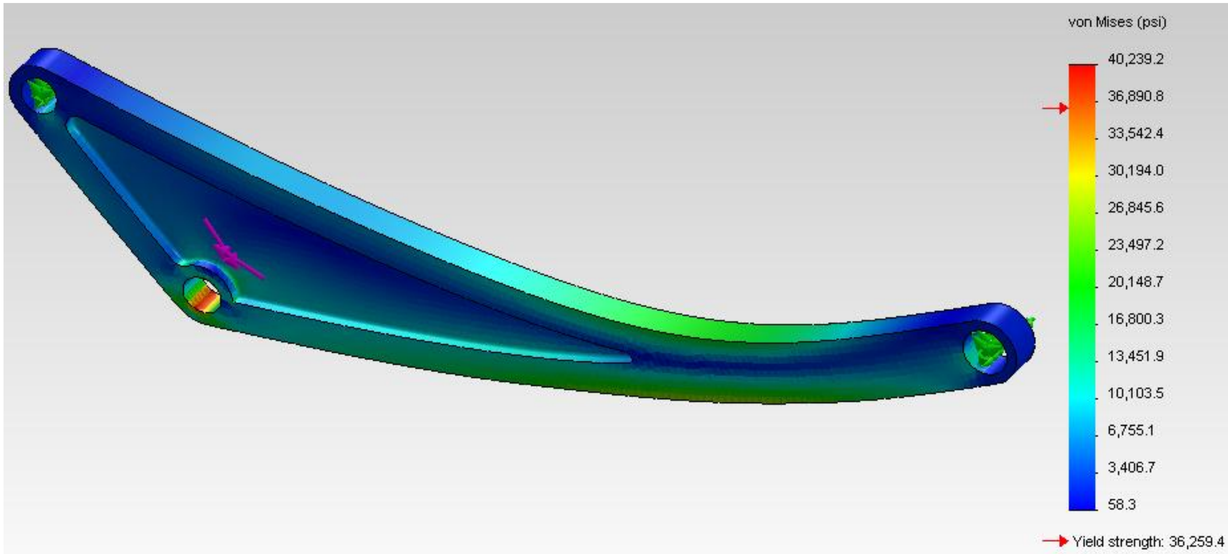


Figure 23: Lower member FEA at maximum bending moment

Although the application angle of the load applied to the lower member is at a greater angle with respect to the lower member and causes a greater bending moment, the overall force on the hoist has already been reduced due to the shifting of the weight of the box about the pivot point. The bending moment creates more stress in the member, but not enough to cause the lower member to fail. The region over the yield stress is due to the stress concentration at the sharp corners in the lower sleeve that were required to apply the force in the right direction.

### 2.3.5 Upper Member

The upper member is made similar to an I-beam with two 1" x 3.5" flanges and a ½" x 3" web. At each end of the beam is a piece of tubing through which the bushings and pin will protrude. For extra strength, each side is supported by a 3/8" brace to support the tubes. An exploded diagram of the upper member can be seen in Figure 24.

| ITEM NO. | PART NUMBER | DESCRIPTION | QTY. |
| --- | --- | --- | --- |
| 1 | upper member plate | 1" plate | 2 |
| 2 | upper member brace | 1/2" plate | 1 |
| 3 | upper member lower end | 3/8" plate | 1 |
| 4 | upper member lower mount | 3.5" tubing 1/2" thick | 1 |
| 5 | upper member upper mount | 3.5" tubing 1/2" thick | 1 |
| 6 | upper member upper end | 3/8" plate | 1 |

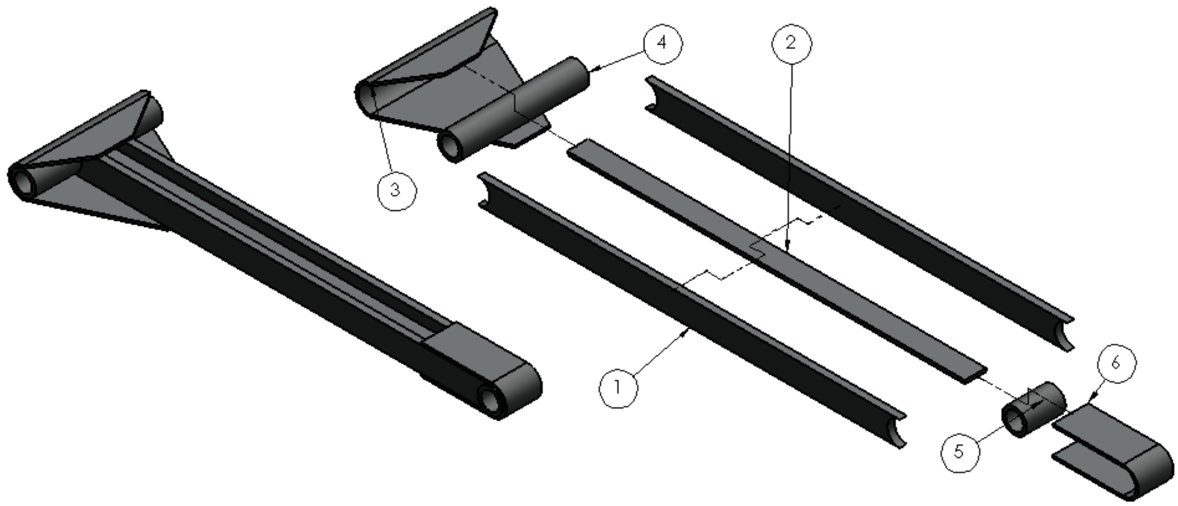


Figure 24: Upper Member Exploded View

The upper member of the hoist can be treated as a simple two force member making the FEA in this case much easier. However, due to the extremely large loads travelling through a single member, the member will be tested in three different sections; the cross-sectional area of the I-beam to insure its' integrity and a bearing force analysis of each end of the member separately as to make sure there is no overlapping error.

#### 2.3.5.1 I-Beam FEA

With a constant cross-section of a beam there should be a constant color throughout the whole area of the beam when it is in evenly distributed tensile load. However, due to the nature of finite element analysis, the FEA results show stress concentration areas on the beam, which is not true since the force is evenly distributed. The overall color of the beam in Figure 25 is green. It can be seen in the accompanying color chart that this stress is far below the maximum yield strength of the ASTM A36 material.

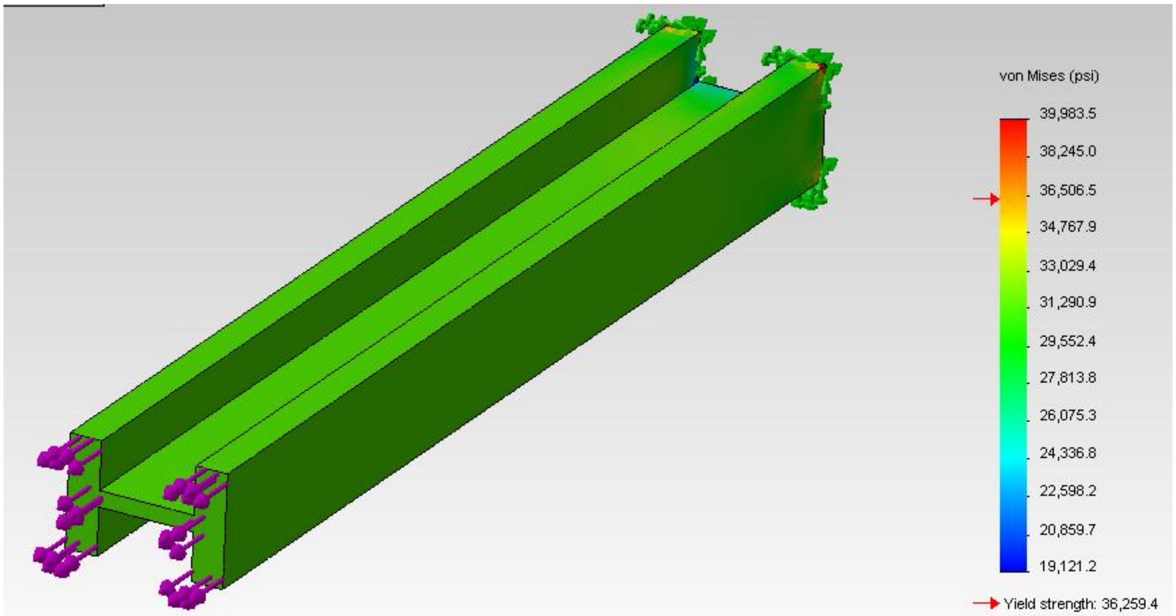


Figure 25: Upper member I-beam FEA medium mesh size

#### 2.3.5.2 Lower Pin Sleeve FEA

The lower pin mount is much longer than the upper pin mount due to the distance between it and the lower members to which it attaches. A description of the two mounting points can be seen in Figure 24. The long distance between the I-beam and the outer edges of the pin causes a large bending moment that must be counteracted with a gusset or brace to stop the pin from bending or deforming. The initial design used a simple gusset on the inside corner of this pin sleeve. The gusset was deemed insufficient to support the sleeve as the FEA showed that the sleeve would deform under such a high bearing load. The new design wraps a bracing gusset around the sleeve, holding it in place.

FEA of the new design showing the new brace can be seen in Figure 26 using nodal analysis.

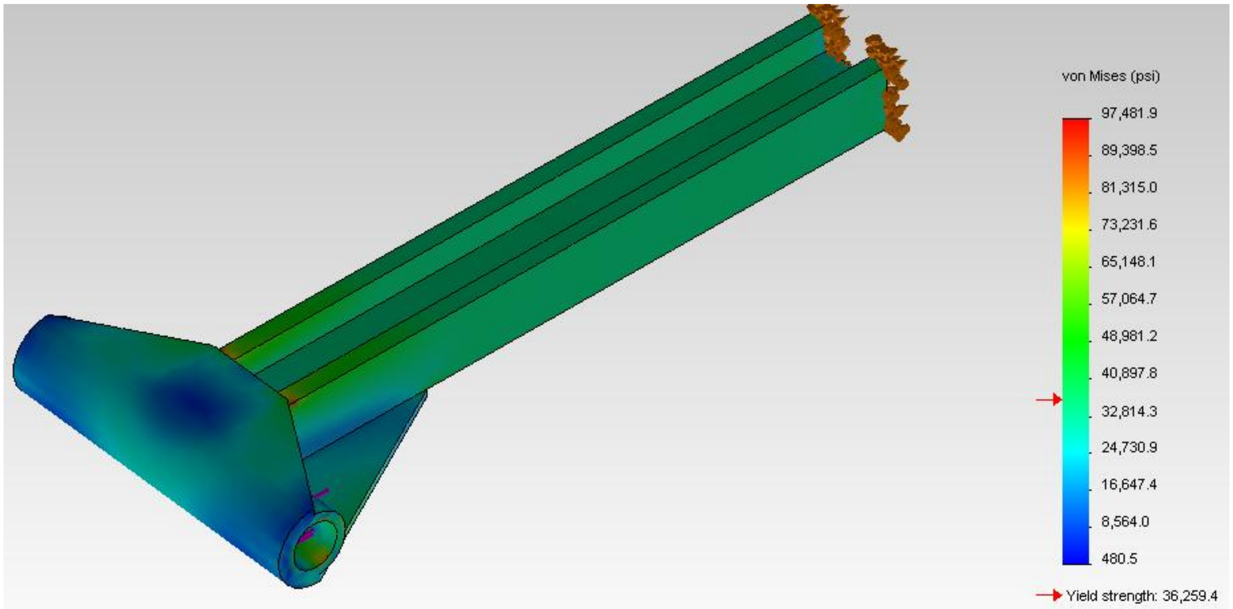


Figure 26: Upper member lower pin sleeve nodal analysis

Figure 26 above shows a greater stress within the I-beam than the yield stress which is not true. The inaccuracy of the FEA is caused by the stress concentrations which theoretically approaches infinity at a sharp corner. Therefore, we are ignoring this inaccuracy and only accepting the lower pin section of the FEA result shown in Figure 26.

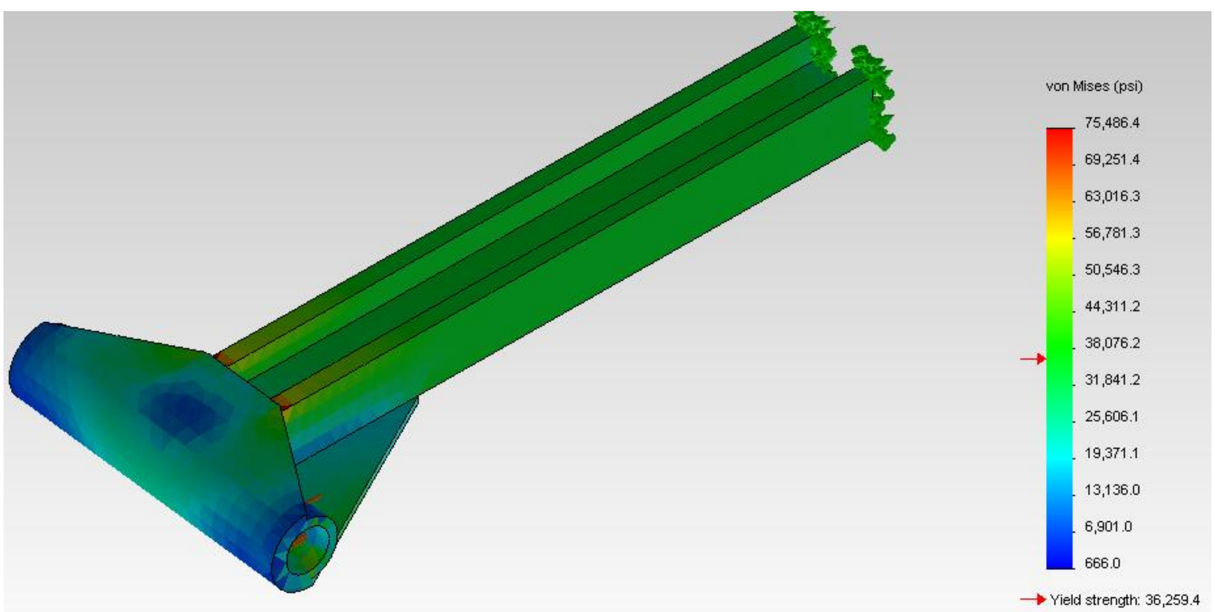


Figure 27: Upper member lower pin sleeve elemental analysis

Figure 27 uses an elemental approach to the FEA, rather than a nodal approach. An elemental approach is preferred for accurate results. From this diagram we can see that the stress in the I-beam is much closer to that shown in Figure 25, and that the overall stress in the member is quite low other than a few areas in corners where there is stress concentration. The stress concentration in the sharp corners would, however, be alleviated by the welds filling these corners.

#### 2.3.5.3 Upper Pin Sleeve FEA

The upper part of the upper member of the hoist which attaches to the box is much shorter than the lower sleeve and therefore does not experience the same type of bending moment. However, because of the small area at which the force is applied, there is still a large stress concentration around the circumference of the sleeve. The sleeve was redesigned with a brace supporting the large loads.

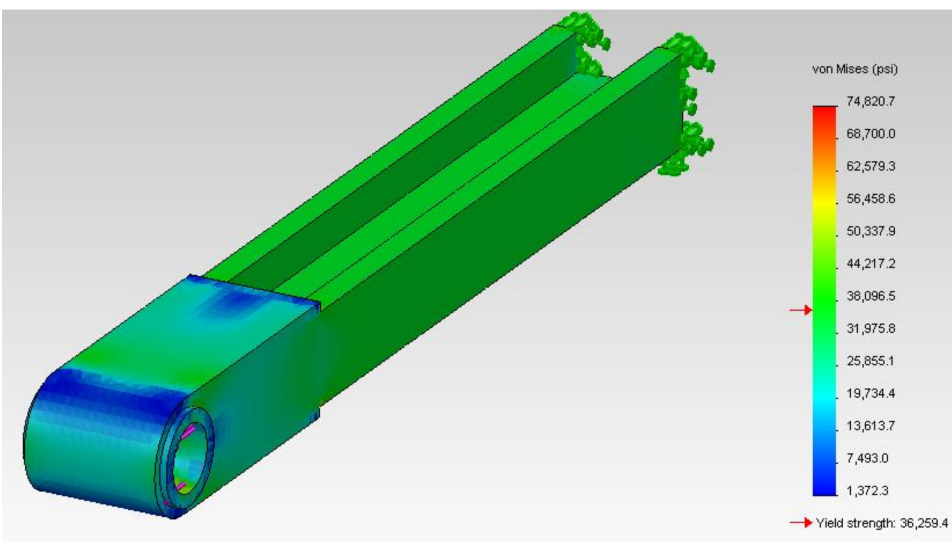


Figure 28: Upper member upper mount FEA

### 2.3.6 Upper Box Mount

The original upper box mount fits inside the end of the upper member. The new design, shown in Figure 29, uses 2" pins to connect the separate members. Therefore, the pin must be able to sit inside the upper mounting bracket. The sleeve in which the pin sits must also be braced to be able to withstand the large loads without deforming. Due to the space constraint we are unable to put a gusset above or beneath the sleeve. Therefore, two gussets were added, item 4, and a top brace, item 3, to either side of the sleeve to keep it from bending.

| ITEM NO. | PART NUMBER | DESCRIPTION | QTY. |
|---|---|---|---|
| 1 | upper mount L-bracket | 3/8" plate | 1 |
| 2 | upper mount pin brace | 2.5" tubing 1/2" thick | 1 |
| 3 | upper mount gusset brace | 1/4" plate | 2 |
| 4 | upper mount gusset | 3/8" plate | 4 |

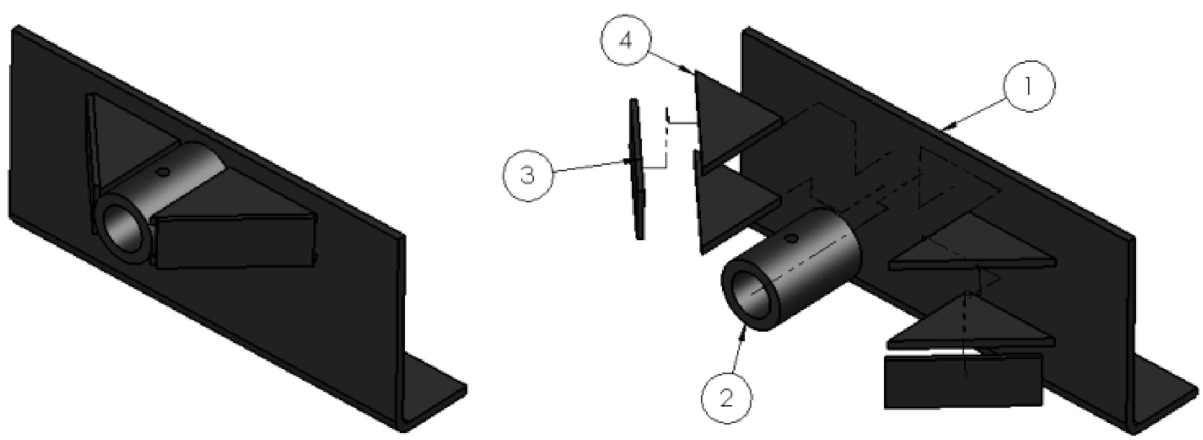


Figure 29: Upper Box mount exploded view

The FEA of the upper box mount in Figure 30 shows a stress concentration at the top of the sleeve where it is welded to the L-bracket. Though, even at the highest stress concentration it is still lower than the yield strength of the material.

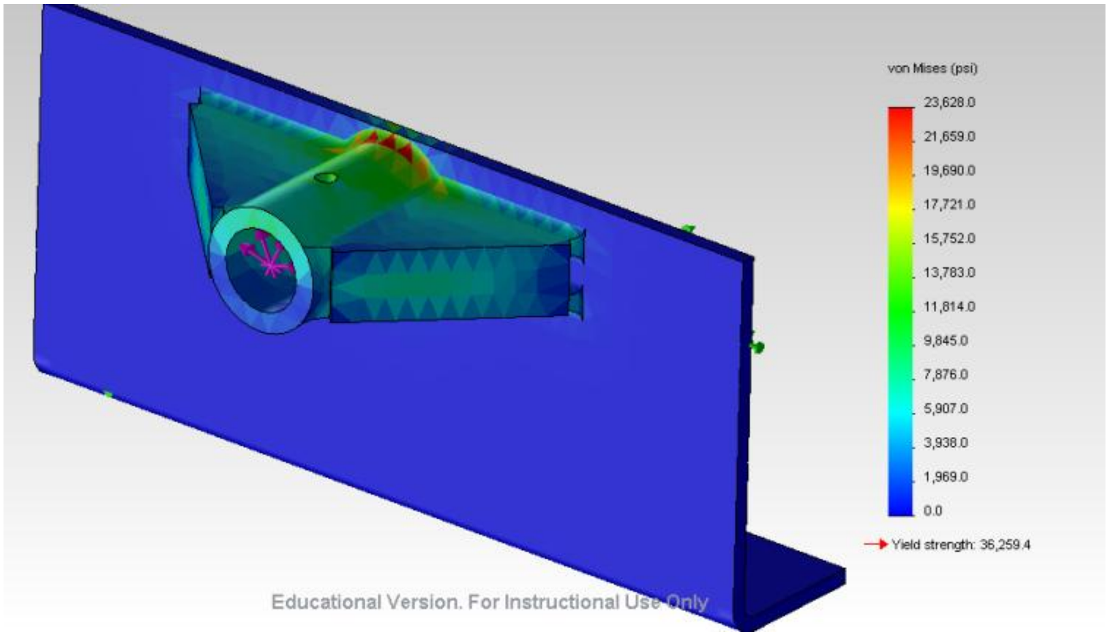


Figure 30: Upper box mount FEA medium mesh size

### 2.3.7 Lower Frame Mount

The lower frame mount is redesigned as shown in Figure 31. The redesign makes it possible to remove the hoist from the frame without having to grind off any welds as in the current design. This makes it easier for maintenance, replacing bushings and other parts if required.

| ITEM NO. | PART NUMBER | DESCRIPTION | QTY. |
|---|---|---|---|
| 1 | lower frame mount cross brace | 3"x4" rect. tubing 3/8" thick | 1 |
| 2 | lower frame mount l-bracket | 4"x5" L-bracket 3/8" thick | 2 |
| 3 | lower frame mount pin brace | 3" tubing 1/2" thick | 3 |
| 4 | lower frame mount pin flange | 1" plate | 2 |
| 5 | lower frame mount pin | 2" rod | 1 |

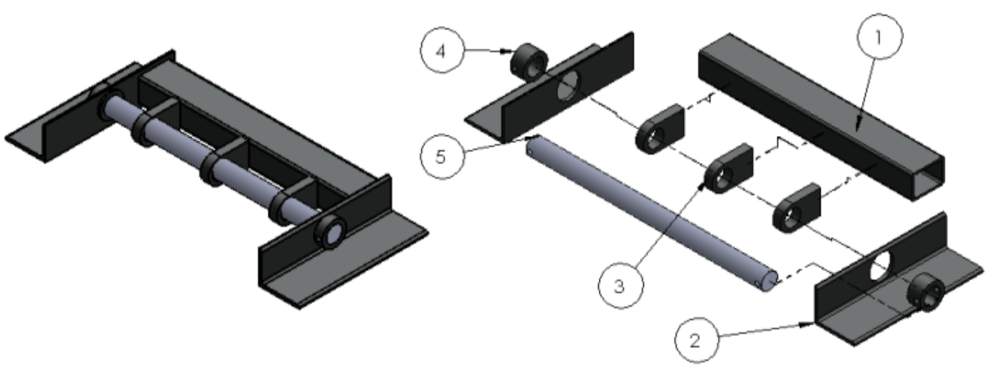


Figure 31: Lower frame mount exploded view

The FEA of the lower frame mount shows high levels of bending stress in the lower pin. Therefore, the three 1” plate braces were added for support. The FEA results can be seen in Figure 32.

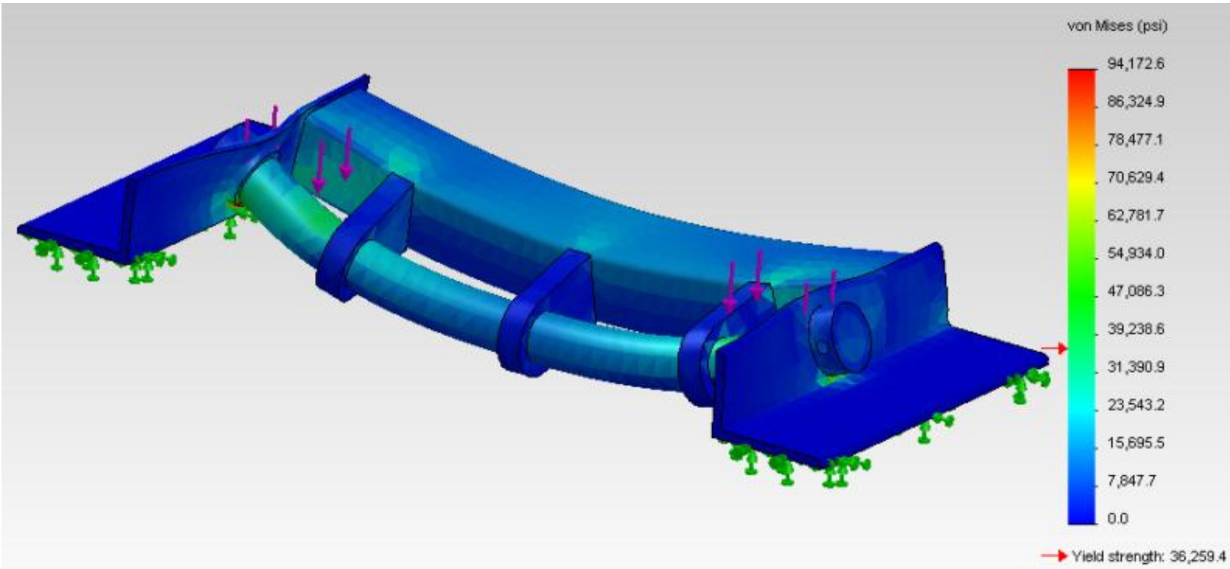


Figure 32: Lower frame mount FEA medium mesh size – Deformation scale of 84

The FEA shows very high stress concentrations due to the sharp corners where the mounting sleeve meets the pin and where the sleeve meets the L-bracket. However, from the color distribution we can see that the overall stress in the member is very low and most of the stress concentrations will be relieved by the welds.

### 2.3.8 Greaseless Bushings

There are ten pivot points on the design which must be able to turn about the pins. Polygon Composites makes composite greaseless bushings that are capable of handling up to 60,000psi. [5] These bushings are used in many different applications including heavy construction equipment and are strong enough to use for our application. Using a ¼” thick bushing at each pivot point will reduce friction allowing for a greater lifting force and will reduce maintenance costs as the bushings are self-lubricating and do not need to be greased. One of the greaseless bushings can be found in Figure 33.

Figure 33: Greaseless bushing for cylinder mount

# 3 Cost Analysis and Manufacturability Assessment

Quattro Consulting performed a cost analysis and manufacturability assessment of the new hoist designs. The purpose behind these analyses is to provide Cancade with a preliminary evaluation in term of the implementation of the proposed designs.

## 3.1 Material Cost Analysis

The analysis is intended to compare the cost of the new designs with Cancade's current design. Due to the limitation of manufacturing data provided by the client, the analysis is limited only to the material cost. It is important to note that cost reduction is not the main objective of this project. Quattro Consulting did the best to obtain the most accurate quote. However, due to the limited resource, the obtained quote may not reflect the cheapest possible quote.

For this analysis, Quattro Consulting made several assumptions as follows:

- If price per unit, such as \$/ft or \$/ft$^2$, is not available the following assumptions apply:
    - Sheet material are ordered in dimensions of 5' x 10'. Material price is obtained from dividing final price by total area square footage
    - Square tubing, round tubing, bar and angle iron are ordered per available minimum length. Material price is obtained from dividing final price by the length in feet
- Quattro Consulting assumes no guarantee of the availability of material other than at the time the quote is obtained
- Quattro Consulting assumes no guarantee of the stability of the material prices

The quotes for the new and current hoists' material are obtained from several different suppliers. The three designs all require A36 steel. This is common steel for agricultural and industrial applications. The material quote is obtained from Russel Metals, Castle Metal and Brunswick Steel. All of them are Winnipeg-based steel suppliers. The list of material and its price is available in Appendix E.

To create a benchmark, the analysis starts with Cancade's current design. The design utilizes A36 mild steel and the total cost of this design is \$412.23. The design requires parts from 11 different types and sizes of A36 steel. The results of Cancade's current hoist cost analysis can be seen in Table IV.

TABLE IV: CANCADE'S CURRENT HOIST COST

| Type | Material | Size | Quantity | Unit | Sub Total |
|---|---|---|---|---|---|
| Plate | A36 | .25" Thick | 6.95 | $ft^2$ | $39.94 |
| | A36 | .375" Thick | 8.51 | $ft^2$ | $73.61 |
| | A36 | .5" Thick | 6.83 | $ft^2$ | $78.83 |
| | A36 | 1" Thick | 1.09 | $ft^2$ | $31.49 |
| | A36 | 1.25" Thick | 0.14 | $ft^2$ | $5.32 |
| Square Tubing | A36 | 3" x 4" x. 25" Thick | 9.66 | ft | $79.00 |
| | A36 | 3" x 3" x .375" Thick | 2.22 | ft | $21.61 |
| Round Tubing | A36 | 2.5" OD x .25" Thick | 0.50 | ft | $5.66 |
| | A36 | 3" OD x .25" Thick | 1.51 | ft | $20.81 |
| | A36 | 4" OD x .25" Thick | 3.81 | ft | $30.58 |
| Angle Iron | A36 | 3" x 5" x .375 Thick | 3.33 | ft | $25.37 |
| Total | | | | | $412.23 |

The material price for the design 1 was totaled at $600.50. The design requires only 7 different types and sizes of A36 Steel. The results of the design 1 cost analysis can be seen in Table V.

TABLE V: DESIGN 1 COST

| Type | Material | Size | Quantity | Unit | Subtotal |
|---|---|---|---|---|---|
| Plate | A36 | .75" Thick | 11.60 | $ft^2$ | $182.62 |
| | A36 | .5" Thick | 6.98 | $ft^2$ | $80.57 |
| | A36 | .375" Thick | 0.45 | $ft^2$ | $3.92 |
| Square Tubing | A36 | 3" x 4" x .375" Thick | 11.83 | ft | $139.16 |
| Round Tubing | A36 | 2.75" OD x 2" ID (.375" Thick) | 3.08 | ft | $55.22 |
| | A36 | 3.25"OD x 2" ID (.625" Thick) | 1.33 | ft | $32.47 |
| Round Bar | A36 | 2" Diameter | 8.08 | ft | $106.54 |
| Total | | | | | $600.50 |

Finally, design 2 is the most expensive design with a total of $1,069.51. The design utilizes 8 different types and sizes of A36 steel. The reason behind the high cost is that design 2 utilizes significantly more 1" steel plate than the other designs. This particular steel plate costs more than any of the thinner plates. The results of the design 2 cost analysis can be found in Table VI.

TABLE VI: DESIGN 2 COST

| Type | Material | Size | Quantity | Unit | Subtotal |
|---|---|---|---|---|---|
| Plate | A36 | Gage 14 | 8.01 | $ft^2$ | $0.16 |
| | A36 | .375" Thick | 5.93 | $ft^2$ | $51.33 |
| | A36 | .5" Thick | 1.25 | $ft^2$ | $14.44 |
| | A36 | 1" Thick | 24.77 | $ft^2$ | $718.31 |
| Round Tubing | A36 | 3" OD (.5" Thick) | 2.58 | ft | $66.12 |
| | A36 | 3.5" OD (.5" Thick) | 2.54 | ft | $78.03 |
| Angle Iron | A36 | 3.5" x 5" x .375" Thick | 2.67 | ft | $20.32 |
| Round Bar | A36 | 2" Diameter | 9.17 | ft | $120.80 |
| Total | | | | | $1,069.51 |

Comparing all three designs, Cancade's current hoist is the cheapest. However, if the manufacturing cost is included, the final cost for each design will be different. Quattro Consulting recommends that Cancade performs an in-depth material breakdown and bulk ordering to reduce the price.

### 3.2 Manufacturability Assessment

Cancade's truck division facility in Brandon is a fully functional workshop. It has the capability to manufacture the line of boxes, hoists, and trailers as well as retrofitting their products on customers' trucks. To manufacture a hoist, processes such as sawing, plasma cutting, bending, welding and powder coating are involved. These processes are available in Cancade's facility, but there are limitations with certain processes. Plasma cutting is only available for material with maximum thickness of 1/2" while all welding is done by hand.[2]

To measure the new designs' manufacturability compared to the current design, Quattro Consulting assessed all of the processes required to manufacture the hoists. However, powder coating were excluded because it is not pertinent to any specific design. Quattro consulting performed the manufacturability assessment from the available 3D CAD models. No prototypes have been built for this purpose. To measure the process, there were several assumptions and benchmarks made for this assessment:

- Welding was measured by the length of the welds
- Bending and sawing were measured by the amount of bends and cuts performed.
- Bolting was measured by counting the bolted connections
- Plasma cutting was measured by the perimeter length of the cut object
- Assembly was measured by the amount of individual parts

This assessment covers all six of the processes involved, however, it emphasizes welding and assembly. The analysis was done to provide the client with the information regarding parts and welds reduction, which are some of the main objectives of this project. Cancade requested a 30% reduction in both welds and parts. Welding and assembly is currently the most labor intensive process in manufacturing Cancade's current hoist.

The manufacturability assessment starts with Cancade's current design. By evaluating Cancade's current design, a benchmark for the other designs was created. The current design contains 55 individual parts and 1307.12" of weld. It contains 10 bending processes and 39 sawing processes. It also involves 1435.78" of plasma cutting. Design 1 is able to reduce the amount of parts to 25 individual parts. This number exceeds the target specifications as it is a 55% reduction of parts compared to the current design. Welding is also reduced to 643.58" of weld or a 51% weld reduction. Plasma cutting reduces to 840.86" or by 41%. Sawing is reduced by 28% to 28 processes. Bending increases to 14 processes. However bending is a less labor intensive process and a small increase is insignificant. Finally, design 2 reduces the amount of parts to 37 individual parts. This number represents a 32.73% part reduction. Welding is reduced to 732.82" or a reduction of 43.94%. Plasma cutting is cut down to 1390.35" or a 3.16% reduction. Bending is reduced to only 2 processes or 80% reduction. Sawing increases insignificantly by 28.21% to 28 sawing processes. The tabulated results of the manufacturability assessment are available in Table VII.

TABLE VII: MANUFACTURABILITY COMPARISON FOR CANCADE'S CURRENT HOIST, DESIGN 1 AND DESIGN 2

| | Cancade's Current | Design 1 | | Design 2 | | |
|---|---|---|---|---|---|---|
| | | Quantity | % Reduction | Quantity | % Reduction | |
| Bolted parts | 0 | 0 | n/a | 4.00 | n/a | bolt |
| Welding | 1307.12 | 643.58 | 51% | 732.82 | 43.94% | in of weld |
| Bending | 10 | 14 | -40% | 2.00 | 80.00% | item |
| Sawing | 39 | 28 | 28% | 28.00 | 28.21% | item |
| Plasma | 1435.78 | 840.86 | 41% | 1390.35 | 3.16% | in of plasma cut |
| Assembly | 55 | 25 | 55% | 37.00 | 32.73% | part |

From the assessment, it is important to note that both new designs exceed the specification of 30% reduction in welds and parts. Design 1 is able to achieve a 51% weld reduction and a 55% part reduction. Design 2 successfully reduces the amount of welds by 43.94% as well as a 32.73% reduction in parts.

# 4 Summary and Recommendation

Quattro Consulting's design 1 is able to lift the 60,000lbs load. The design reduces the amount of welds by 51% and parts by 55%. These values exceed the requirement for 30% reduction for both welds and parts. The material used for design 1 is A36 steel. The hoist maximum dumping angle was increased to 46.5°. As the result of increased dumping angle, the new hoist must go slightly beyond the constrained space when fully collapsed. The maximum dumping angle is slightly lower than the target specifications. It is a compromise to avoid extending the hoist too far outside the constrained space.

In order to be implemented, several minor details on design 1 will still need to be evaluated. First is to constrain the pivoting pins. This can be done in many ways such as using cross pins or welding washers on the end. The re-routing of the hydraulic hoses also needs to be examined to ensure a safe route avoiding any pinch points. Finally, the installation of a safety prop is recommended for maintenance purposes.

Design 2 is capable of lifting a 60,000lbs load with the maximum dumping angle of 50°. These values meet the target specifications. The amount of weld reduction is 43.94% while the amount of parts is reduced by 32.73%. The weld and part reductions of design 2 exceed the target specification of 30%. Design 2 uses A36 steel. The space constraint is compromised in order to produce a stronger hoist while achieving a higher dumping angle.

The first recommendation for future work for design 2 is to evaluate a way to bolt the upper member to the box frame eliminating welds. The bolting method assures that the hoist can be fully disassembled for maintenance purposes. Utilizing higher strength alloy steel can further reduce the hoist weight and the amount of parts. The re-routing of the hydraulic lines and the installation of a safety prop should also be considered.

Both designs are not able to meet the fully collapsed space constraint as stated in the desired target specifications. The ability to meet the constraint is limited by the need to achieve a higher dumping angle. Depending on the truck frame design, exceeding the space may either be tolerable or cause interference. In case of interference, modifying the truck frame is necessary.

Both designs Quattro Consulting presents have advantages that will benefit Cancade. Design 1 has a large percentage of part and weld reduction. Design 2 is able to lift at a higher dumping angle with a slightly lower percentage of part and weld reduction compare to design 1. The decision of choosing the implemented design will depend on the client's business plan. However, it must be noted that both of Quattro Consulting designs exceed any other manufacturer's hoist.

In term of cost and manufacturing, Quattro Consulting recommends a more in depth material breakdown to determine all the required parts. A detailed manufacturing plan must also be considered before mass producing the hoist. Depending on the amount of hoist orders, bulk purchasing of material can be done.

Quattro Consulting has presented the final hoist designs for Cancade Company Ltd. From the target specifications we were given, both designs have been optimized to the best of our ability.

## Works Cited

[1] Cancade Compant Ltd., 12 2011. [Online]. Available: http://www.cancade.com/. [Accessed 02 12 2011].

[2] M. Rosumowitsch, Interviewee, *Design Engineer. Cancade Company Ltd..* [Interview]. 15 September 2011.

[3] R. Livicker, Interviewee, *Inside Sales. ASA Alloys.* [Interview]. 23-27 11 2011.

[4] Russel Metals, "Tube and Pipe," 12 2011. [Online]. Available: http://www.russelmetals.com/pdf/english/service/pdf_catalogue/Sec_06_Tube_and_Pipe.pdf . [Accessed 15 11 2011].

[5] M. Rosumowitsch, "Truck assembly design position," 2011.

[6] J. Hildebrand, Interviewee, *Truck assembly lifted position.* [Interview]. 10 2011.

# Appendix A –

# Concept Selection

## List of Tables

## A-1 Concept Analysis & Selection

Quattro Consulting brainstormed ideas for the new hoist design as well as models some conceptual designs in SolidWorks. As a result, there were 11 different designs generated. The designs then were roughly sketched and further evaluated by using screening and scoring matrices. The generated conceptual designs are shown below with brief descriptions.

TABLE I: CONCEPTUAL DESIGNS GENERATED

| Design # | Description | Preliminary Sketch |
|---|---|---|
| 1 | Design 1 is Cancade's current hoist design | |
| 2 | The design encompasses a sliding mechanism which would be attached to the lower member of the hoist. The slider provides a pushing (horizontal) force to the lower member to provide more lifting force. The design would increase the number of parts and may interfere with existing structural members of the hoist and truck. | 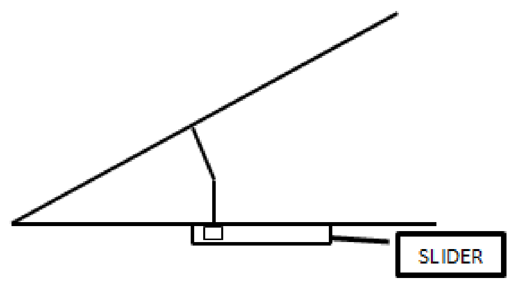  |
| 3 | Design 3 was inspired from the concept of a scissor lift. The cylinder pushes at the central joint of the two members as shown to initiate vertical movement. This design is more complex than the current design and may increase the number of parts as well as increase the complexity of manufacturing. | 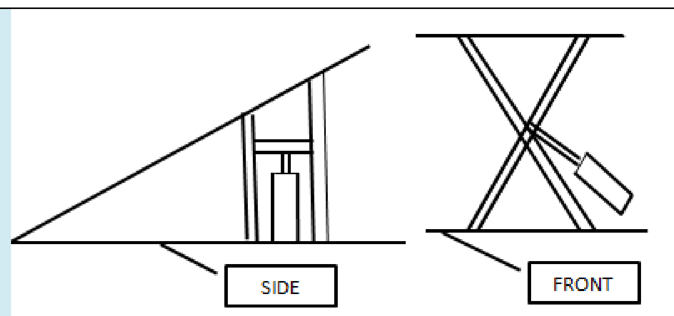  |

| | | |
|---|---|---|
| 4 | The concept of this design is very simple. It consists of using a large cylinder to lift the box. Though it is the most simple of designs, it is not very feasible as finding such a large cylinder is impractical. Also this design would violate the vertical and horizontal constraints provided by Cancade Ltd. | 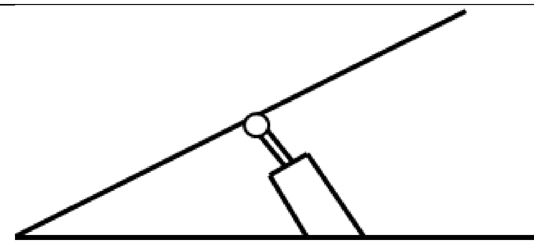 |
| 5 | Concept 5 consists of a supporting cylinder. The supporting cylinder would assist the initial lift of the box which will in turn reduce the force experienced by the structure of the hoist. | 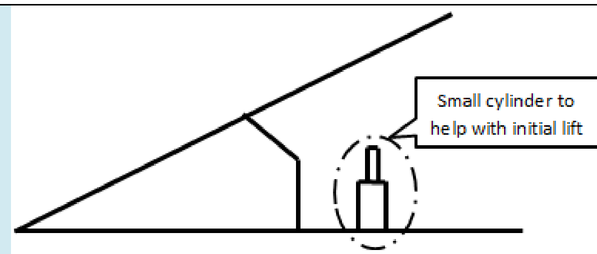 |
| 6 | Design 6 is similar to the previous concept. A cam would be used to provide support with the initial lift of the box. | 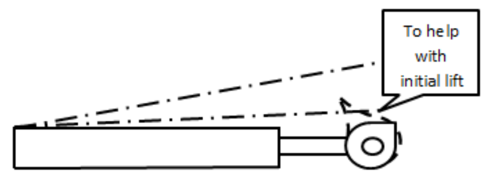 |
| 7 | The horizontal pin to pin distance would be reduced in this design while keeping a similar hoist structure. | 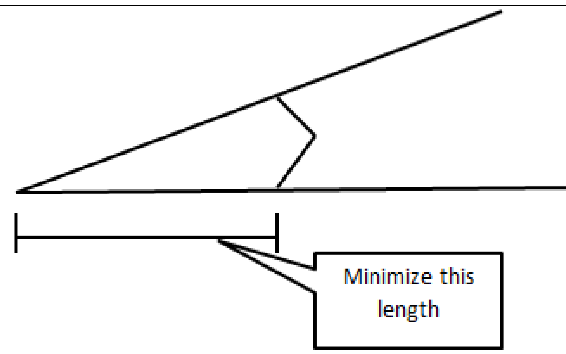 |
| 8 | For this concept, the position of the cylinder was changed to the outside and the cylinder performs a push motion to the lower motion. This motion would rotate the lower member upwards and motion would be following by the upper member. | 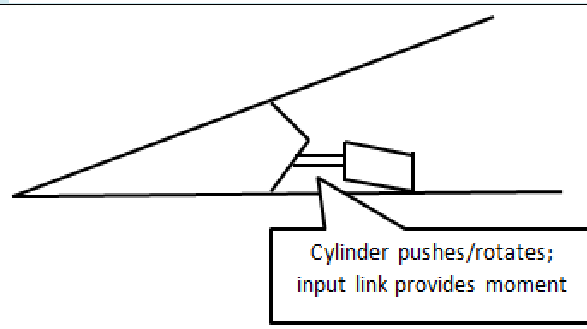 |

| | | |
|---|---|---|
| 9 | The position of the cylinder was changed for concept 9. In the current design, the cylinder is attached within the upper and lower member. For this design, the cylinder would push from the truck frame to the upper member. | 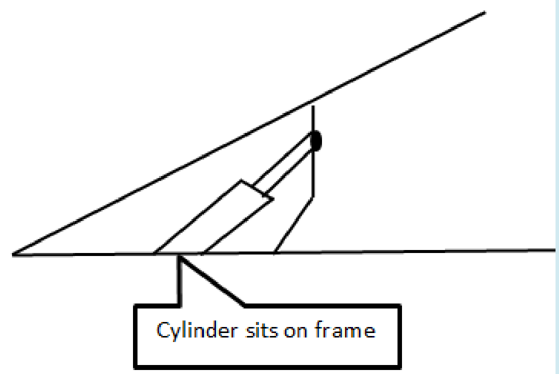  |
| 10 | Concept 10 is very similar to the previous conceptual design. The cylinder would be attached to the frame as before but perform a pull motion rather than pushing the lower member. For this conceptual design, the members would have to very robust and strong. | 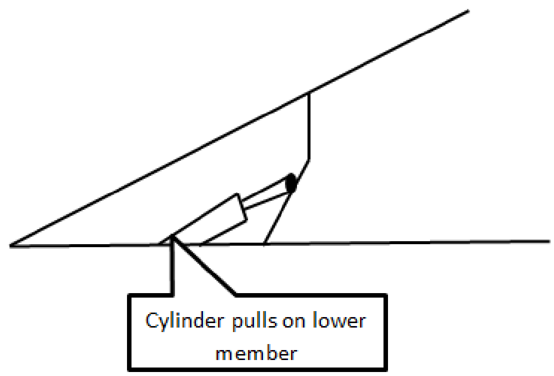  |
| 11 | The concept is very similar to designs 5 & 6. The mechanism of concept 11 would aid in the initial lift of the box. The cylinder slides along a cam type member which gives the cylinder a better initial angle of attack. | 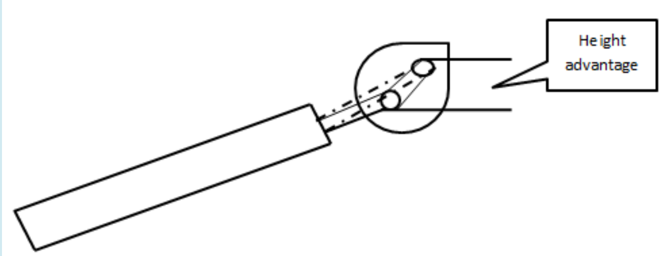  |
| 12 | The last conceptual design encompasses the use of a linkage mechanism assisted by a cylinder between the linkages as shown in the figure. This design is more complex than the current hoist and can make the manufacturing process difficult. | 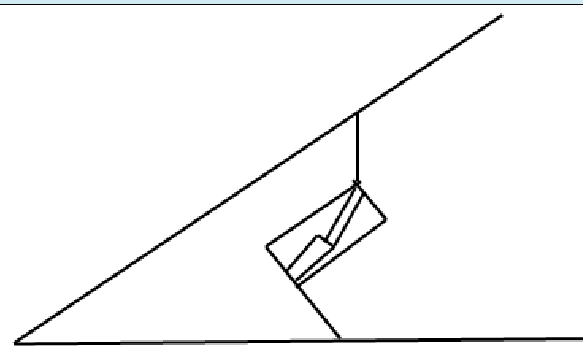 |

The above designs were discussed in more detail and in accordance to the criteria formulated in the House of Quality. These criteria were inserted into a screening matrix and the best possible designs were found. The screening matrix can be seen in TABLE II: SCREENING MATRIX.

Design 1 from the conceptual designs generated was not included in the screen matrix as the detail of the design was much higher than the other conceptual designs.

TABLE II: SCREENING MATRIX

| | Conceptual Designs | | | | | | | | | | |
|---|---|---|---|---|---|---|---|---|---|---|---|
| **CRITERIA** | 2 | 3 | 4 | 5 | 6 | 7 | 8 | 9 | 10 | 11 | 12 |
| **Simple Design** | 0 | - | + | 0 | 0 | + | + | + | + | 0 | - |
| **Easy to Manufacture** | - | 0 | + | 0 | 0 | + | + | + | + | 0 | - |
| **Efficient** | 0 | - | - | + | + | + | 0 | 0 | 0 | + | 0 |
| **Work with Current Specs** | - | - | - | 0 | + | + | 0 | 0 | + | + | - |
| **Safe** | 0 | 0 | 0 | 0 | 0 | 0 | 0 | 0 | 0 | 0 | 0 |
| **Corrosion Resistant** | - | - | 0 | 0 | - | 0 | 0 | 0 | 0 | - | 0 |
| **User Friendly** | 0 | 0 | 0 | 0 | 0 | 0 | 0 | 0 | 0 | 0 | 0 |
| **Robust** | - | + | 0 | 0 | 0 | 0 | 0 | + | 0 | - | + |
| **Total** | -4 | -3 | 0 | +1 | +1 | +4 | +2 | +3 | +3 | 0 | -2 |

The screening matrix used the following measurement for the criteria:

TABLE III: LEGEND FOR THE SCREENING MATRIX

| Legend | |
|---|---|
| + | Meets the criteria |
| - | Does not meet criteria |
| 0 | Neutral/Not Applicable |

From the above screening process, it can be seen that designs 5, 6, 7, 8, 9 & 10 scored the highest out of the 11 conceptual designs.

To proceed with the next step, designs 5, 6, 7, 8, 9 and 10 were divided into two categories as follows:

TABLE IV: TOP DESIGNS SUMMARY

| Designs | Additional Mechanisms |
|---|---|
| 7, 8, 9 & 10 | 5 & 6 |

Design 5 and 6 consist of supplementary machinery which aid the hoist structure but do not have a direct impact on the structure. In other words, they do not change the design of the existing hoist structure. Design 7, 8, 9 and 10 have a direct influence on the current design of the hoist and for that reason they were categorized separately.

To further narrow down the concepts, a scoring matrix is used. The scoring matrix can be seen in Table V. At this level, design 1 was incorporated into the scoring matrix in order to compare the current design to the top conceptual designs.

TABLE V: SCORING MATRIX

| | **DESIGNS** | | | | | | |
|---|---|---|---|---|---|---|---|
| **CRITERIA** | 1 | 5 | 6 | 7 | 8 | 9 | 10 |
| **Simple Design [0.15]** | 3 | 1 | 1 | 3 | 3 | 3 | 3 |
| **Easy to Manufacture [0.15]** | 3 | 1 | 1 | 3 | 3 | 3 | 3 |
| **Efficient [0.10]** | 2 | 3 | 3 | 3 | 0 | 0 | 0 |
| **Work with Current Specs [0.25]** | 3 | 1 | 2 | 3 | 0 | 0 | 3 |
| **Safe [0.10]** | 0 | 0 | 0 | 0 | 0 | 0 | 0 |
| **Corrosion Resistant [0.05]** | 0 | 0 | 0 | 0 | 0 | 0 | 0 |
| **User Friendly [0.10]** | 0 | 0 | 0 | 0 | 0 | 0 | 0 |
| **Robust [0.10]** | 0 | 0 | 0 | 0 | 0 | 0 | 0 |
| **Total** | 1.85 | 0.85 | 1.10 | 1.95 | 0.90 | 0.90 | 1.65 |

A weighted percentage was assigned to each of the criteria as shown in Table V above. Performing this step helped weigh the criteria relative to each other which further enhanced the selection of the most effective designs.

The legend for the scoring matrix is shown in Table VI:

TABLE VI: LEGEND FOR THE SCORING MATRIX

| Legend | Description |
|---|---|
| **3** | Fully Satisfies Criteria |
| **2** | Neutral |
| **1** | Minimally Meets Criteria |

The percentage is multiplied by the number assigned to each design. A sample calculation can be seen below:

$$Design\ 5; \quad Total = (1 * 0.15) + (1 * 0.15) + (3 * 0.10) + (1 * 0.25) = 0.85$$

From the scoring matrix, the top designs were design 1, 6 and 7.

# Appendix B –

# Stress Calculations

## List of Figures

## List of Tables

## B-1 Background

The objectives of the force analysis of the 3D models are as follows:

- To understand the forces experienced by hoist members of both models corresponding to dumping angles
- To aid the design process of the parts that will withstand the occurring forces
- To understand at which dumping angle the models experience the most forces. In other words, it will help determine critical dumping angles
- To determine the maximum bending moment experienced by the lower member.

The following sections display valuable information regarding analysis of the two designs. The information is presented in terms of graphs to easily portray the general trend. It is important to note that the data displayed in the graphs is available from the detailed calculation of this analysis is located in section B-3.

## B-2 Results Preliminary Force Analysis

In order to determine the force experienced by the two designs, the first step was to determine the equivalent weight experienced by the hoist. It is important to note that even though the box design load is 60000lbs, the force experienced by the hoist through its top mounting point is not the same. The reason for this is because the centroid of the load shifts as a function of the dumping angle. As the dumping angle increases, the centroid of the load shifts closer to the pivot point. After the hoist has been lifted above a certain angle, the center of mass falls behind the pivot point of the box. The equivalent weight placed at the top mounting point of the hoist is shown in Error! Reference source not found..

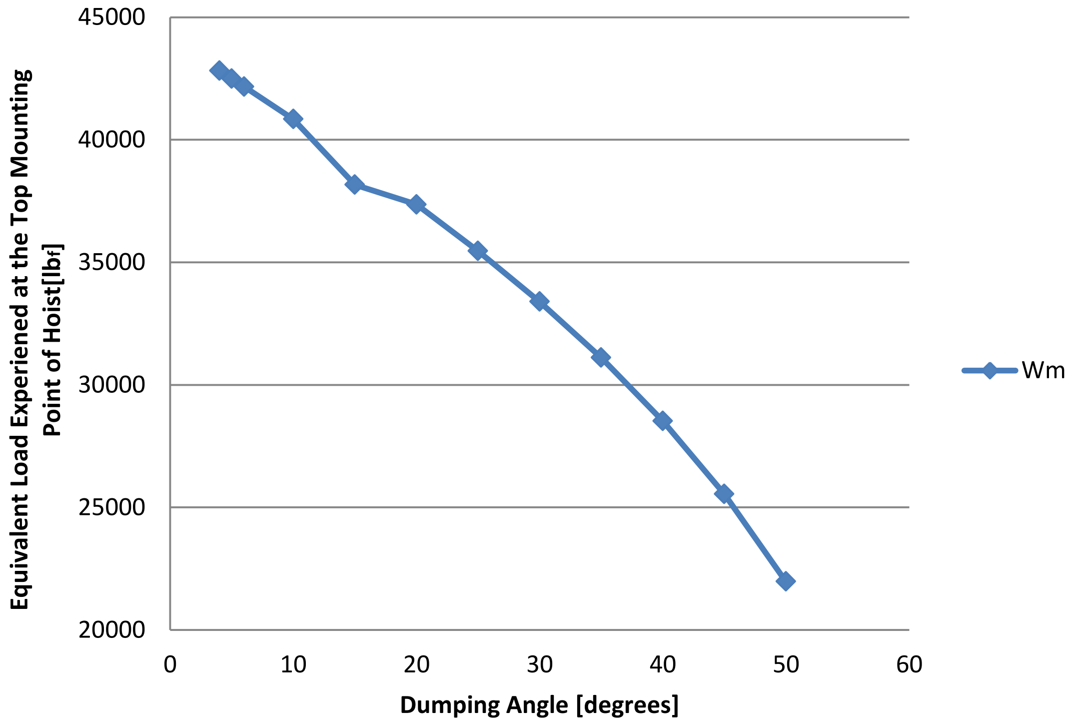


Figure 1: Equivalent Load Placed on the Top Mounting Point Of The Hoist As A Function Of The Dumping Angle

Now that the load on the hoist is known, the analysis to determine the internal forces experienced by the hoist for both CAD models was performed.

## B-2.1 Design 1 Analysis

Design 1 consists of a hoist in which both the lower and the upper member have equal lengths (66"). The horizontal pin-to-pin along the frame and the pin-to-pin along the box are of equal lengths as well (155"). Before determining the forces experienced by the hoist members, the external forces were calculated. Figure 2 below is a simplified system of Design 1.

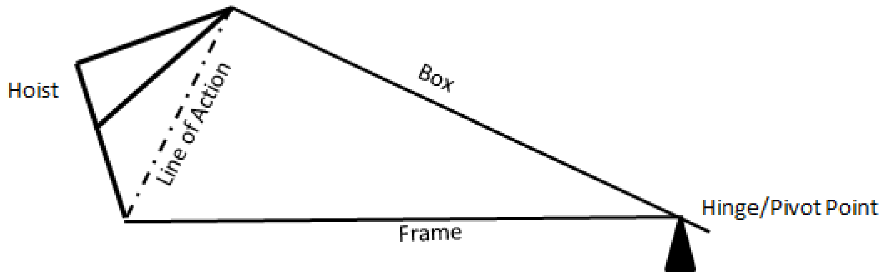


Figure 2: Simple Depiction of Entire System for Design 1

The hoist in Figure 2 is removed to determine the external forces of the system and replaced with the line of action. A free body diagram used to determine the external forces is shown in the Figure 3.

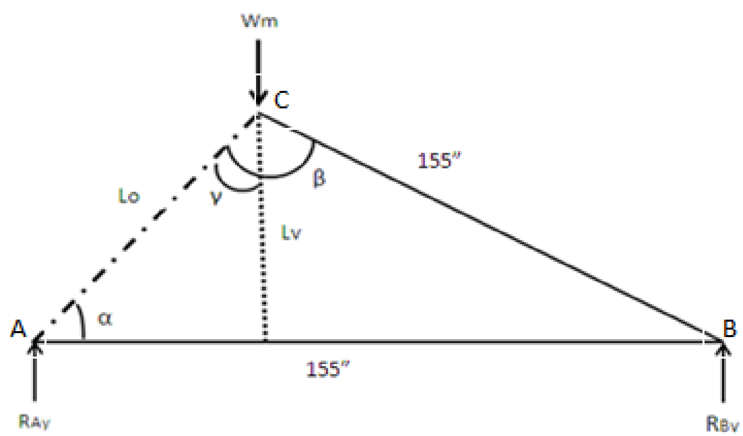


Figure 3: Free Body Diagram to Determine External Forces for Design 1

By performing simple static calculations, the reaction forces displayed in the free body diagram were determined. These reaction forces were then plotted as a function of the dumping angle to observe the trend of the reaction forces. The reaction forces at points A and B are plotted as shown in Figure 4 and Figure 5.

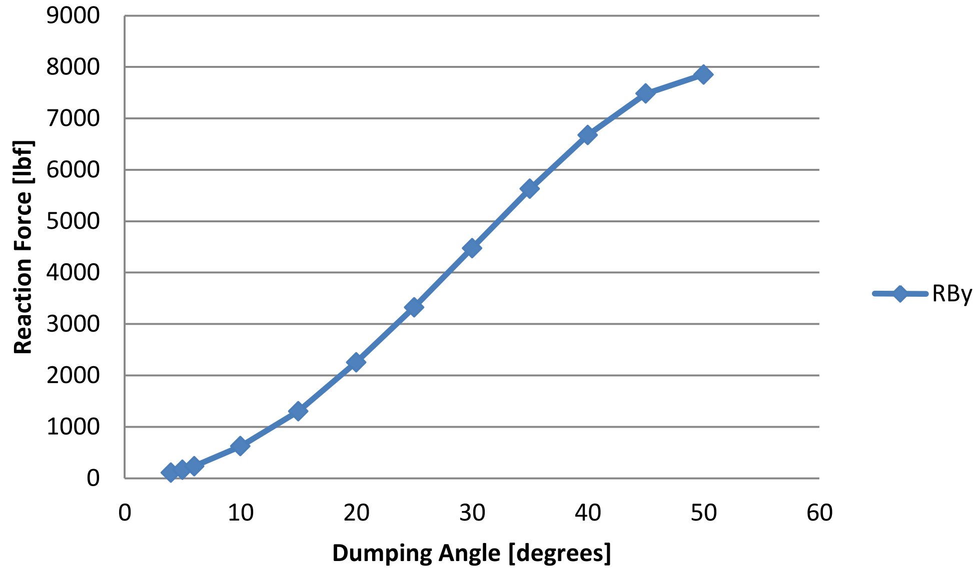


Figure 4: Reaction Force at Point B as a Function of Dumping Angle - Design 1

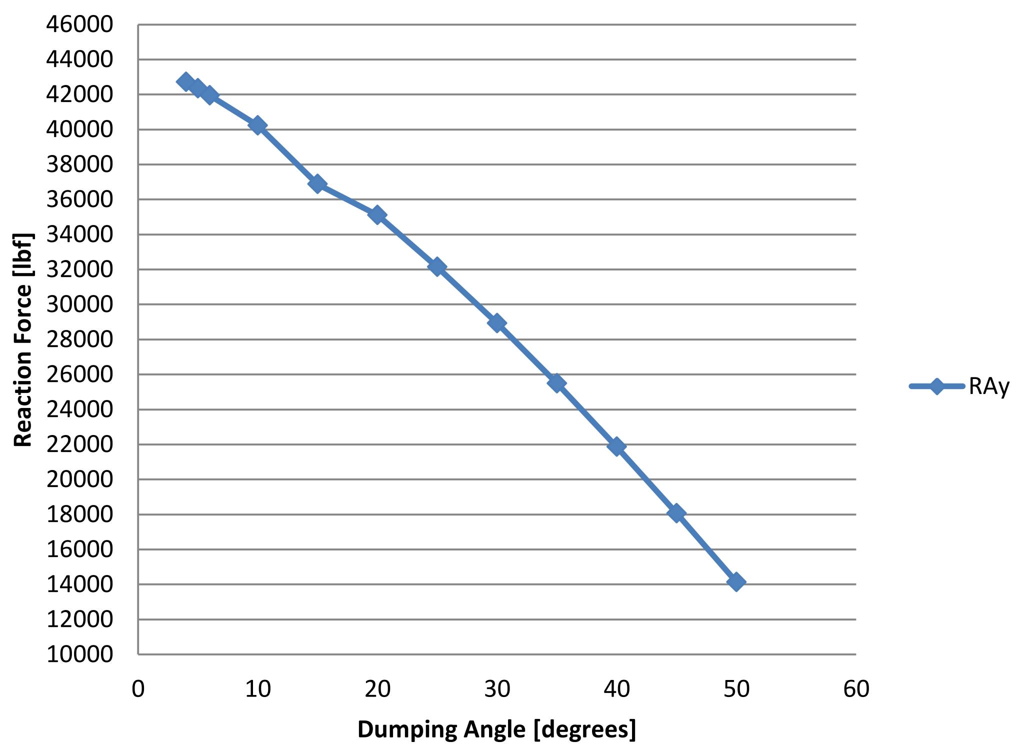


Figure 5: Reaction Force at Point A as a Function of Dumping Angle - Design 1

As it can be seen from the plots, the reaction forces at points A and B essentially experience opposite trends. The force at point A decreases as a function of the dumping angle while the reaction force at point B increases. The reason is that as the box is lifted, the centroid of mass shifts closer to the hinge. Therefore, the reaction force point A will decrease while the reaction force at point B increases to compensate for the load shift.

Once the reaction forces were known, the force experienced by hoist was determined. This force is directed along the line of action as shown in Figure 2. The force was calculated by determining the internal force experienced along the line of action.

The force along the line of action is essentially the load experienced by the hoist. The force along the line of action decreases as the hoist continues to lift as shown in Figure 6. This is largely due to the fact that the centroid of the mass shifts away from the hoist as the dumping angle getting larger.

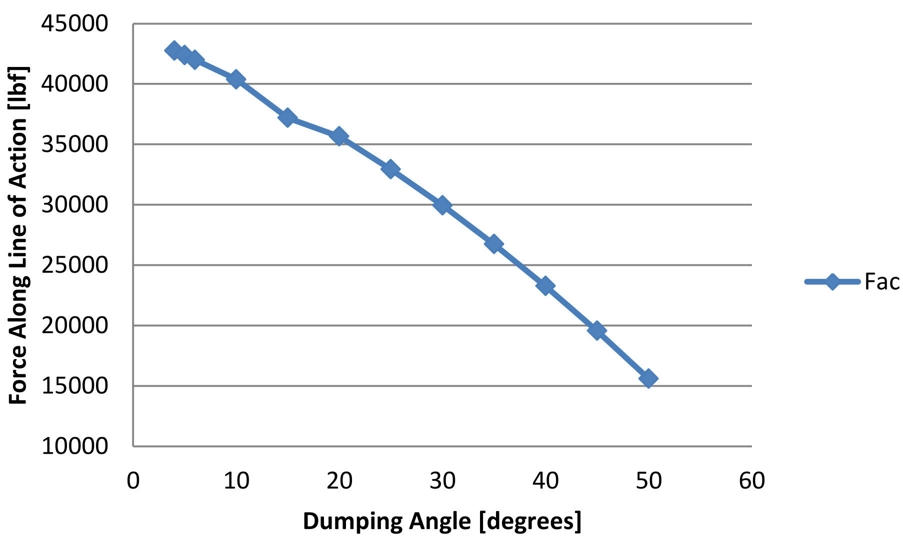


Figure 6: Force Along of Line of Action - Design 1

As a result, the forces experienced by the hoist members were determined. They were determined by simplifying the hoist as a simple truss structure. Figure 7 shows the illustration of the hoist as a simplified truss structure.

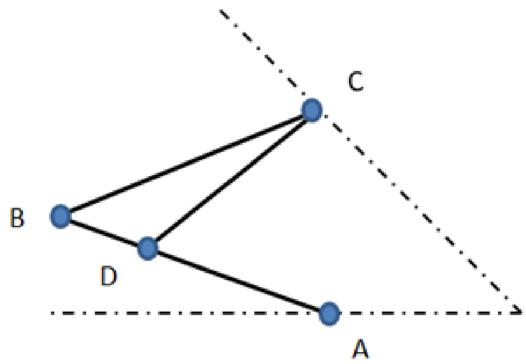


Figure 7: Simplified Truss Structure of Hoist

As the dumping angle increase, the force experienced by the top member of the hoist decreases. This phenomenon can be observed in Figure 8.

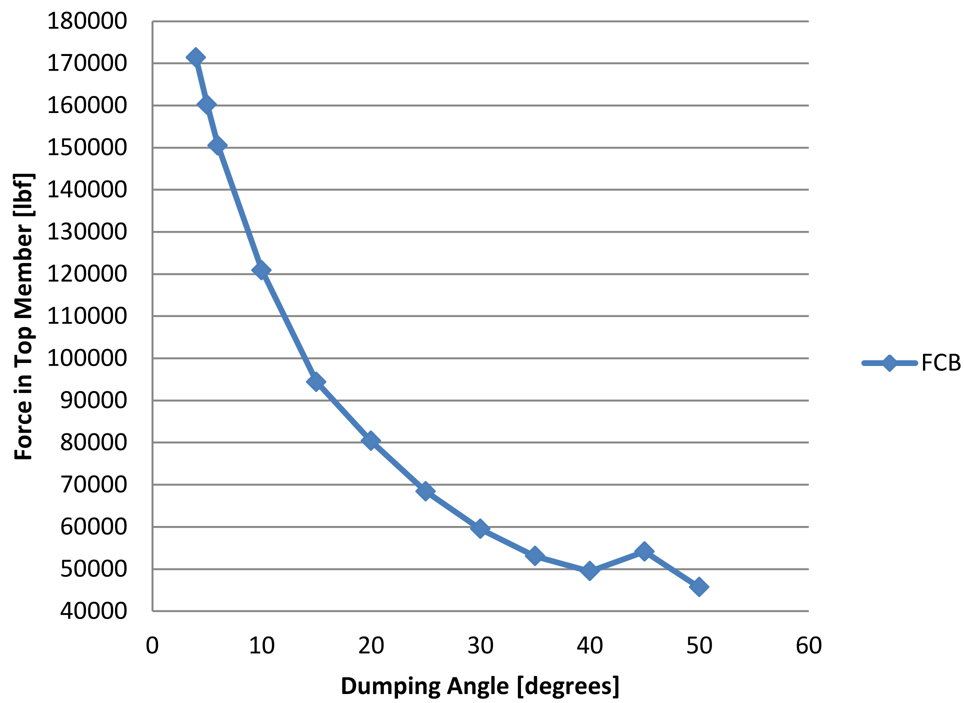


Figure 8: Force in Top Member as a Function of the Dumping Angle - Design 1

Figure 9 displays a unique behavior in regards to the force experienced by the lower section of the lower member (section DA). From the plot, it is observed that the member experiences a decrease in force followed by a sudden increase at approximately 20°. The reason for this behavior is not clearly seen in the graph. However through the detailed calculations, it was observed that the lower member is initially in compression and changes to tension after reaching a certain dumping angle. Therefore, the compressive force experienced by the member decreases with the increase in the dumping angle but once the dumping angle reaches approximately 20°, the member is in tension and the force in the member increases.

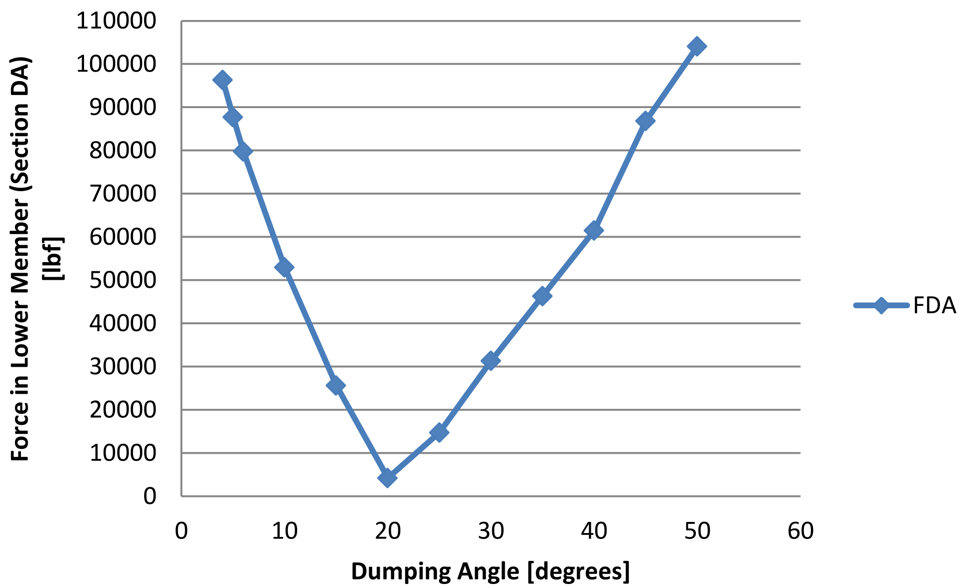


Figure 9: Force is Lower Member (Section DA) as a Function of Dumping Angle - Design 1

The upper section of the lower member essentially behaves as a two-force member, similar to that of the behavior of the hoist's upper member. In general the force experienced by section BD (upper section) of the lower member decreases with the increase in the dumping angle. However, the force jumps as the dumping angle becomes closer to 50°. This phenomenon can be explained by the hoist being incapable of safely lifting to the dumping angle of 50°. In other words, the member is being "stretched" at the larger dumping angles. Therefore, an increase in force is seen. Figure 10 displays the force experienced in the upper section (section BD) of the hoist as a function of the dumping angle.

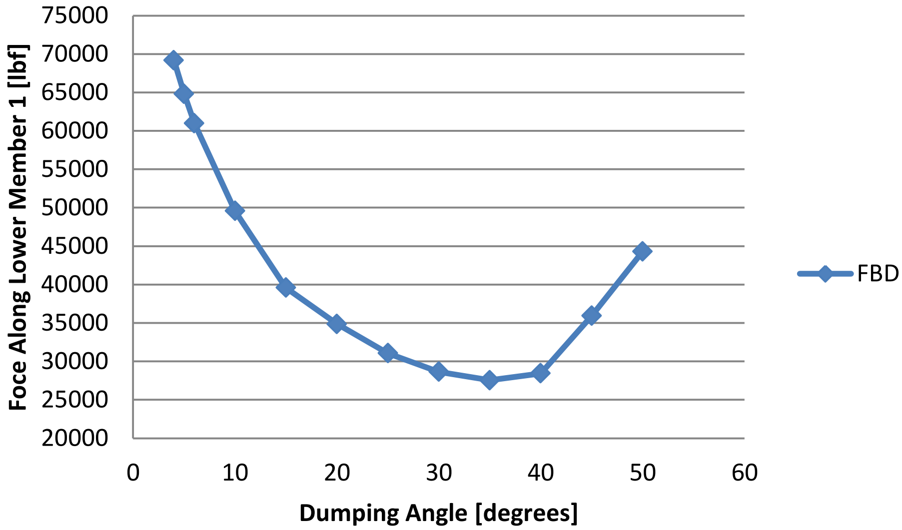


Figure 10: Force is Lower Member (Section BD) as a Function of Dumping Angle - Design 1

Although it is not as severe, a hint of the same phenomenon also occurs on the upper member. It can be seen in the previously shown Figure 8. The upper member experiences an increase in force as the dumping angle of 50° is approached. The reasoning for this is similar to the explanation for the bottom member.

The force experienced by the cylinder decreases with the increasing dumping angle. However, the force in the cylinder jumps towards the end of the lifting cycle. Similarly, it is due to the fact that hoist cannot reach the maximum dumping angle. Therefore, the members experience an increase in force shown in Figure 11.

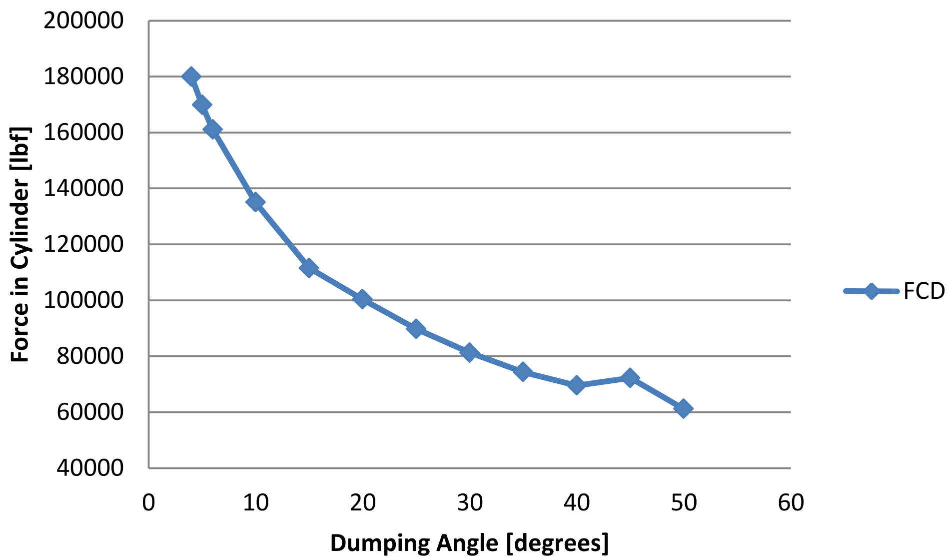


Figure 11: Force is Cylinder as a Function of Dumping Angle - Design 1

The final calculation for Design 1 was to determine the angle at which the maximum bending moment occurs on the lower member. This step is not necessary for the upper member and the cylinder because they are treated as two-force members. The maximum bending moment was simply calculated by treating the lower member as beam pinned at both ends. Next, the force exerted by the cylinder was applied to the lower member. This process was done for the entire range of incrementing dumping angle. The purpose is to determine at which dumping angle that the lower member experiences the maximum bending moment. The results of this process are presented in Figure 12. From the graph, it can be concluded that the maximum bending moment occurs at approximately 10°.

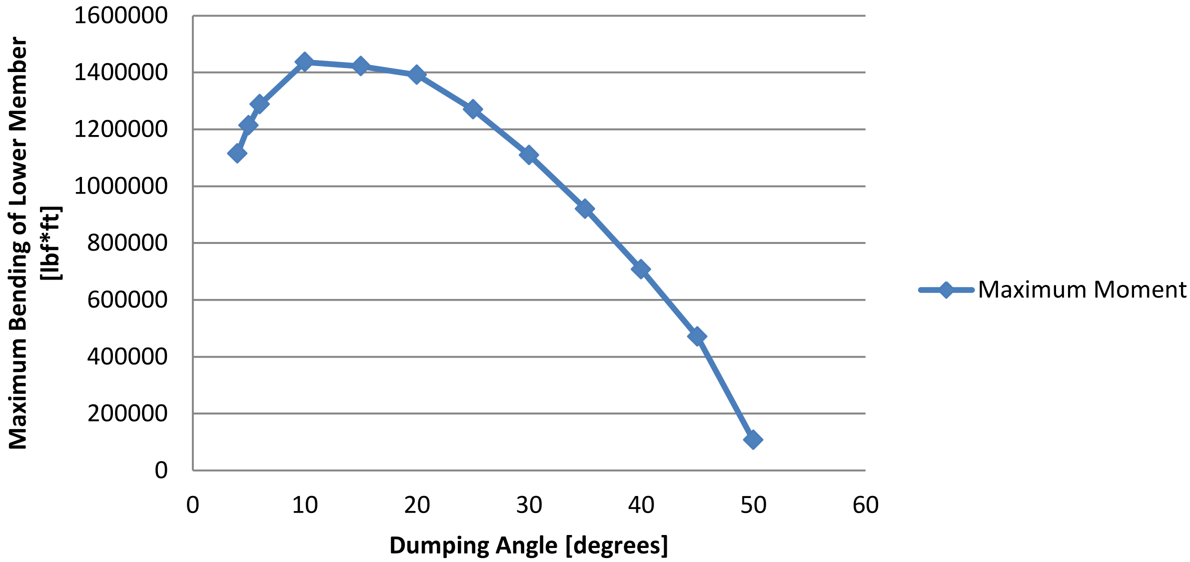


Figure 12: Maximum Bending Moment Experienced by Lower Member - Design 1

### B-2.2 Design 2 Analysis

Design 2 encompasses lower and upper members of different lengths and also different pin-to-pin distances from the original design. The lower member length is 81.91" and the upper member is 59.91". The distance between the hinges to lower mount of the hoist (horizontal pin-to-pin) has been also changed to 125" and the pin-to-pin along the box is kept the same as it cannot be compromised.

A unique feature of Design 2 is that the line of action that connects the hoist top mounting point to the bottom mounting point changes in direction as the dumping angle increases. This is illustrated by the schematic on Figure 13.

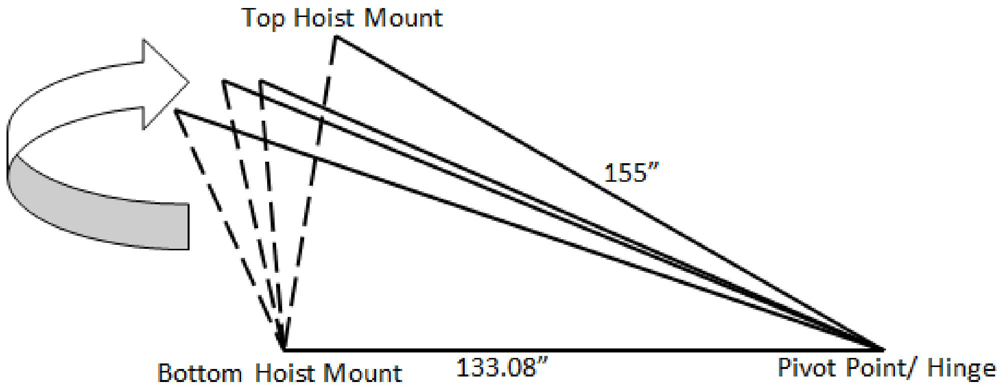


Figure 13: Varying Line of Action for Design 2

The reason for the change of the line of action is due to the fact that the horizontal pin-to-pin distance was reduced. From a to-scale drawing, it was determined that the line of action passes the vertical at a dumping angle of 30°. Therefore, Design 2 was analyzed using two different cases. These cases correlate to a dumping angle less than 30° and also when the dumping angle is greater than 30°. Figure 14 and Figure 15 were generated to illustrate the two cases and to determine the external forces experienced by the system.

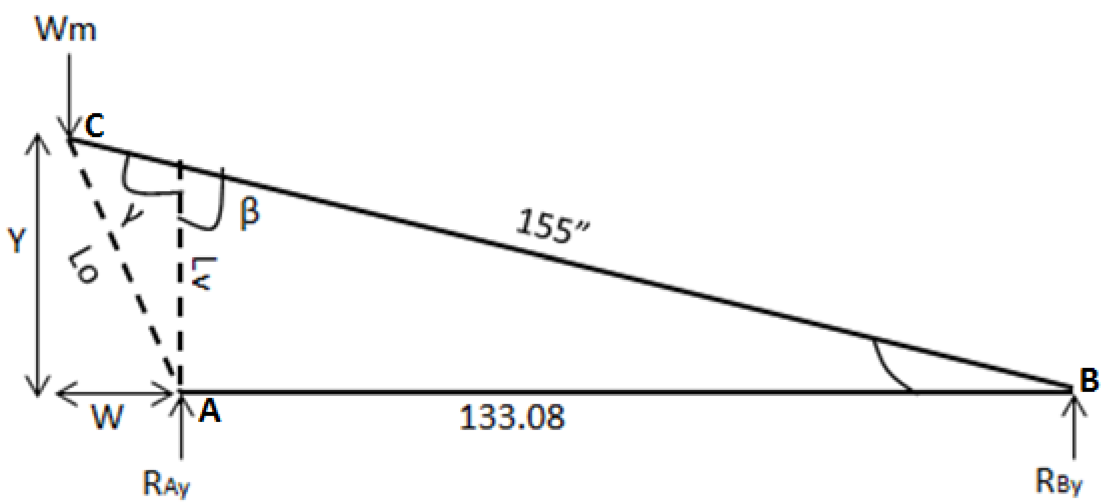


Figure 14: Free Body Diagram for External Forces - Design 2 Case 1

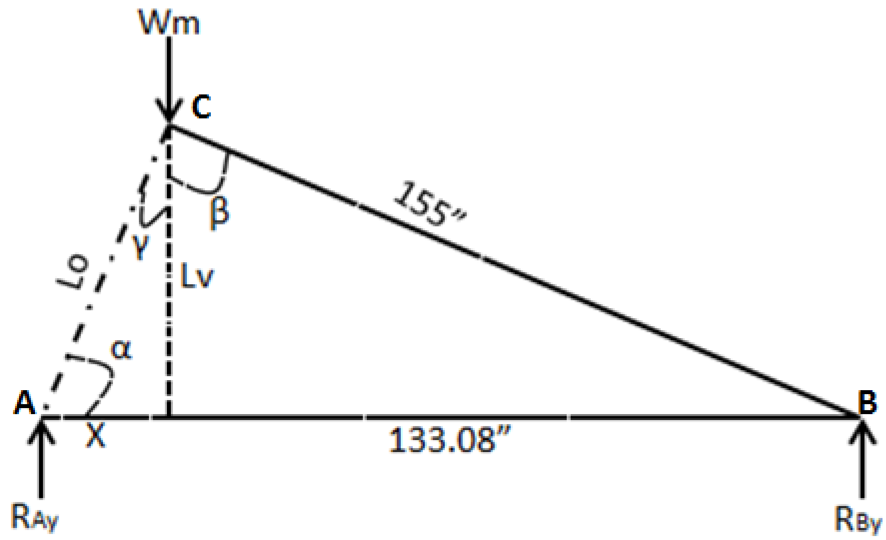


Figure 15: Free Body Diagram for External Forces - Design 2 Case 2

Using static equilibrium equations, the reaction forces for both cases was determined and plotted as shown in Figure 16 and Figure 17. Similarly to Design 1, the reaction force at point A decreases as the center of mass shifts closer to the pivot point or hinge.

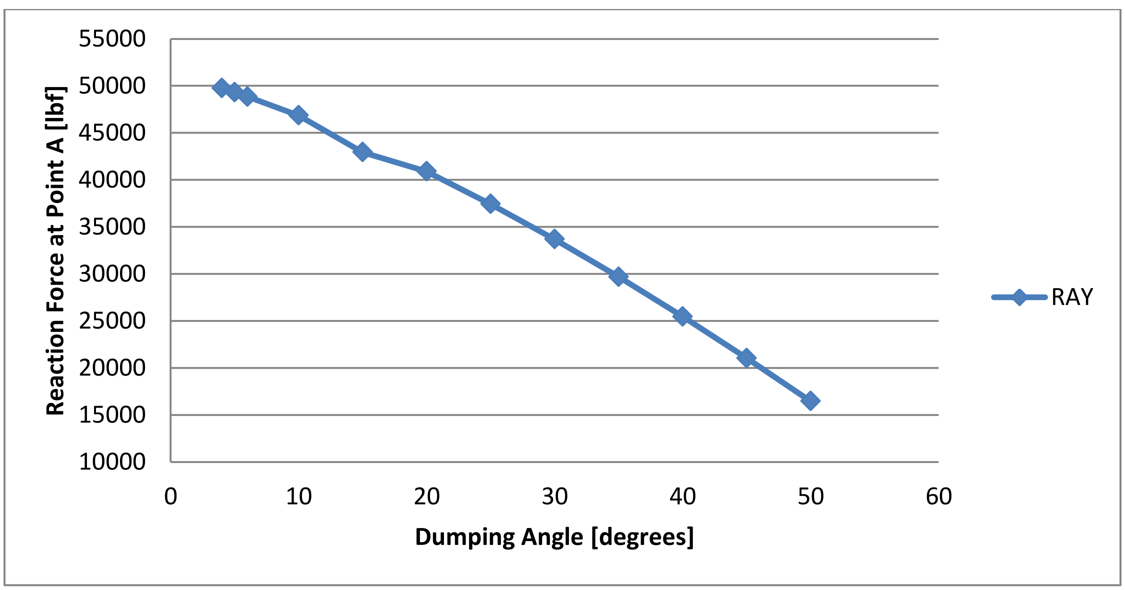


Figure 16: Reaction Force at Point A - Design 2

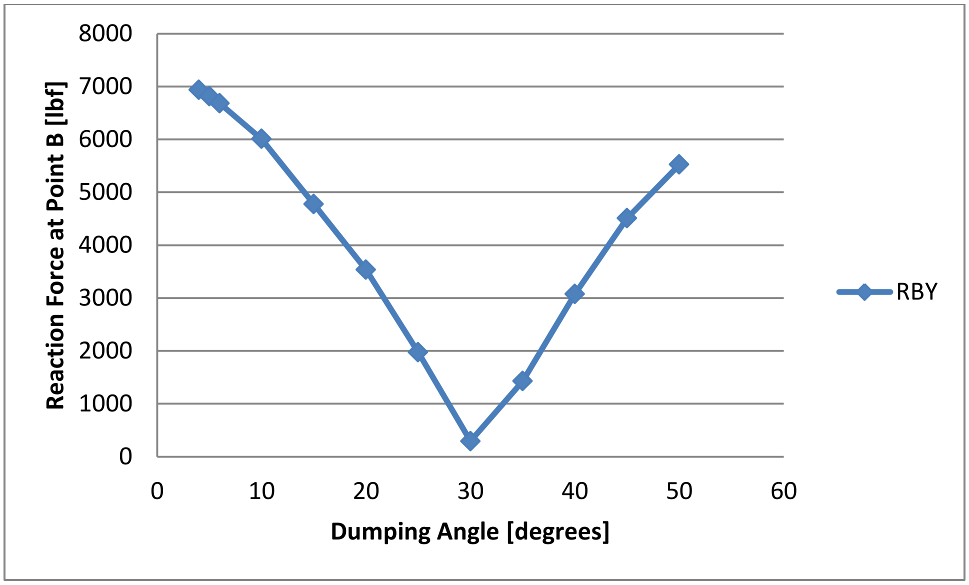


Figure 17: Reaction Force at Point B - Design 2

However, the force experienced by the hinge is not the same as for Design 1. It initially reduces and then increases after it passes a certain dumping angle. This is largely due to the fact that the line of action changes as a function of the dumping angle. To better explain this phenomenon, a phase called equilibrium state was established. The equilibrium state is reached when the line of action is collinear with the vertical line. The equilibrium state can be clearly seen in Figure 18.

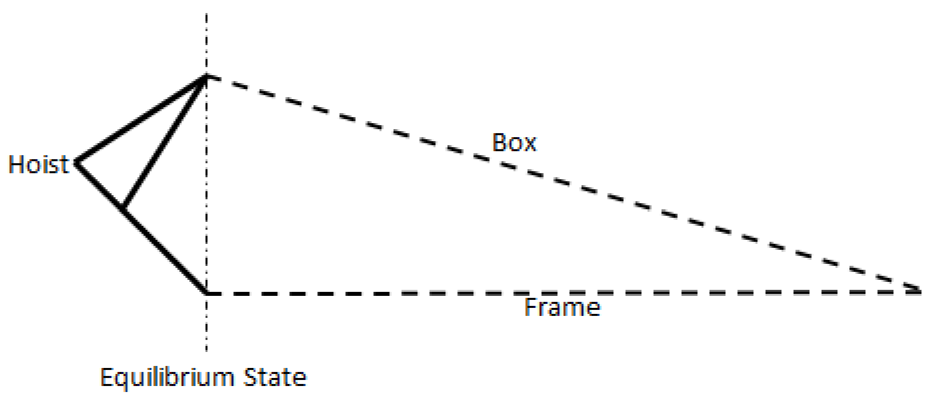


Figure 18: Established Equilibrium State for Design 2

As a result, as the hoist approaches the equilibrium state, the reaction force at point B decreases. As soon as the hoist passes the equilibrium state, the reaction force at point B increases.

Once the reaction forces of the system were determined, the force along the line of action was found. This force is what the hoist experiences. The line of action is represented as the dashed line in Figure 14 and Figure 15. The force along the line of action was determined using simple statics.

Figure 19 below shows the force along the line of action plotted as a function of the dumping angle. The trend of the force along the line of action is very similar to that of Design 1. However, it is important to note that the magnitude of this force is greater than it is in Design 1. This is due to the awkward position of the hoist in the first 30° of lift. The hoist experiences large forces before it passes the equilibrium state and decrease substantially after this point.

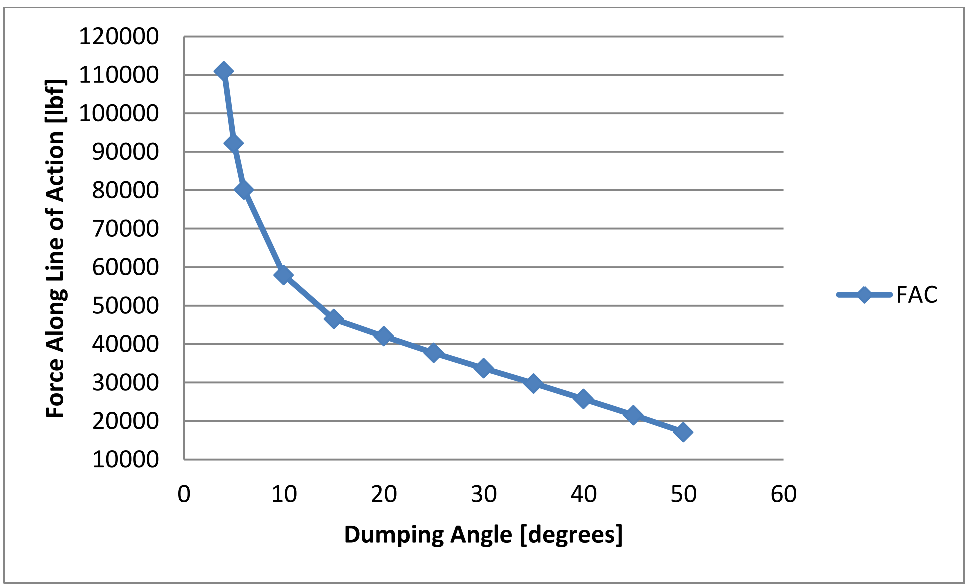


Figure 19: Force along Line of Action - Design 2

Now that the force experienced by the hoist was determined, the internal forces experienced by hoist members were computed. First, the hoist was assumed to be a simple truss structure. By applying the force along the line of action at the top of the hoist, the force in each member was calculated as a function of the dumping angle. Figure 20 illustrates design 2 treated as a simple truss structure.

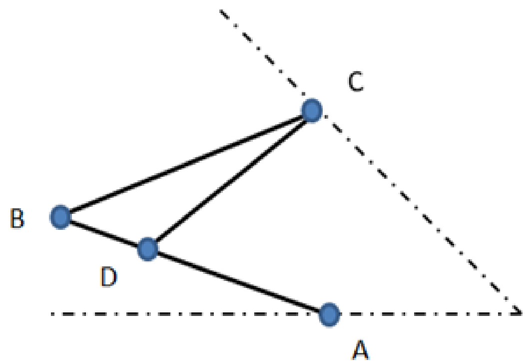


Figure 20: Simplified Truss Structure of Hoist

Figure 21 shows the force in the top member of the hoist as a function of the dumping angle.

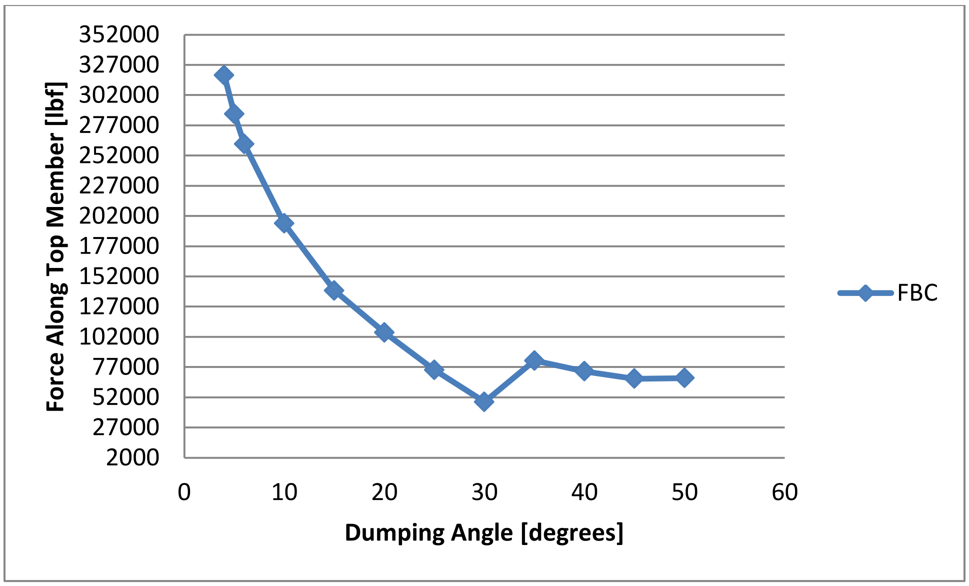


Figure 21: Force Along Top Member as a Function of Dumping Angle - Design 2

The force in the top member decreases as the dumping angle increases. This is very similar to the observation made in the first design. However, it is important to note that the increase in force seen in the plot at approximately 30° is due to the change in the hoist position. Contrary to Design 1, where the force jumps at the final stage of the lift, the sudden force increase in Design 2 happens because of the existence of the equilibrium state as discussed earlier. However, the general trend can be established; the force in the top member decreases as the dump angle increases.

Figure 22 represents the force experienced by the cylinder as a function of the dumping angle. The force on the cylinder decreases as the box is raised. The increase in force experienced at 30° is simply due to the hoist passing its equilibrium point.

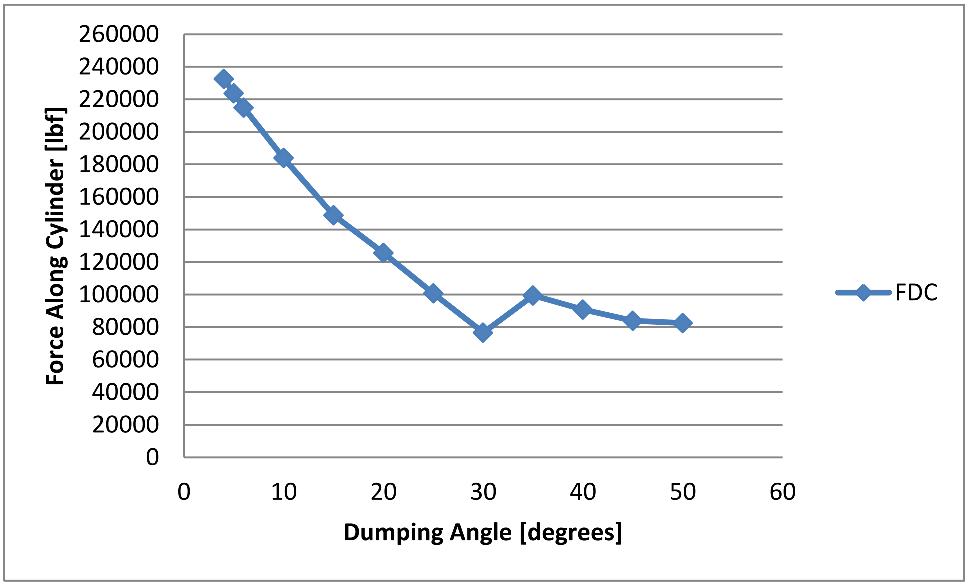


Figure 22: Force Along Cylinder as a Function of Dumping Angle - Design 2

The lower member is divided into two sections as shown in Figure 20. Similarly to Design 1, the lower member experiences a decrease in force followed by an increase. This is largely due to the fact that the lower member is initially in compression and then changes to tension. When the member is in compression the force decreases as dumping angle increases. Once the member is in tension however, the force increases. Figure 24 and Figure 25 show the force along the lower member of the hoist.

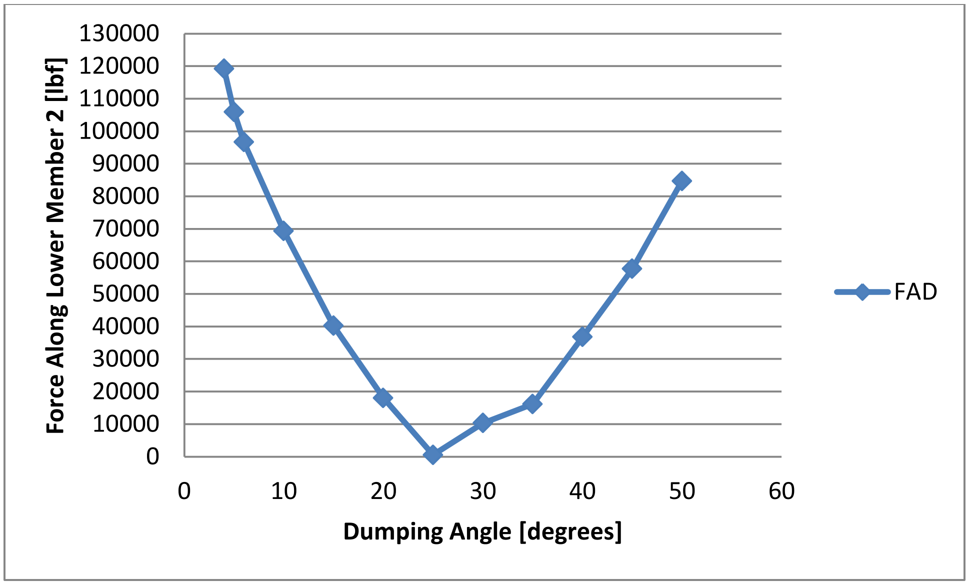


Figure 23: Force Along Lower Member (Section AD) as a Function of Dumping Angle - Design 2

Ideally the force in section DB should decrease with an increase in the dumping angle but since section DB and AD are the same member, a similar trend is seen in section DB as seen in DA previously.

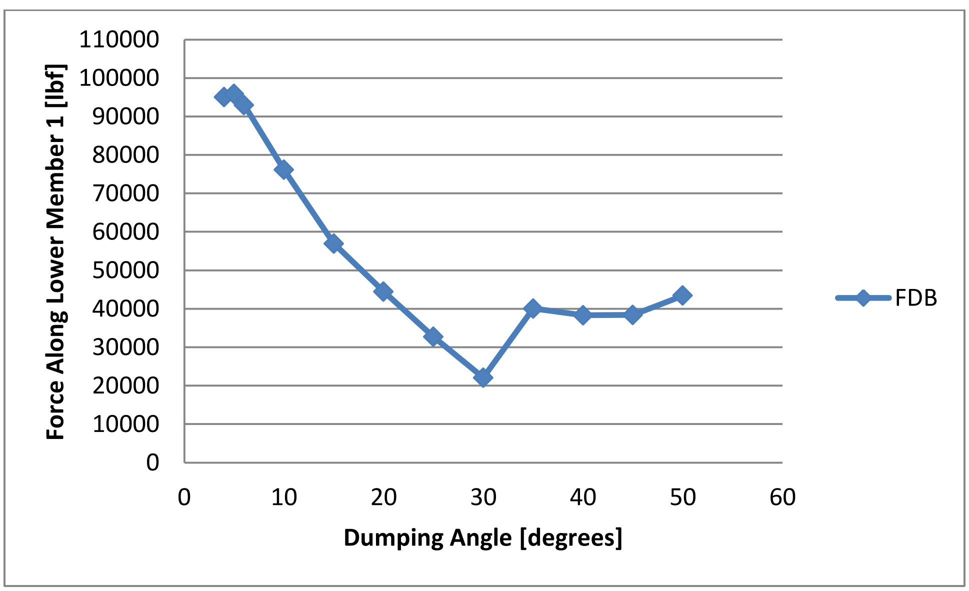


Figure 24: Force Along Lower Member (Section DB) as a Function of Dumping Angle - Design 2

The final calculation for Design 2 was determining the maximum bending moment in the lower member. This step is not necessary for the top member and the cylinder as they are two force members. The maximum bending moment was calculated by treating the lower member as a beam pinned at both ends. The force exerted by the cylinder was then applied to the lower member. This was done to determine at which dumping angle the lower member experiences the maximum bending moment.

Figure 25 displays the moment experienced by the lower member as a function of the dumping angle. From the graph we can conclude the maximum bending moment occurs approximately at 10˚.

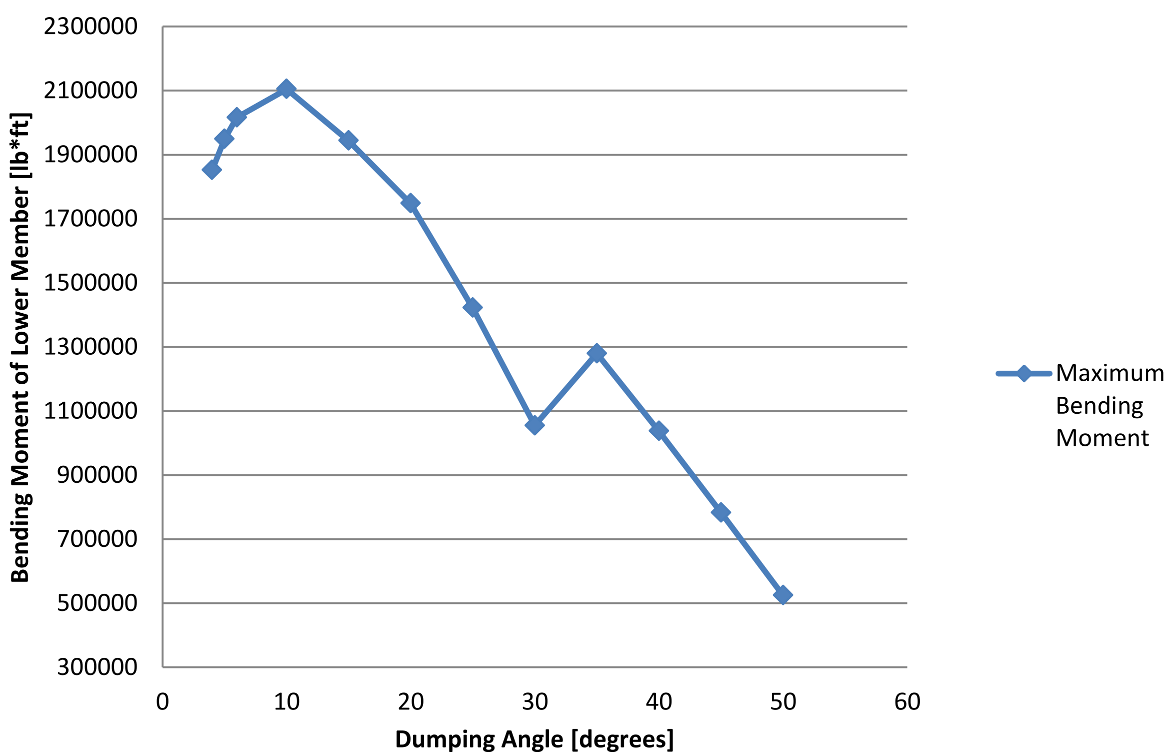


Figure 25: Maximum Bending Moment of Lowe Member - Design 2

### B-2.3 Conclusion

The maximum forces experienced by both of the designs occur at smaller angles. As a result, the critical dumping angle occurs in the first 10°. This key observation is used to further develop the components of the two designs. If the hoists are designed so that they are able to withstand the force experienced during the initial lift of the box, they will not fail at any point after that.

Hence, the forces experienced in the members of both designs were calculated at a dumping angle of 0° when the hoists are fully compacted. The results for both designs are tabulated in Table I and II below. The detail of the calculation can be found in section B-3. Maximum bending moment occurs at 10° for both design 1& 2.

TABLE I: FORCES EXPERIENCED AT 0 DEGREE OF DUMP ANGLE - DESIGN 1

| **Design 1** | **Lower Member** | | **Cylinder** | **Top Member** |
|---|---|---|---|---|
| Dumping Angle | FDA [lbs] | FBD [lbs] | FCD [lbs] | FCB [lbs] |
| **0** | -156,175.57 | -156,175.57 | **-161,089.33** | **156,389.80** |

TABLE II: FORCES EXPERIENCED AT 0 DEGREE OF DUMP ANGLE - DESIGN 2

| **Design 2** | **Lower Member** | | **Cylinder** | **Top Member** |
|---|---|---|---|---|
| Dumping Angle | FDA [lbs] | FBD [lbs] | FCD [lbs] | FCB [lbs] |
| **0** | -48585.57 | -59,817.80 | -183,706.80 | 177,891.07 |

## B-3 Details of All Calculations

As the dumping angle increases, the centroid of the mass placed on the hoist will not be in the same location. Therefore to determine the impact of the mass on the hoist, the first step was to find the mass placed on the hoist as a function of the dumping angle. In order to calculate the equivalent weight, a SolidWorks model of the load placed on the box was created and divided up into 4 different cross sections.

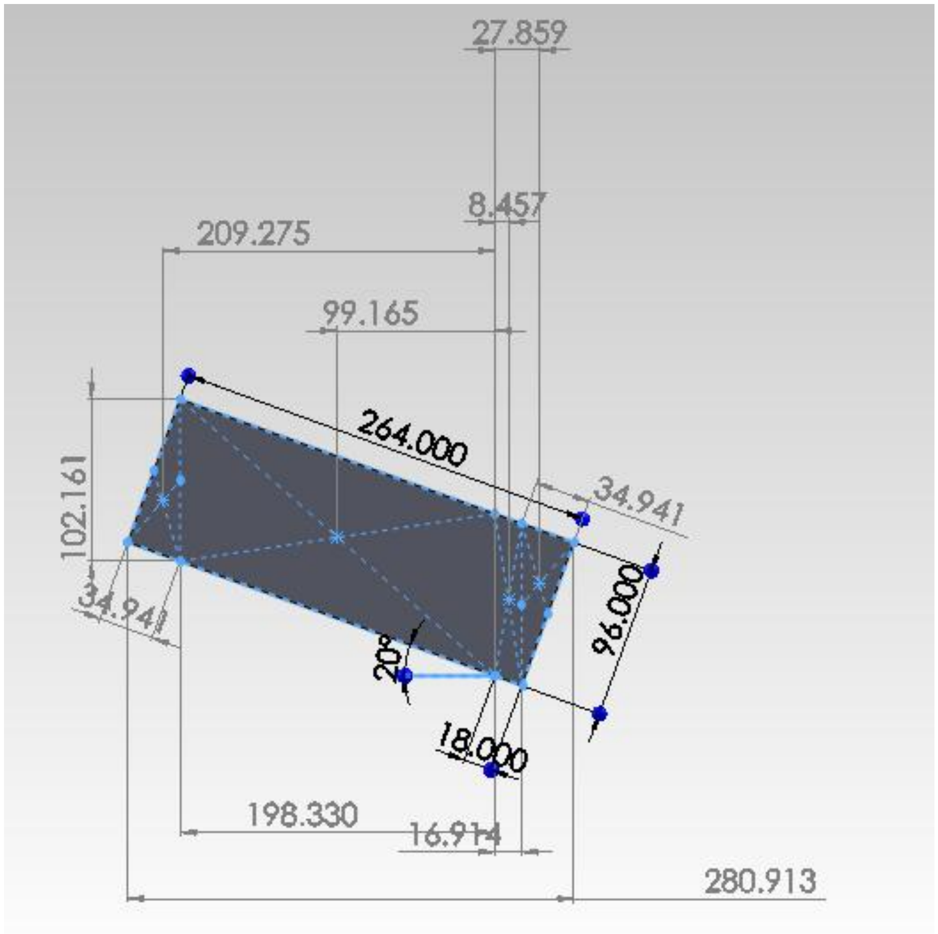


Figure 26: SolidWorks Model Used to Find Load on Hoist in Terms of Dumping Angle

Essentially the solid bar is an equivalent depiction of the 60 000 pounds placed on the hoist. As the box is lifted higher by the hoist; the center of mass of the box shifts closer to the pivot point. As it can be seen in Figure 26, the mass is divided up into two triangles and two rectangles. As we increase the angle, the dimensions of all the sections change as well as the centroid changes.

The first step was to calculate the density of the mass by using the area. This was done by:

$$Density = \frac{Total\ Mass}{Area\ of\ Box} = \frac{Total\ Mass}{Length\ of\ Box * Height\ of\ Box} = \frac{60000\ lbs}{264*69} = 2.367 lbs/in^2$$

As mentioned previously, the mass applied on the hoist is divided into four sections. Therefore each section exhibits a force in accordance to the area. As a result, the dimension of each section were found to calculate the area associated with each section which in turn was used to calculate the force in accordance to each section. For example, let us consider a case of dump angle equal to 20˚.

The figure below shows each section labeled:

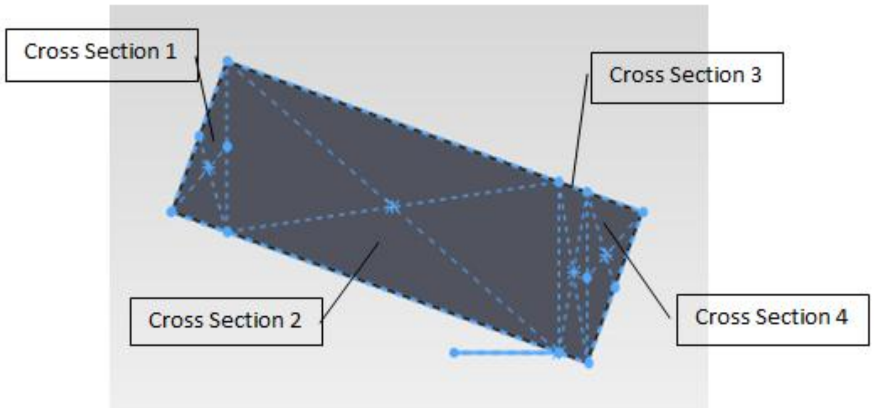


Figure 27: Cross Sections Shown of Equivalent Load

Considering Figure 26, we can find the area of each corresponding section from the SolidWorks model. As well we can directly obtain the distance of the centroid of each section from the pivot point. This information is tabulated in the table below.

TABLE III: AREA OF CROSS SECTION AT DUMP ANGLE OF 20 DEGREES°

| Cross Section | Dimensions [in] | Area [in2] | Distance From Fulcrum [in] |
|---|---|---|---|
| **1** | B=34.961; H= 96 | ½ *B*H = 1678.12 | 202.98 |
| **2** | L=102.161; W=198.33 | L*W = 20261.591 | 99.17 |
| **3** | L=102.161; W=16.914 | L*W= 1727.95 | -8.46 |
| **4** | B=34.961; H=96 | ½ *B*H = 1678.128 | -27.86 |

Now that we have obtained the area of each section, we can determine the force by simply multiplying the area with the density found previously.

TABLE IV: FORCE EXERTED BY THE DIFFERENT SECTIONS OF BOX

| Cross Section | Force in Each Section of the Represented Box [lbs] |
|---|---|
| **1** | Area*2.37lbs/in² = 3972.13 |
| **2** | Area*2.37lbs/in² = 47959.19 |

| | |
|---|---|
| **3** | Area*2.37lbs/in² = 4090.06 |
| **4** | Area*2.37lbs/in² = 3972.13 |

Next the centroid of whole mass in accordance to the dumping angle can be found as:

$$Centroid = \frac{\sum F * Distance\ from\ Fulcrum}{Total\ Mass}$$

$$Centroid = \frac{\sum(3972.13 * 209.38) + (47959.19 * 99.17) + (4090.06 * -8.46) + (3972.13 * -27.86)}{60000}$$

$$\therefore\ Location\ of\ Centroid = 96.52"\ Along\ the\ Box\ from\ the\ Fulcrum$$

Essentially we have determined that the 60 000lb load has a new centroid which is at 96.52" along the box at a dumping angle of 20˚. Again this is due to the fact that the box is lifting a certain angle which shifts the centroid of the mass towards the fulcrum due to gravity. From the information obtained we can now determine the equivalent weight placed on the mounting point of the hoist.

The figure below shows a schematic which will aid in the explanation for finding the weight (Wm) placed on the hoist's mounting point to the box.

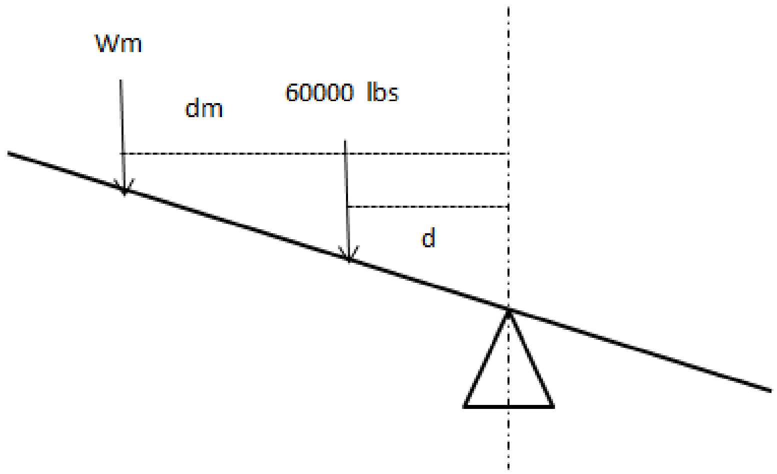


Figure 28: Schematic of Determining Force Experienced by Hoist as a Function of Dumping Angle

As shown in the figure above, Wm represents the equivalent weight placed on the hoist's mounting point as function of the dumping angle. Dm represents the distance of Wm from the pivot point. The same principles apply to the 60000 lbs load which is at a distance d from the pivot point. Distance d is the horizontal distance of the 60000 lbs load from the pivot point. This can be simply found by using trigonometry as follows:

$$d = \cos(20) * Location\ of\ Centriod\ Along\ Box$$

$$d = \cos(20) * 96.52" = 90.70"$$

As a result the weight Wm can be found as:

$$W \quad = \frac{d}{dm} * 60000 = \frac{90.70}{96.52} * 60000 = 37362.19$$

In a similar fashion, Table V was tabulated as shown for different values of the dumping angle.

TABLE V: SUMMARY FOR CALCULATIONS TO DETERMINE FORCE APPLIED TO HOIST AS A FUNCTION OF DUMPING ANGLE

| Dump Angle = 4˚ | | | | | | | | |
|---|---|---|---|---|---|---|---|---|
| Distance | **[in]** | | | **Area [in²]** | **Force [lbs]** | **Centre of Gravity [in]** | **Force @ mounting point - vertical** | |
| **1** | 240.936 | 6.713 | 96 | 322.224 | 762.704208 | 110.354; left of fulcrum-horizontal | dm | 154.622428” |
| **2** | 119.352 | 96.234 | 238.704 | 22971.4407 | 54373.4002 | | Wm | 42821.8497 lb |
| **3** | -8.978 | 96.234 | 17.956 | 1727.9777 | 4090.12323 | 110.623; left of fulcrum-along the box | | |
| **4** | -20.188 | 6.713 | 96 | 322.224 | 762.704208 | | | |
| **Dump Angle = 5˚** | | | | | | | | |
| Distance | **[in]** | | | **Area [in²]** | **Force** | **Centre of Gravity** | **Force @ mounting point - vertical** | |
| **1** | 239.486 | 8.399 | 96 | 403.152 | 954.260784 | 109.363; left of fulcrum-horizontal | dm | 154.410178” |
| **2** | 118.348 | 96.367 | 236.697 | 22809.7798 | 53990.7488 | | Wm | 42495.7952 lb |
| **3** | -8.966 | 96.367 | 17.932 | 1728.05304 | 4090.30156 | 109.781; left of fulcrum-along the box | | |
| **4** | -20.72 | 8.399 | 96 | 403.152 | 954.260784 | | | |
| **Dump Angle = 6˚** | | | | | | | | |
| Distance | **[in]** | **[in]** | **[in]** | **Area [in²]** | **Force** | **Centre of Gravity** | **Force @ mounting point - vertical** | |
| **1** | 237.963 | 10.09 | 96 | 484.32 | 1146.38544 | 108.339; left of fulcrum-horizontal | dm | 154.150894” |
| **2** | 117.309 | 96.529 | 234.618 | 22647.4409 | 53606.4927 | | Wm | 42168.778 lb |
| **3** | -8.951 | 96.529 | 17.901 | 1727.96563 | 4090.09464 | 108.936; left of fulcrum-along the box | | |
| **4** | -21.246 | 10.09 | 96 | 484.32 | 1146.38544 | | | |
| **Dump Angle = 10˚** | | | | | | | | |
| Distance | **[in]** | **[in]** | **[in]** | **Area [in²]** | **Force** | **Centre of Gravity [in]** | **Force @ mounting point - vertical** | |

| | | | | | | | | |
|---|---|---|---|---|---|---|---|---|
| **1** | 231.149 | 16.927 | 96 | 812.496 | 1923.17803 | 103.914; left of fulcrum-horizontal | dm | 152.645202” |
| **2** | 112.796 | 97.481 | 225.592 | 21990.9338 | 52052.5402 | | Wm | 40845.2371 lb |
| **3** | -8.863 | 97.481 | 17.727 | 1728.04569 | 4090.28414 | 105.517; left of fulcrum-along the box | | |
| **4** | -23.283 | 16.927 | 96 | 812.496 | 1923.17803 | | | |
| **Dump Angle = 15˚** | | | | | | | | |
| Distance | **[in]** | **[in]** | **[in]** | **Area [in²]** | **Force** | **Centre of Gravity** | **Force @ mounting point - vertical** | |
| **1** | 221.053 | 25.723 | 96 | 1234.704 | 2922.54437 | 95.240; left of fulcrum-horizontal | dm | 149.718503” |
| **2** | 106.386 | 96.387 | 212.271 | 20460.1649 | 48429.2103 | | Wm | 38167.4777 lb |
| **3** | -8.693 | 96.387 | 17.387 | 1675.88077 | 3966.80978 | 98.599; left of fulcrum-along the box | | |
| **4** | -25.669 | 16.927 | 96 | 812.496 | 1923.17803 | | | |
| **Dump Angle = 20˚** | | | | | | | | |
| Distance | **[in]** | **[in]** | **[in]** | **Area [in²]** | **Force** | **Centre of Gravity** | **Force @ mounting point - vertical** | |
| **1** | 209.275 | 34.961 | 96 | 1678.128 | 3972.12898 | 90.698; left of fulcrum-horizontal | dm | 145.652356” |
| **2** | 99.165 | 102.161 | 198.33 | 20261.5911 | 47959.1862 | 96.519; left of fulcrum-along the box | Wm | 37362.1886 lb |
| **3** | -8.457 | 102.161 | 16.914 | 1727.95115 | 4090.06038 | | | |
| **4** | -27.859 | 34.961 | 96 | 1678.128 | 3972.12898 | | | |
| **Dump Angle = 25˚** | | | | | | | | |
| Distance | **[in]** | **[in]** | **[in]** | **Area [in²]** | **Force** | **Centre of Gravity** | **Force @ mounting point - vertical** | |
| **1** | 195.904 | 44.766 | 96 | 2148.768 | 5086.13386 | 83.018; left of fulcrum-horizontal | dm | 140.477707” |
| **2** | 91.19 | 105.92 | 182.38 | 19318.4191 | 45726.6981 | 91.600; left of fulcrum- | Wm | 35458.2394 lb |

| | | | | | | | | |
|---|---|---|---|---|---|---|---|---|
| | | 4 | | | | along the box | | |
| **3** | -8.157 | 105.924 | 16.314 | 1728.04414 | 4090.28047 | | | |
| **4** | -29.837 | 44.766 | 96 | 2148.768 | 5086.13386 | | | |
| **Dump Angle = 30˚** | | | | | | | | |
| Distance | **[in]** | | | **Area [in²]** | **Force** | **Centre of Gravity** | **Force @ mounting point - vertical** | |
| **1** | 181.042 | 55.426 | 96 | 2660.448 | 6297.28042 | 74.713; left of fulcrum-horizontal | dm | 134.233938” |
| **2** | 82.521 | 110.851 | 165.042 | 18295.0707 | 43304.4324 | 86.272; left of fulcrum-along the box | Wm | 3395.4369 lb |
| **3** | -7.794 | 110.851 | 15.588 | 1727.94539 | 4090.04673 | | | |
| **4** | -31.588 | 55.426 | 96 | 2660.448 | 6297.28042 | | | |
| **Dump Angle = 35˚** | | | | | | | | |
| Distance | **[in]** | **[in]** | **[in]** | **Area [in²]** | **Force** | **Centre of Gravity** | **Force @ mounting point - vertical** | |
| **1** | 164.803 | 67.22 | 96 | 3226.56 | 7637.26752 | 65.840; left of fulcrum-horizontal | dm | 126.968567” |
| **2** | 73.224 | 117.194 | 146.448 | 17162.8269 | 40624.4113 | 80.376; left of fulcrum-along the box | Wm | 31113.1129 lb |
| **3** | -7.372 | 117.194 | 14.745 | 1728.02553 | 4090.23643 | | | |
| **4** | -33.099 | 67.22 | 96 | 3226.56 | 7637.26752 | | | |
| **Dump Angle = 40˚** | | | | | | | | |
| Distance | **[in]** | **[in]** | **[in]** | **Area [in²]** | **Force** | **Centre of Gravity** | **Force @ mounting point - vertical** | |
| **1** | 147.309 | 80.554 | 96 | 3866.592 | 9152.22326 | 56.465; left of fulcrum-horizontal | dm | 118.736889” |
| **2** | 63.37 | 125.319 | 126.739 | 15882.8047 | 37594.5988 | 73.710; left of fulcrum-along the box | Wm | 28533.0404 lb |

| | | | | | | | | |
|---|---|---|---|---|---|---|---|---|
| **3** | -6.894 | 125.319 | 13.789 | 1728.02369 | 4090.23208 | | | |
| **4** | -34.358 | 80.554 | 96 | 3866.592 | 9152.22326 | | | |
| **Dump Angle = 45°** | | | | | | | | |
| Distance | **[in]** | **[in]** | **[in]** | **Area [in²]** | **Force** | **Centre of Gravity** | **Force @ mounting point - vertical** | |
| **1** | 128.693 | 96 | 96 | 4608 | 10907.136 | 46.661; left of fulcrum-horizontal | dm | 109.601551” |
| **2** | 53.033 | 135.765 | 106.066 | 14400.0505 | 34084.9195 | 65.988; left of fulcrum-along the box | Wm | 25543.8507 lb |
| **3** | -6.364 | 135.765 | 12.728 | 1728.01692 | 4090.21605 | | | |
| **4** | -35.355 | 96 | 96 | 4608 | 10907.136 | | | |
| **Dump Angle = 50°** | | | | | | | | |
| Distance | **[in]** | **[in]** | **[in]** | **Area [in²]** | **Force** | **Centre of Gravity** | **Force @ mounting point - vertical** | |
| **1** | 109.099 | 114.408 | 96 | 5491.584 | 12998.5793 | 36.501; left of fulcrum-horizontal | dm | 99.6320795” |
| **2** | 42.293 | 149.349 | 84.585 | 12632.6852 | 29901.5658 | 56.785; left of fulcrum-along the box | Wm | 21981.4439 lb |
| **3** | -5.785 | 149.349 | 11.57 | 1727.96793 | 4090.10009 | | | |
| **4** | -36.084 | 114.408 | 96 | 5491.584 | 12998.5793 | | | |

## B-3.1 Forces Analysis of 3D Models

As the force experienced by the hoist was known in terms of dumping angle, the forces experienced by the two redesigned hoists was determined. The purpose of the force analysis is that it will serve as a guide for both models when performing FEAs in SolidWorks. In other words, the force analysis will be used to assure that hoist members will not fail under determined loads. Therefore the hoist will be designed to withstand the determined loads which will influence material selection and designs on hoist members.

The following sections contain force analysis on both 3D models perused for the hoist re-design.

### B-3.1.1 Design One

Design one encompasses both upper and lower members of equivalent length (66”) and keeping the same pin-to-pin distances as the original design.

### B-3.1.2 External Force Analysis

In order to determine the forces experienced by the members of the hoist, the first step was to determine the external forces. Keep in mind the value of Wm found previously is not necessarily the load experienced by the hoist as some of Wm will dissipate to the hinge (pivot point). Figure 29 shows the free body diagram of the entire system. The dashed line in the figure represents the line of action of the force experienced by the hoist. Essentially, the top of the hoist is attached at point C and the bottom is attached to point A. The force along the line of action will effectively be the force experienced by the hoist.

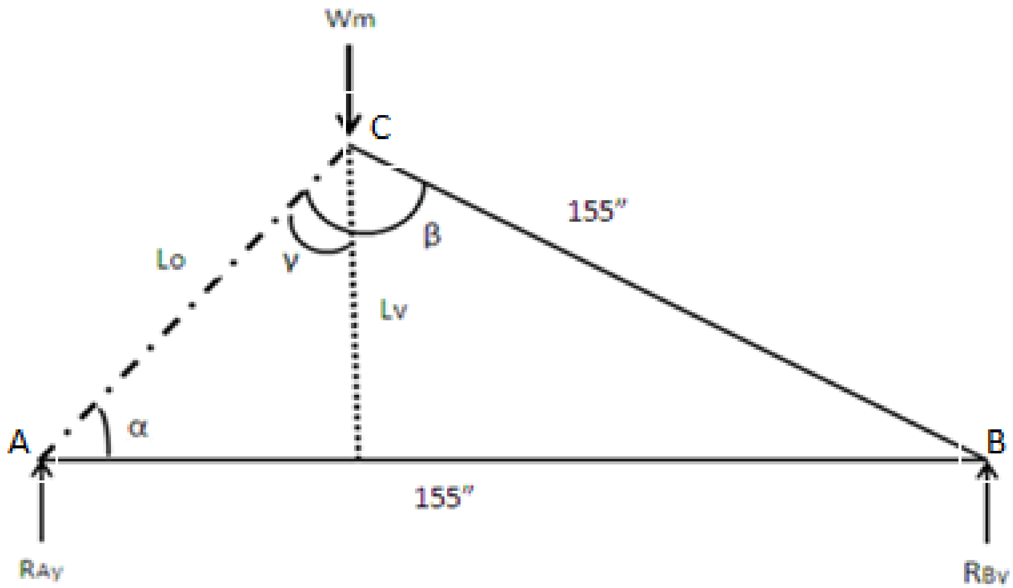


Figure 29: External Forces FBD - Design 1

The table below shows the results of the external forces as well as parameters used in the calculations. In addition a sample calculation is provided following the table to illustrate how the values in the table are obtained.

TABLE VI: SUMMARY OF REACTION FORCES - DESIGN 1

| D Angle [degrees] | $W_M$ [lbf] | $R_{By}$ [lbf] | $R_{Ay}$ [lbf] | α [°] | β [°] | γ [°] | Lo [in] | Lv [in] |
|---|---|---|---|---|---|---|---|---|
| 4 | 42821.85 | 104.311 | 42717.53 | 88 | 88 | 2 | 10.81 | 10.81 |
| 5 | 42495.8 | 161.70 | 42334.08 | 87.5 | 87.5 | 2.5 | 13.52 | 13.50 |
| 6 | 42168.78 | 231.00 | 41937.77 | 87 | 87 | 3 | 16.22 | 16.20 |
| 10 | 40845.24 | 620.53 | 40224.70 | 85 | 85 | 5 | 27.01 | 26.91 |
| 15 | 38167.48 | 1300.52 | 36866.95 | 82.5 | 82.5 | 7.5 | 40.46 | 40.11 |
| 20 | 37362.19 | 2253.21 | 35108.97 | 80 | 80 | 10 | 53.83 | 53.01 |
| 25 | 35458.24 | 3322.16 | 32136.07 | 77.5 | 77.5 | 12.5 | 67.09 | 65.50 |
| 30 | 33395.44 | 4474.14 | 28921.29 | 75 | 75 | 15 | 80.23 | 77.50 |
| 35 | 31113.11 | 5626.74 | 25486.37 | 72.5 | 72.5 | 17.5 | 93.21 | 88.90 |
| 40 | 28533.04 | 6675.46 | 21857.57 | 70 | 70 | 20 | 106.02 | 99.63 |
| 45 | 25543.85 | 7481.62 | 18062.23 | 67.5 | 67.5 | 22.5 | 118.63 | 109.60 |
| 50 | 21981.44 | 7852.04 | 14129.39 | 65 | 65 | 25 | 131.01 | 118.73 |

***Sample Calculation:***

First we can calculate both Lo and Lv as follows:

$$Lv = 155 * \sin(20) = 53.01"$$

$$Using\ cosine\ law: Lo = acos\left(155^2 + 155^2 - (2 * 155 * 155 * \cos(20))\right) = 53.83"$$

Also all other angles can be found as follows:

$$\alpha = \text{acos}((155^2 + 53.83^2 - 155^2)\,/(2 * 53.83 * 155)) = 80°$$

$$\beta = \text{acos}((155^2 + 53.83^2 - 155^2)\,/(2 * 53.83 * 155)) = 80° = \alpha$$

$$\gamma = 180 - 90 - \alpha = 10°$$

To find the external forces, a moment is taken about point A and therefore:

$$M_A = 0\,;\ (R_{By} * 155) - (W_m * (\sin(\gamma) * Lo)) = 0$$

$$\therefore R_{By} = \frac{\text{W}_M * \sin(\gamma) * Lo}{155}$$

$$\therefore R_{Ay} = W_m - R_{By}$$

Following the calculation of the external forces, the force along the line of action was determined. It is important to note that the force along the line of action is essentially the fore experienced by the hoist. This line of action is represented by the dashed line in Figure 29.

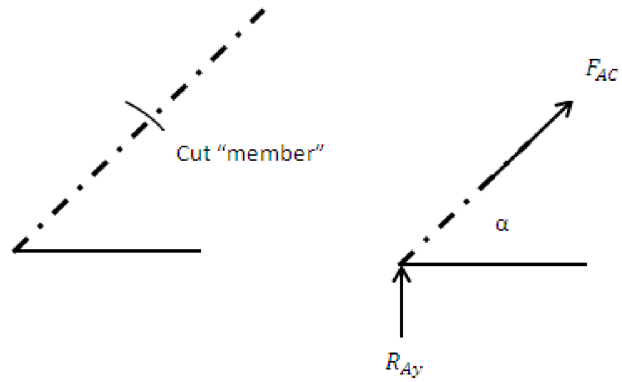


Therefore:

$$F_{AC} = \frac{R_{Ay}}{\sin(\alpha)}$$

For all other dumping angles, the force along the line of action was found as displayed in Table VII.

TABLE VII: SUMMARY OF FORCE A LONG LINE OF ACTION (FORCE EXPERIENCED BY HOIST)

| D Angle [°] | $F_{AC}$ [lbf] | $F_{ACy}$ [lbf] | $F_{ACx}$ [lbf] |
|---|---|---|---|
| 4 | -42743.58 | -42717.5 | -1491.73 |
| 5 | -42374.42 | -42334.1 | -1848.35 |
| 6 | -41995.33 | -41937.8 | -2197.87 |
| 10 | -40378.36 | -40224.7 | -3519.21 |
| 15 | -37185.08 | -36867 | -4853.63 |
| 20 | -35650.59 | -35109 | -6190.66 |
| 25 | -32916.33 | -32136.1 | -7124.4 |
| 30 | -29941.53 | -28921.3 | -7749.44 |
| 35 | -26723.2 | -25486.4 | -8035.82 |
| 40 | -23260.35 | -21857.6 | -7955.51 |
| 45 | -19550.42 | -18062.2 | -7481.62 |
| 50 | -15590.07 | -14129.4 | -6588.65 |

As the force along the line of action was known, it was applied to the hoist and the force experienced by the members was calculated. A simplified truss equivalent of the hoist can be seen below in Figure 30.

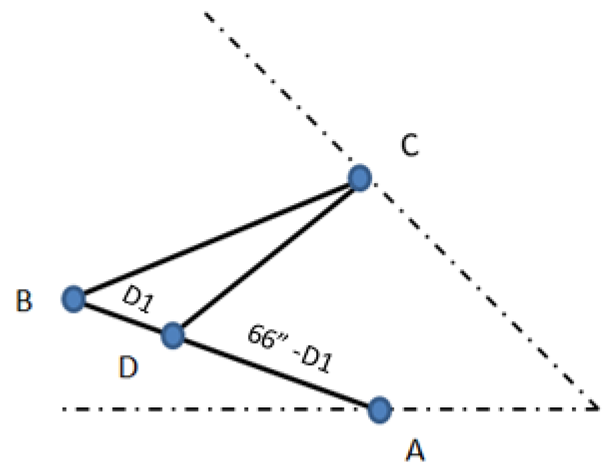


Figure 30: Simplified Truss Representation of Hoist

The force along the line of action can be seen in Figure 31 to better understand the point of application of the fore.

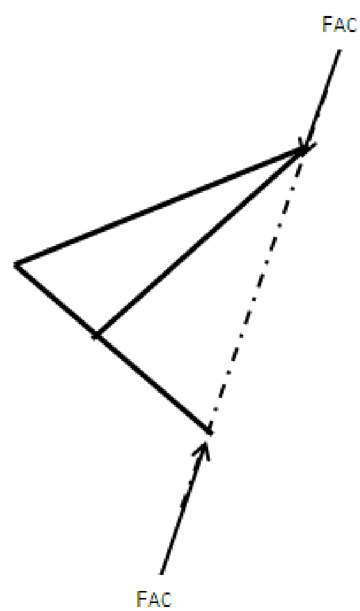


Figure 31: Application of Force Experienced by the Hoist

### B-3.1.3 Internal Force Analysis

Now the forces in each member was found starting at point C as shown in figure 5.

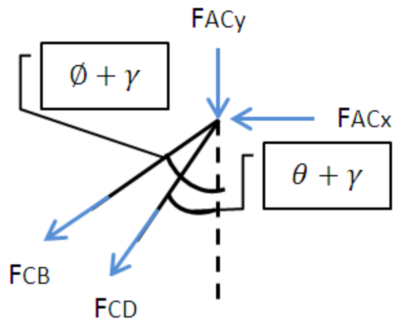


$$\sum F_y = 0;\ -\cos(\theta+\gamma) * F_{CD} - \cos(\theta+\gamma) * F_{CB} - F_{ACy} = 0$$

$$\sum F_x = 0;\ -\sin(\theta+\gamma) * F_{CD} - \sin(\theta+\gamma) * F_{CB} - F_{ACx} = 0$$

These two equations were solved simultaneously to obtain values for both $F_{CB}$ &$F_{CD}$. This was achieved using a simple matrix formulation as shown below:

$$\begin{matrix} -\cos(\theta+\gamma) & -\cos(\emptyset+\gamma) \\ -\sin(\theta+\gamma) & -\sin(\emptyset+\gamma) \end{matrix} * \begin{matrix} F_{CD} \\ F_{CB} \end{matrix} = \begin{matrix} F_{ACy} \\ F_{ACx} \end{matrix}$$

Next point B was chosen to solve for the force in member BD as follows:

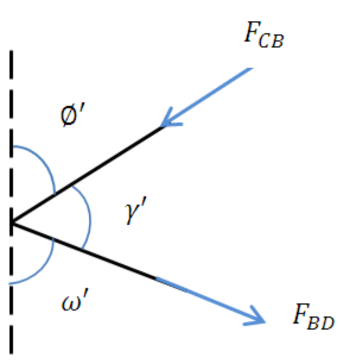

$$\sum F_y = 0; \; -\cos(\emptyset') * F_{CB} - \cos(\omega') * F_{BD} = 0 \quad \therefore F_{BD} = \frac{-\cos(\emptyset') * F_{CB}}{\cos(\omega')}$$

Finally, the force in member DA was calculated at point D as follows:

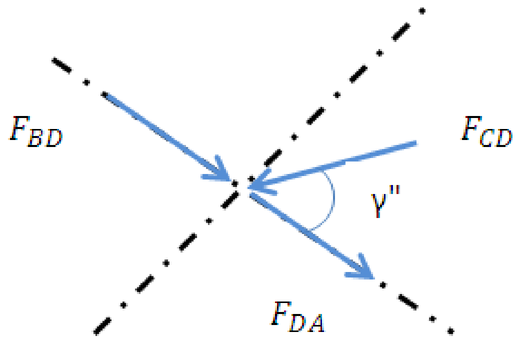


$$\sum F_y = 0; \; F_{BD} + F_{DA} - \cos(\gamma") * F_{CD} = 0$$

$$F_{DA} = \cos(\gamma") * F_{CD} - F_{BD}$$

In a similar fashion, all the forces in members of the hoist of design 1 were calculated. Table VIII shows the summary of the results.

TABLE VIII: SUMMARY OF FORCES IN HOIST MEMBERS AT DIFFERENT DUMPING ANGLES

| D Angle [°] | $F_{DA}$ [lbf] | $F_{BD}$ [lbf] | $F_{CD}$ [lbf] | $F_{CB}$ [lbf] |
|---|---|---|---|---|
| 4 | -96321.94 | -69189.83 | -179935.50 | 171316.80 |
| 5 | -87699.45 | -64809.86 | -169866.40 | 160212.60 |
| 6 | -79761.60 | -60981.33 | -161096.40 | 150450.30 |
| 10 | -52919.05 | -49567.63 | -135057.50 | 120880.20 |
| 15 | -25626.54 | -39593.26 | -111514.8 | 94349.84 |
| 20 | -4217.87 | -34859.30 | -100305.00 | 80337.59 |
| 25 | 14724.54 | -31051.40 | -89734.74 | 68408.25 |
| 30 | 31308.58 | -28641.18 | -81247.73 | 59491.73 |
| 35 | 46283.39 | -27546.81 | -74332.11 | 53011.83 |
| 40 | 61467.72 | -28427.23 | -69524.87 | 49446.88 |
| 45 | 86818.71 | -35932.32 | -72216.60 | 54135.45 |
| 50 | 104082.96 | -44304.81 | -61170.40 | 45667.42 |

All angled presented in the equations above were simply calculated from geometry. Table IX shows the values for each angle at the corresponding dumping angle.

TABLE IX: SUMMARY OF ANGLES USED IN CALCULATIONS

| D Angle | $\theta$ [˚] | $\gamma'$ [˚] | ∅ [˚] | $\beta'$ [˚] | $\omega$ [˚] | $\omega'$ [˚] | $\gamma''$ [˚] | d1 [in] |
|---|---|---|---|---|---|---|---|---|
| 4 | 71.60 | 9.40 | 85.29 | 87.29 | 6.70 | 83.29 | 23.097 | 39.83 |
| 5 | 69.75 | 11.75 | 84.12 | 86.62 | 8.37 | 81.62 | 26.12 | 37.19 |
| 6 | 67.94 | 14.12 | 82.93 | 85.93 | 10.06 | 79.93 | 29.11 | 35.09 |
| 10 | 61.17 | 23.62 | 78.18 | 83.18 | 16.81 | 73.18 | 40.63 | 26.66 |
| 15 | 53.64 | 35.70 | 72.14 | 79.64 | 25.35 | 64.64 | 54.20 | 25.83 |
| 20 | 46.99 | 48.13 | 65.93 | 75.93 | 34.06 | 55.93 | 67.071 | 23.23 |
| 25 | 41.03 | 61.10 | 59.44 | 71.94 | 43.05 | 46.94 | 79.51 | 21.20 |
| 30 | 35.55 | 74.86 | 52.56 | 67.56 | 52.43 | 37.56 | 91.88 | 19.32 |
| 35 | 30.32 | 89.85 | 45.073 | 62.57 | 62.42 | 27.57 | 104.59 | 17.36 |
| 40 | 25.06 | 106.87 | 36.56 | 56.56 | 73.43 | 16.56 | 118.37 | 14.95 |
| 45 | 19.19 | 127.98 | 26.00 | 48.50 | 86.49 | 3.50 | 134.80 | 11.04 |
| 50 | 5.23 | 165.96 | 7.015 | 14.03 | 90 | 0 | 167.75 | 9.69 |

The last calculation for the analysis of design 1 included finding the maximum bending moment of the lower member. This calculation was not needed for the upper member as it is only a two-force member.

TABLE X: MAXIMUM BENDING MOMENT IN LOWER MEMBER

| D Angle [˚] | Maximum Moment [lb*ft] |
|---|---|
| 4 | 1114793 |
| 5 | 1214342 |
| 6 | 1288067 |
| 10 | 1436441 |
| 15 | 1421955 |
| 20 | 1391376 |
| 25 | 1269851 |
| 30 | 1109746 |
| 35 | 920282.3 |
| 40 | 707336.9 |
| 45 | 471158 |
| 50 | 107235.5 |

The maximum moment was found by considering the lower member as a beam with pin connections at each end. The load of the cylinder was applied in accordance to different dumping angles and hence the bending moment caused by the cylinder is measured. A sample calculation for a dumping angle of 20˚ is shown below.

## *Sample Calculation:*

From Table VIII the corresponding force exerted by the cylinder at a dumping angle of 20˚ is 100305 lb*f*.

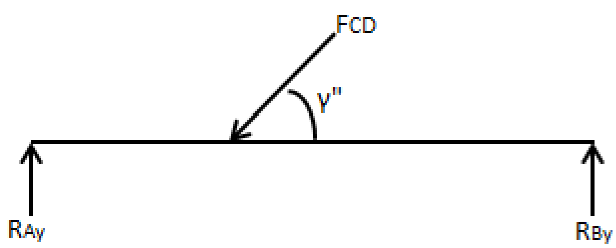


Figure 32: Free Body Diagram of Lower Member for Bending Moment – Design 1

TABLE XI: MAXIMUM BENDING MOMENT DESIGN 1 - SUPPLEMENTARY CALCULATIONS

| D Angle | γ" | $F_{CD}$ [lb*f*] | $F_{CD}$ : y-direction[lb*f*] | $R_{AY}$[lb*f*] | $R_{BY}$ [lb*f*] |
|---|---|---|---|---|---|
| 4 | 23.09739 | 179935.5 | 70587.85 | 42599.77 | 27988.08 |
| 5 | 26.1271 | 169866.4 | 74803.01 | 42151.5 | 32651.51 |
| 6 | 29.11359 | 161096.4 | 78380.24 | 41676.91 | 36703.33 |
| 10 | 40.63818 | 135057.5 | 87960.25 | 39523.47 | 48436.78 |
| 15 | 54.20736 | 111514.8 | 90453.98 | 35394.92 | 55059.07 |
| 20 | 67.07141 | 100305 | 92380.03 | 32551.36 | 59828.67 |
| 25 | 79.51688 | 89734.74 | 88236.94 | 28346.78 | 59890.15 |
| 30 | 91.88138 | 81247.73 | 81203.93 | 23775.53 | 57428.4 |
| 35 | 104.5998 | 74332.11 | 71931.93 | 18920.28 | 53011.65 |
| 40 | 118.3745 | 69524.87 | 61172.17 | 13855.5 | 47316.67 |
| 45 | 134.8001 | 72216.6 | 51242.68 | 8573.056 | 42669.63 |
| 50 | 167.7524 | 61170.4 | 12976.54 | 1904.209 | 11072.33 |

The external forces are solved by using simple static equilibrium equations. As the external forces are known, the next step was to "cut" the member at different values of $F_{CD}$ in order to determine at which angle the maximum bending moment occurs. This was done by determining the shear force which in turn was used to find the maximum bending moment. Let us consider the case when the dumping angle is equal to 20˚.

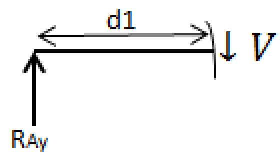


Figure 33: Determining Shear Force in Lower Member - Design 1

As it can be clearly seen, the shear force in simply equal to the reaction force. The distance d1 is the distance from point A to right before the point of application of $F_{CD}$.

Therefore the bending moment is calculated as follows:

$$Maximum\ Bending\ Moment = V * d1$$

### B-3.1.4 Design Two

Design two encompasses a lower member of length 81.91" and an upper member with a length of 59.91." The horizontal pin-to-pin has been also changed to 133.08" and the pin-to-pin along the box up the mounting point is kept the same as it cannot be compromised.

### B-3.1.4 External Force Analysis

A unique feature of design two is that the line of action as discussed earlier changes in direction as the dumping angle increases. This is illustrated by the schematic shown on the next page:

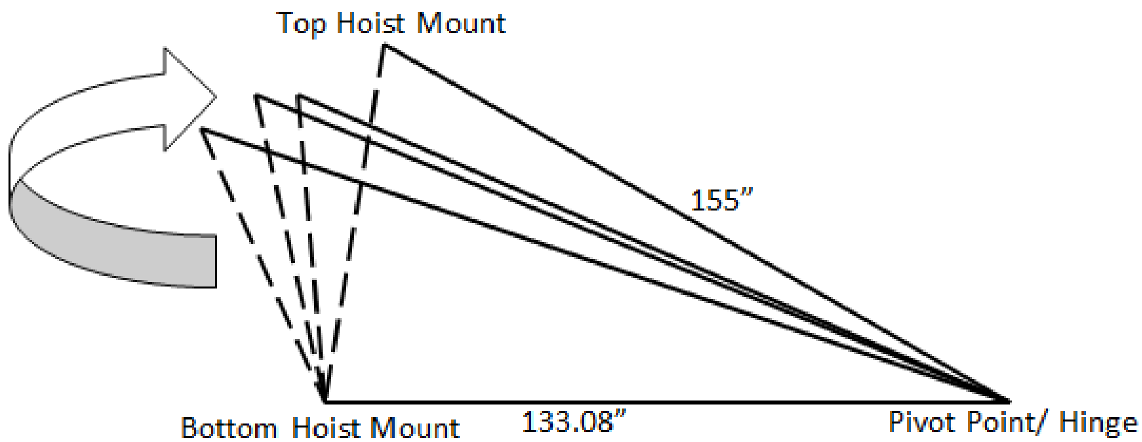


Figure 34: Varying Line of Action for Design 2

The reason for the change in line of action is simply due to the fact that the horizontal pin-to-pin was reduced. After scaled drawings, it is determined that the line of action passes the vertical point after a dumping angle of 30˚ and therefore design two is analyzed using two different cases.

### *Case 1(Dump Angle < 30˚)*

Similar to the previous design, parameters were set to define the entire system to determine the external forces. For case 1, Figure 35 shows the setup of systems.

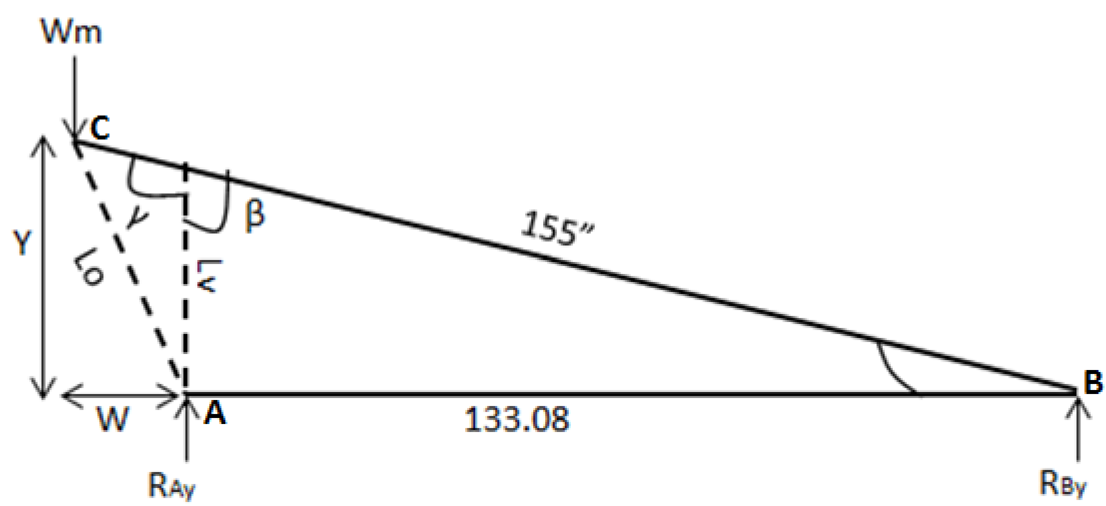


Figure 35: Free Body Diagram for External Forces - Design 2 Case 1

The results obtained from case 1 for the external forces are presented in the table below:

TABLE XII: SUMMARY OF RESULTS EXTERNAL FORCE ANALYSIS - DESIGN 2 CASE 1

| D Angle[˚] | Wm [lbf] | Lv [in] | Lo [in] | β [˚] | $R_{AY}$ [lbf] | $R_{BY}$ [lbf] | Y [in] | W [in] |
|---|---|---|---|---|---|---|---|---|
| **4** | 42821.85 | 9.30551 | 24.10802 | 86 | 49755.54 | -6933.69 | 10.81225 | 21.54743 |
| **5** | 42495.8 | 11.64255 | 25.25246 | 85 | 49308.91 | -6813.12 | 13.50914 | 21.33518 |
| **6** | 42168.78 | 13.98675 | 26.58374 | 84 | 48847.3 | -6678.52 | 16.20191 | 21.07589 |
| **10** | 40845.24 | 23.46471 | 33.27815 | 80 | 46852 | -6006.76 | 26.91547 | 19.5702 |
| **15** | 38167.48 | 35.65734 | 43.43243 | 75 | 42941.03 | -4773.55 | 40.11695 | 16.6435 |
| **20** | 37362.19 | 48.43534 | 54.48469 | 70 | 40893.41 | -3531.22 | 53.01312 | 12.57736 |
| **25** | 35458.24 | 62.05389 | 65.92279 | 65 | 37430.71 | -1972.47 | 65.50583 | 7.402707 |
| **30** | 33395.44 | 76.83089 | 77.50866 | 60 | 33686.27 | -290.838 | 77.5 | 1.158938 |

*Sample Calculations (consider D Angle = 20°):*

First we can calculate both Lo and Lv as follows:

$$Lv = 133.08 * \tan(20)$$

$$Using\ cosine\ law: Lo = acos\left(133.08^2 + 155^2 - (2 * 155 * 133.08 * \cos(20))\right)$$

Also all other angles can be found as follows:

$$\beta = 180° - 90° - 20°$$

To find the external forces, a moment is taken about point B and therefore:

$$M_B = 0\ ;\ (-R_{Ay} * 133.08) + (W_m * (\cos(20) * 155)) = 0$$

$$\therefore R_{Ay} = \frac{W_m * \cos(20) * 155}{133.08}$$

$$\therefore R_{By} = W_m - R_{Ay}$$

### *Case 2 (Dump Angle >30˚)*

Similar to case 1, parameters were defined on the entire structure to determine the external forces. Figure 36 shows the free body diagram and other parameters used to determine the external forces on the structure.

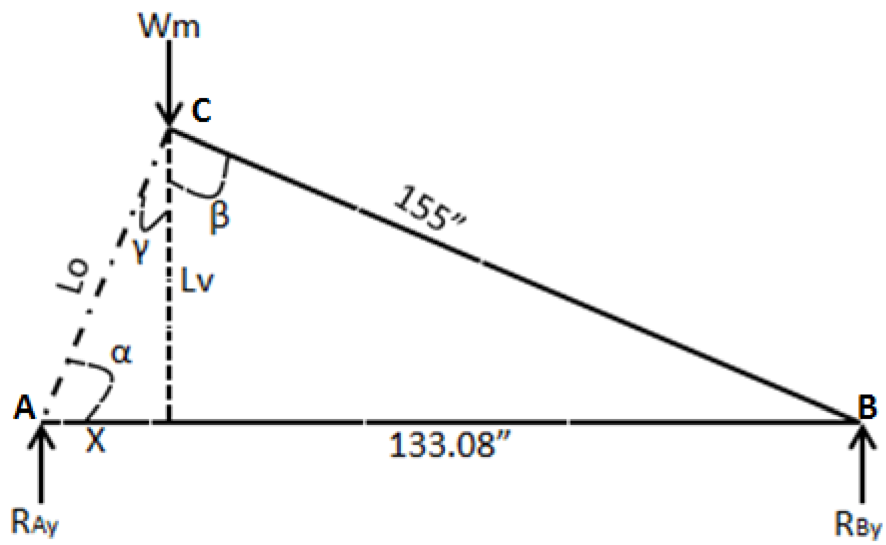


Figure 36: External Forces Free Body Diagram - Design 2 Case 2

The results obtained from case 2 for the external forces are presented in the table below:

TABLE XIII: SUMMARY OF RESULTS EXTERNAL FORCE ANALYSIS - DESIGN 2 CASE 2

| D Angle | Wm [lbf] | Lv [in] | X [in] | Lo [in] | β [˚] | α [˚] | $R_{ay}$ [lbf] | $R_{By}$ [lbf] |
|---|---|---|---|---|---|---|---|---|
| **35** | 31113.11 | 88.90435 | 6.106433 | 89.11381 | 55 | 86.07079 | 29685.42 | 1427.692 |
| **40** | 28533.04 | 99.63208 | 14.33811 | 100.6585 | 50 | 81.81076 | 25458.76 | 3074.281 |
| **45** | 25543.85 | 109.6016 | 23.47345 | 112.087 | 45 | 77.91154 | 21038.1 | 4505.747 |
| **50** | 21981.44 | 118.7369 | 33.44292 | 123.3567 | 40 | 74.26982 | 16457.31 | 5524.131 |

*Sample Calculations:*

First we can calculate both Lo and Lv as follows:

$$Lv = 155 * \sin(20)$$

$$Using\ cosine\ law: Lo = acos\left(133.08^2 + 155^2 - (2 * 155 * 155 * \cos(20))\right)$$

Also all other angles can be found as follows:

$$\alpha = \text{asin}(Lv/Lo)$$

$$\beta = 180° - 90° - 20°$$

$$\gamma = \text{asin}(X/Lv)$$

To find the external forces, a moment is taken about point B and therefore:

$$M_A = 0\ ;\ (-R_{Ay} * 133.08) - (W_m * (133.08 - \text{X}))$$

$$\therefore R_{Ay} = \frac{W_m * (133.08 - \text{X})}{133.08}$$

$$\therefore R_{By} = W_m - R_{Ay}$$

Following the calculation of the external forces, the force along the line of action was determined. It is important to note that the force along the line of action is essentially the fore experienced by the hoist.

*Case 1:*

The results for case 1 are shown in Table XIV:

TABLE XIV: RESULTS FOR FORCE A LONG LINE OF ACTION - DESIGN 2 CASE 1

| D Angle [˚] | α [˚] | $F_{AC}$ [lbf] | $F_{ACy}$ [lbf] | $F_{ACx}$ [lbf] |
|---|---|---|---|---|
| **4** | 26.64698 | -110940 | -49755.5 | -99156.4 |
| **5** | 32.34143 | -92172.5 | -49308.9 | -77874.3 |
| **6** | 37.55097 | -80147.6 | -48847.3 | -63541.9 |
| **10** | 53.97915 | -57927.6 | -46852 | -34066 |
| **15** | 67.46768 | -46489.9 | -42941 | -17815.1 |
| **20** | 76.65335 | -42028.6 | -40893.4 | -9701.96 |
| **25** | 83.55245 | -37669 | -37430.7 | -4229.98 |
| **30** | 89.14326 | -33690 | -33686.3 | -503.746 |

*Sample Calculation:*

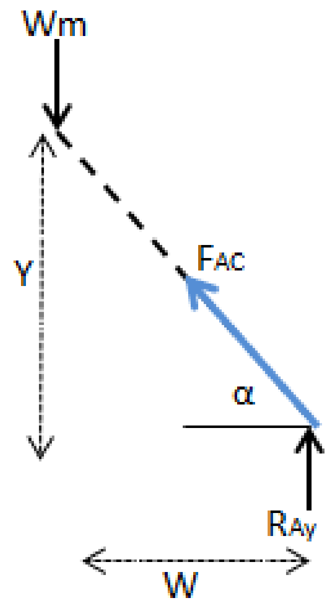


$$F_{AC} = \frac{-R_{Ay}}{\sin(\alpha)}$$

*Case 2:*

The results for case 2 are shown in Table XV.

TABLE XV: RESULTS FOR FORCE A LONG LINE OF ACTION - DESIGN 2 CASE 2

| D Angle [˚] | α [˚] | $F_{AC}$ [lbf] | $F_{ACy}$ [lbf] | $F_{ACx}$ [lbf] |
|---|---|---|---|---|
| **35** | 86.07079 | -29755.4 | -29685.4 | -2038.96 |
| **40** | 81.81076 | -25721 | -25458.8 | -3663.79 |
| **45** | 77.91154 | -21515.2 | -21038.1 | -4505.75 |
| **50** | 74.26982 | -17097.6 | -16457.3 | -4635.3 |

*Sample Calculation:*

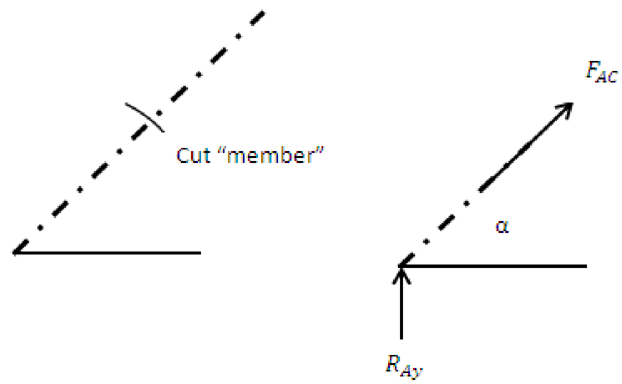


$$F_{AC} = \frac{-R_{Ay}}{\sin(\alpha)}$$

As the force along the line of action was known, it was applied to the hoist and the force experienced by the members was calculated. A simplified truss equivalent of the hoist can be seen below:

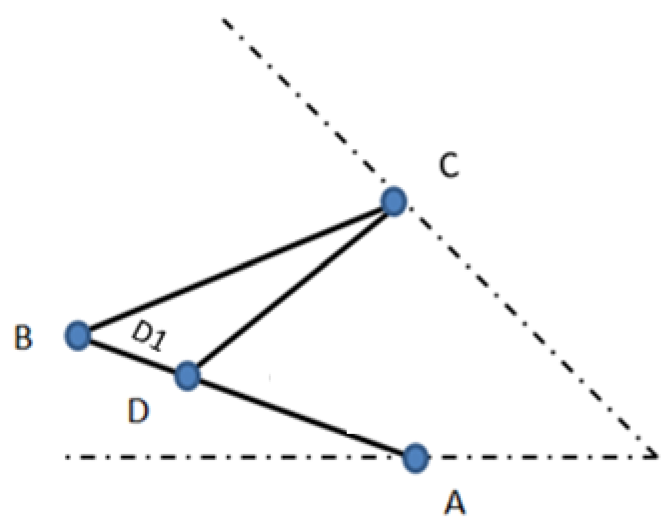


Figure 37: Simplified Truss Representation of the Hoist

The force a long line of action can be seen in Figure 38 to better understand the point of application of the force.

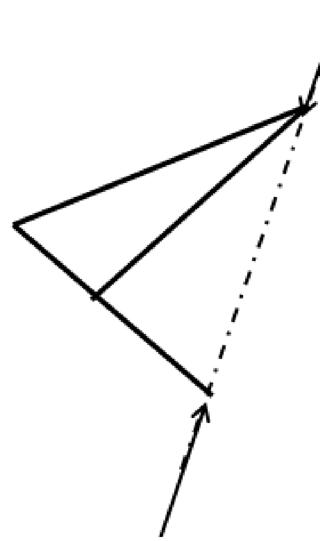


Figure 38: Application of Force along Line of Action Experienced by the Hoist

### B-3.1.5 Internal Force Analysis

As a result of force $F_{AC}$, the forces in the members of the hoist were calculated and shown in the table below. Sample calculations are shown following the table.

TABLE XVI: SUMMARY OF FORCES IN HOIST MEMBERS AT DIFFERENT DUMPING ANGLES

| D Angle [°] | $F_{DA}$ [lbf] | $F_{BD}$ [lbf] | $F_{CD}$ [lbf] | $F_{CB}$ [lbf] |
|---|---|---|---|---|
| **Case 1** | | | | |
| 4 | -118921 | -94925.3 | -232185 | 318054.5 |
| 5 | -105598 | -95705.4 | -223004.9 | 285914.1 |
| 6 | -96201.2 | -92787.2 | -214052.4 | 261105.1 |
| 10 | -68527.8 | -76068.1 | -182799.9 | 195555.3 |
| 15 | -39290.9 | -57846 | -148711.7 | 142420 |
| 20 | -16584.9 | -47774.2 | -129372.6 | 113542.7 |
| 25 | 3469.579 | -40501.1 | -112320.9 | 92532.04 |
| 30 | 23162.62 | -39169.9 | -104090.7 | 85346.37 |
| **Case 2** | | | | |
| 35 | 16163.05 | -40033.1 | -99373.29 | 82325.78 |
| 40 | 36760.25 | -38302.3 | -90761.88 | 73362.56 |
| 45 | 57720.06 | -38382.2 | -83811.13 | 67275.03 |
| 50 | 84710.35 | -43416.2 | -82411.75 | 67831.21 |

### *Case 1(Dump Angle < 30˚)*

As done for design 1, we begin at point C to calculate the forces in the upper member and the cylinder. It is important to note that the direction of $F_{ACx}$ has changed due to the line of action of hoist for angles under 30˚.

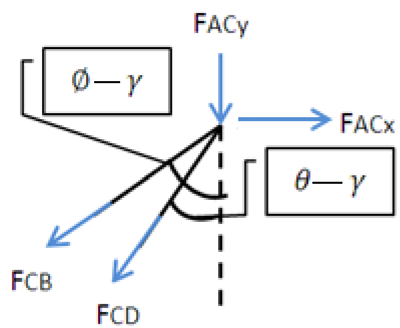


$$\sum F_y = 0; -\cos(\theta-\gamma) * F_{CD} - \cos(\theta-\gamma) * F_{CB} - F_{ACy} = 0$$

$$\sum F_x = 0; -\sin(\theta-\gamma) * F_{CD} - \sin(\theta-\gamma) * F_{CB} + F_{ACx} = 0$$

Now we solve these two equations simultaneously to obtain values for both $F_{CB}$ &$F_{CD}$. This can be achieved using a simple matrix formulation as shown below:

$$\begin{matrix} -\cos(\theta-\gamma) & -\cos(\emptyset-\gamma) \\ -\sin(\theta-\gamma) & -\sin(\emptyset-\gamma) \end{matrix} * \begin{matrix} F_{CD} \\ F_{CB} \end{matrix} = \begin{matrix} F_{ACy} \\ -F_{ACx} \end{matrix}$$

Next we move onto point B to solve for the force in member BD as follows:

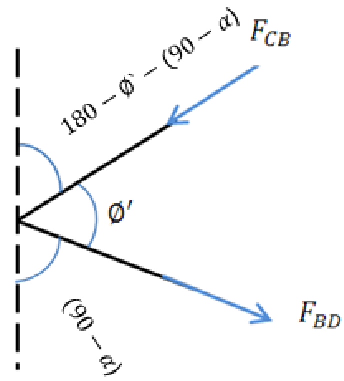


$$\sum F_y = 0;\ -\cos(180 - (90 - \alpha) - \emptyset') * F_{CB} - \cos(90 - \alpha) * F_{BD} = 0$$

$$\therefore F_{BD} = \frac{-\cos(180 - (90 - \alpha) - \emptyset') * F_{CB}}{\cos(90 - \alpha)}$$

Finally, the force in member DA is calculated at point D as follows:

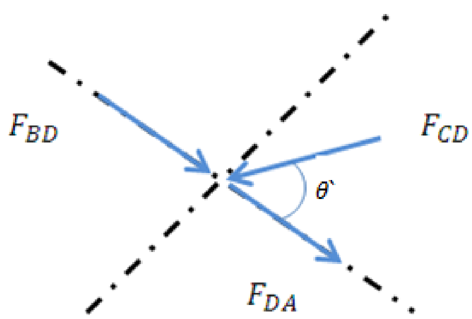


$$\sum F_y = 0;\ F_{BD} + F_{DA} - \cos(\theta`) * F_{CD} = 0$$

$$F_{DA} = \cos(\theta`) * F_{CD} - F_{BD}$$

### *Case 2 (Dump Angle >30°)*

In the same fashion as case 1, the internal forces in the hoist for case 2 were found.

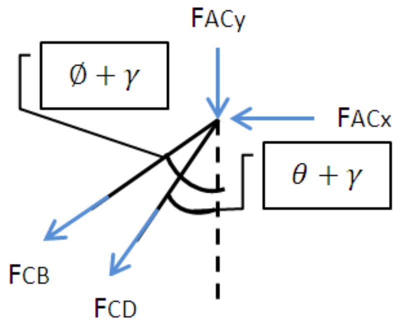


$$\sum F_y = 0; -\cos(\theta+\gamma) * F_{CD} - \cos(\theta+\gamma) * F_{CB} - F_{ACy} = 0$$

$$\sum F_x = 0; -\sin(\theta+\gamma) * F_{CD} - \sin(\theta+\gamma) * F_{CB} - F_{ACx} = 0$$

Now we solve these two equations simultaneously to obtain values for both $F_{CB}$ &$F_{CD}$. This can be achieved using a simple matrix formulation as shown below:

$$\begin{matrix} -\cos(\theta+\gamma) & -\cos(\emptyset+\gamma) \\ -\sin(\theta+\gamma) & -\sin(\emptyset+\gamma) \end{matrix} * \begin{matrix} F_{CD} \\ F_{CB} \end{matrix} = \begin{matrix} F_{ACy} \\ F_{ACx} \end{matrix}$$

Next we move onto point B to solve for the force in member BD as follows:

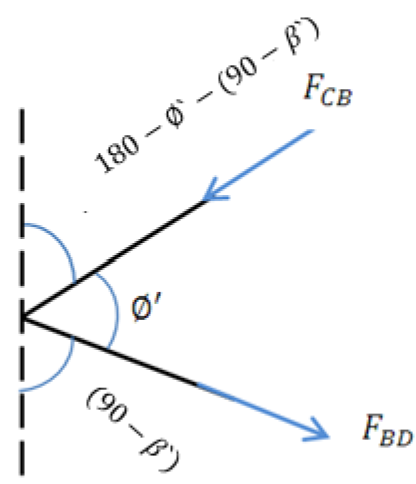

$$\sum F_y = 0;\ -\cos(180-(90-\beta`)-\emptyset') * F_{CB} - \cos(90-\beta`) * F_{BD} = 0$$

$$\therefore F_{BD} = \frac{-\cos(180-(90-\beta`)-\emptyset') * F_{CB}}{\cos(90-\beta`)}$$

Finally, the force in member DA is calculated at point D as follows:

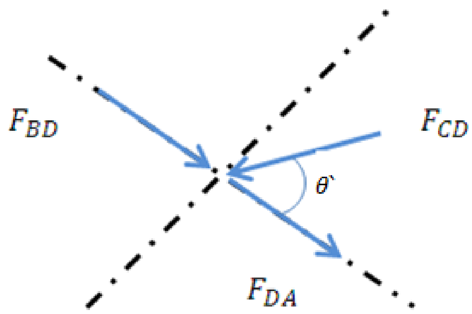


$$\sum F_y = 0;\ F_{BD} + F_{DA} - \cos(\theta`) * F_{CD} = 0$$

$$F_{DA} = \cos(\theta`) * F_{CD} - F_{BD}$$

The last calculation for the analysis of design 2 included finding the maximum bending moment of the lower member. As mentioned prior this calculation is not needed for the upper member as it is only a two-force member.

TABLE XVII: MAXIMUM BENDING MOMENT IN LOWER MEMBER

| D Angle | Maximum Bending Moment |
|---|---|
| 4 | 1852399 |
| 5 | 1949547 |
| 6 | 2016388 |
| 10 | 2104930 |
| 15 | 1943974 |
| 20 | 1747762 |
| 25 | 1422126 |
| 30 | 1054601 |
| 35 | 1279686 |
| 40 | 1037344 |
| 45 | 782768.1 |
| 50 | 524439.7 |

The maximum moment was found by considering the lower member as a beam with pin connections are each end. The load of the cylinder was applied in accordance to different dumping angles and hence the bending moment caused by the cylinder is measured. A sample calculation for a dumping angle of 20˚ is shown below.

*Sample Calculation:*

From Table XVI the corresponding force exerted by the cylinder at a dumping angle of 20˚ is 129372.6 lbf.

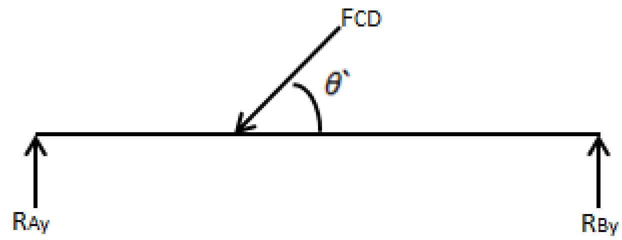


Figure 39: Free Body Diagram of Lower Member for Bending Moment – Design 2

The external forces were solved by using simple static equilibrium equations. As the external forces are known, the next step was to "cut" the member at different values of $F_{CD}$ in order to determine at which angle gives the maximum bending moment. This was done by determining the shear force which in turn is used to find the maximum bending moment. Let us consider the case when the dumping angle is equal to 20˚.

TABLE XVIII: MAXIMUM BENDING MOMENT DESIGN 2 - SUPPLEMENTARY CALCULATIONS

| D Angle [˚] | $F_{CD}$ [lbf] | $F_{CD}$; Y-direction [lbf] | θ' [˚] | d1 [in] | $R_{ay}$ [lbf] | $R_{By}$ [lbf] |
|---|---|---|---|---|---|---|
| **4** | 232557.1 | 90585.96 | 22.92473 | 39.424 | 43599.39 | 46986.57 |
| **5** | 223533.9 | 96186.96 | 25.48669 | 36.814 | 43230.28 | 52956.68 |
| **6** | 214737.5 | 100829.5 | 28.00493 | 34.687 | 42698.55 | 58130.94 |
| **10** | 183840.9 | 112475.4 | 37.72036 | 28.938 | 39736.06 | 72739.31 |
| **15** | 148720.1 | 112610 | 49.21748 | 24.728 | 33995.77 | 78614.26 |
| **20** | 125578.5 | 108937 | 60.1672 | 21.898 | 29123.16 | 79813.79 |
| **25** | 100664.1 | 95035.76 | 70.74979 | 19.704 | 22861.27 | 72174.49 |
| **30** | 76580.23 | 75669.3 | 81.15384 | 17.809 | 16451.98 | 59217.32 |
| **35** | 99373.29 | 99334.69 | 91.59718 | 16.013 | 19419.25 | 79915.44 |
| **40** | 90761.88 | 88659.06 | 102.3575 | 14.142 | 15307.1 | 73351.97 |
| **45** | 83811.13 | 76649.73 | 113.8577 | 11.958 | 11189.95 | 65459.78 |
| **50** | 82411.75 | 65887.95 | 126.9179 | 8.934 | 7186.39 | 58701.56 |

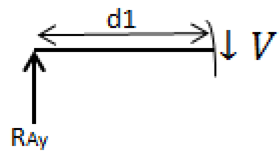


As it can be clearly seen, the shear force in simply equal to the reaction force. The distance d1 is the distance from point A to right before the point of application of $F_{CD}$.

Therefore the bending moment is calculated as follows:

$$Maximum\ Bending\ Moment = V * d1$$

# Appendix C –

# Details of Design 1

## List of Figures

## C-1 Design 1 Convergence Study

To ensure the validity of the FEA analysis convergences, studies were performed for each member. This was done by increasing the mesh density to see if the maximum stress increases substantially. If the stress increases significantly, it could mean that some features are not set up properly in the FEA program.

The first member looked at was the lower member. In Figure 1 the plot shows the results with the initial mesh density, while Figure 2 shows the results after the mesh density is increased.

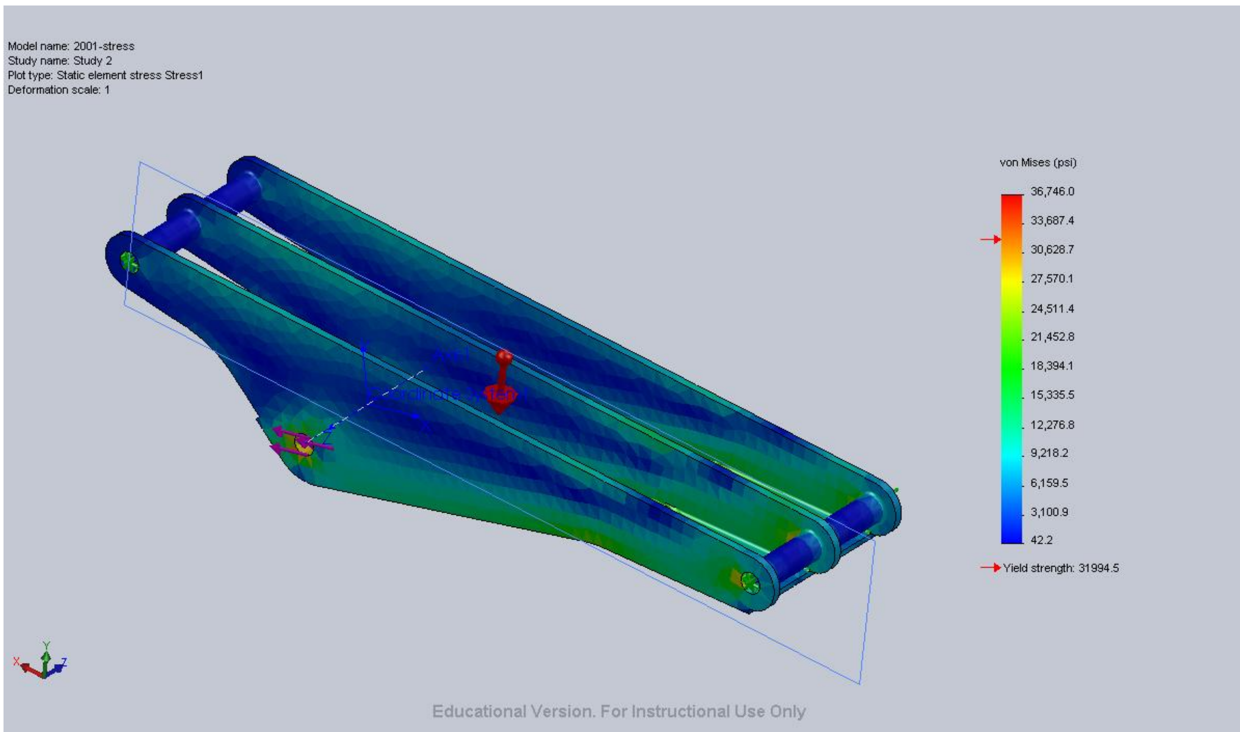


Figure 1: Lower Member Convergence 1

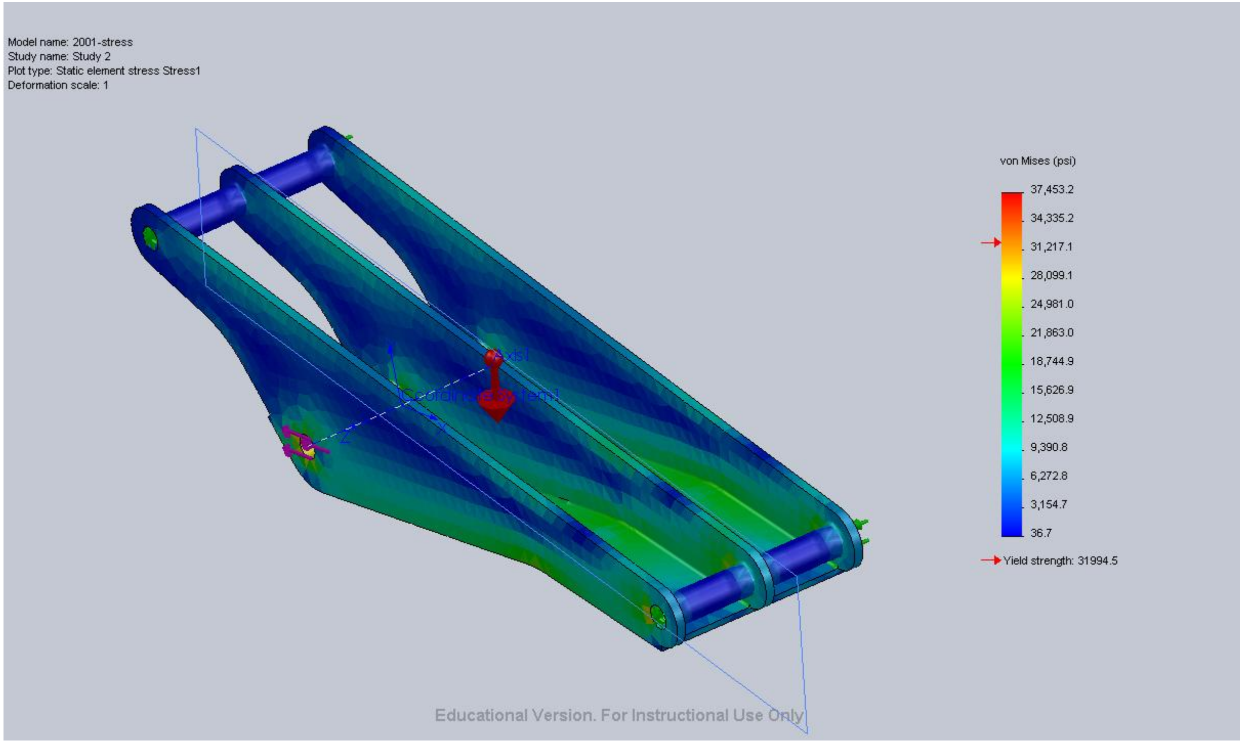


Figure 2: Lower Member Convergence 2

The stress in with the lower mesh density is shown as 36,746psi while with the increased mesh density the stress is 37,452psi. Since there is only a 2% increase in the stresses, the results are valid.

The next member looked at was the lower member. Figure 3 shows the stresses with the initial mesh density while Figure 4 shows the stresses after the mesh density was increased.

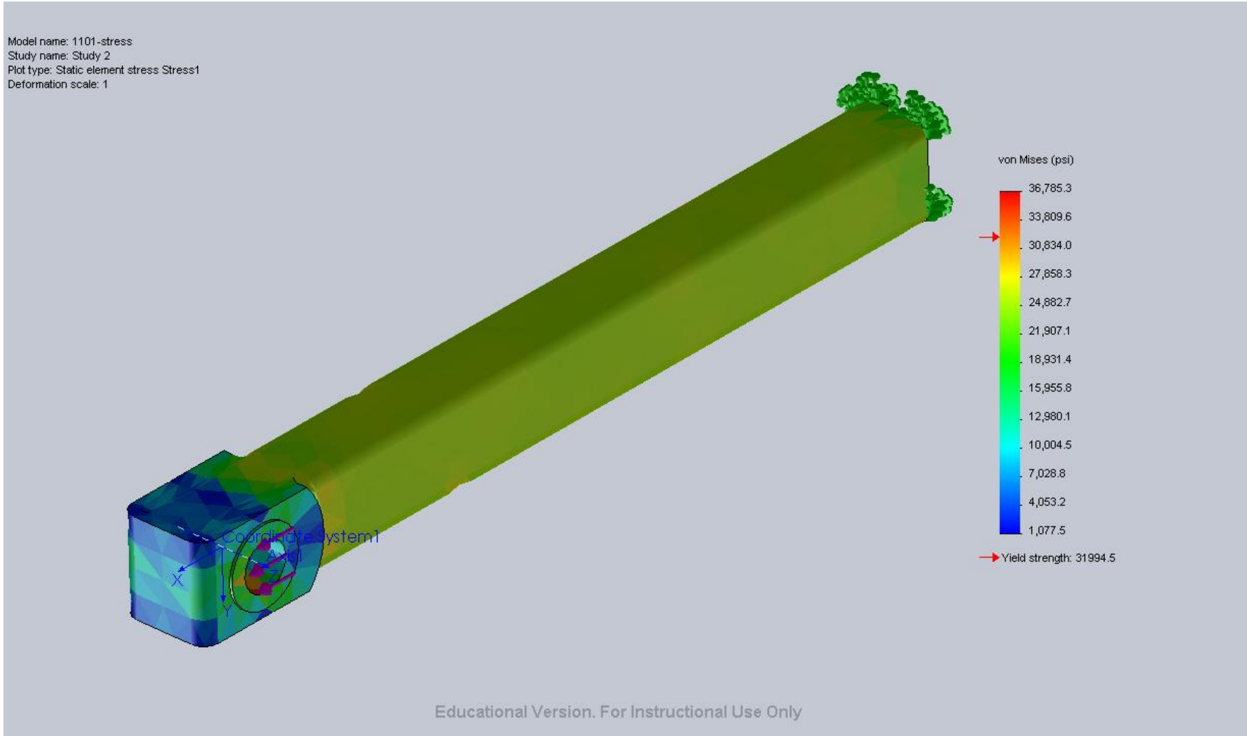


Figure 3: Lower Member Convergence 1

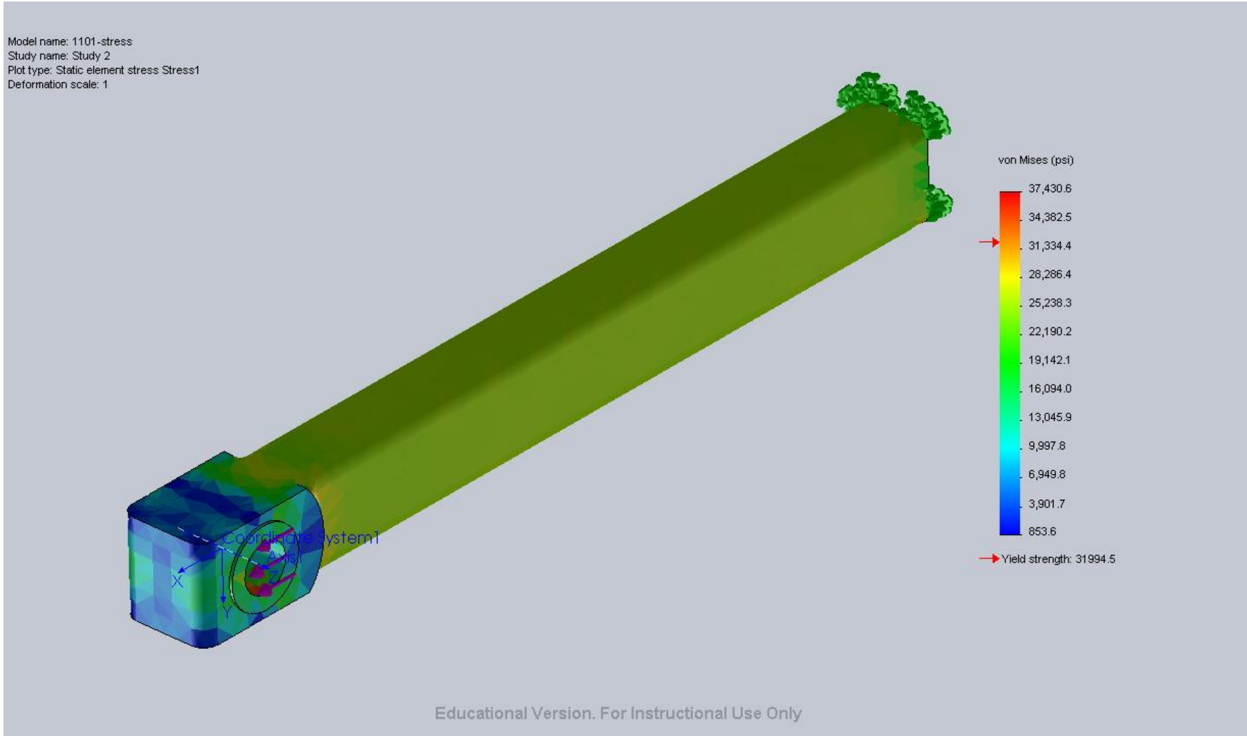


Figure 4: Lower Member Convergence 2

The stress in the initial plot is 36,785psi while the stress in the plot with the higher mesh density is 37,430psi. This shows convergence as the stress increased only by 1.8% and therefore the results are valid.

The frame mount was looked at next. The stress with the initial mesh density is shown in Figure 5 while the stress after the mesh density is increased is shown in Figure 6.

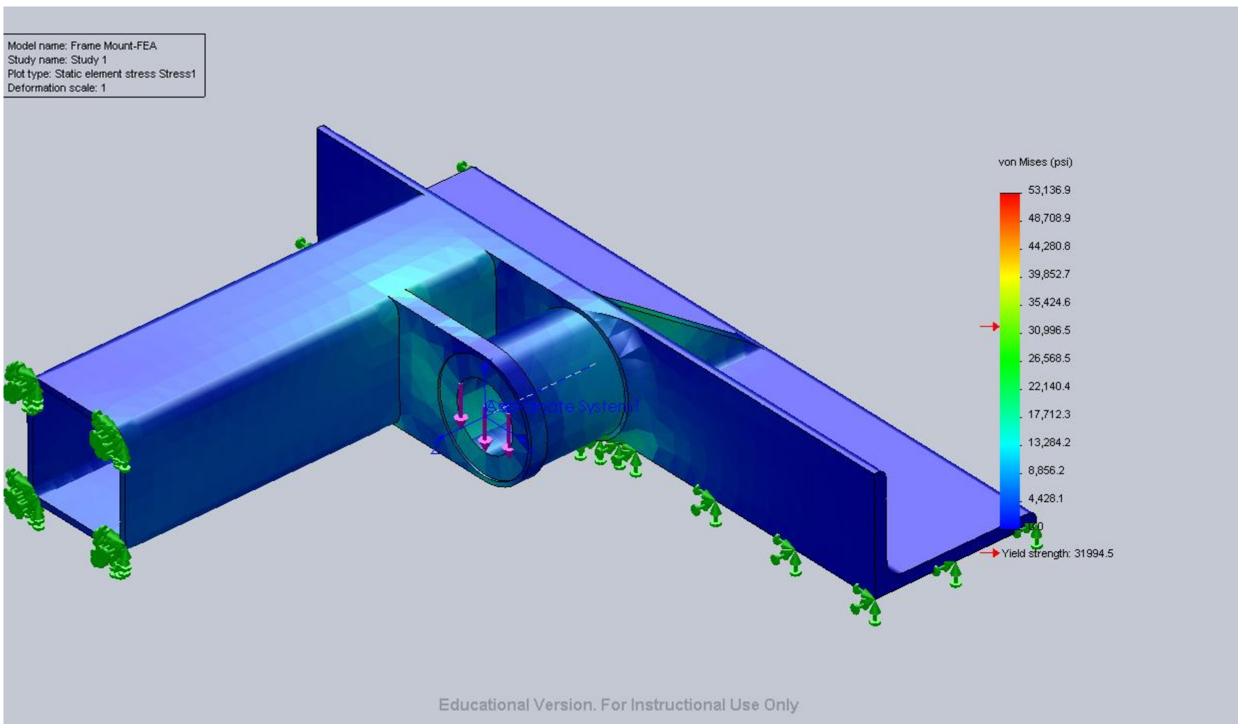


Figure 5: Frame Mount Convergence 1

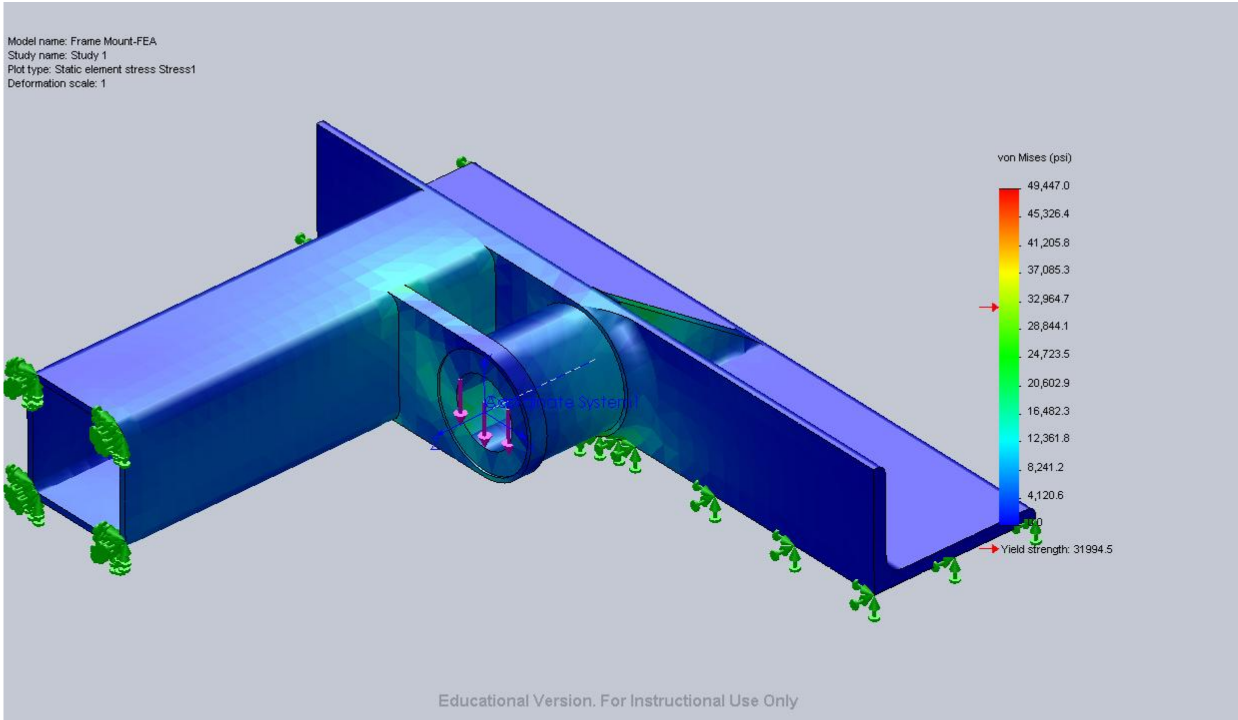


Figure 6: Frame Mount Convergence 2

The maximum stress in this member went down with an increase in mesh density. The stresses in areas of concern around the round tube and the gusset remained constant. The results therefore are valid for these areas.

The last member that was looked at is the box mount. Figure 7 shows the stresses with the initial mesh density and Figure 8 has the stresses after the mesh density has been increased.

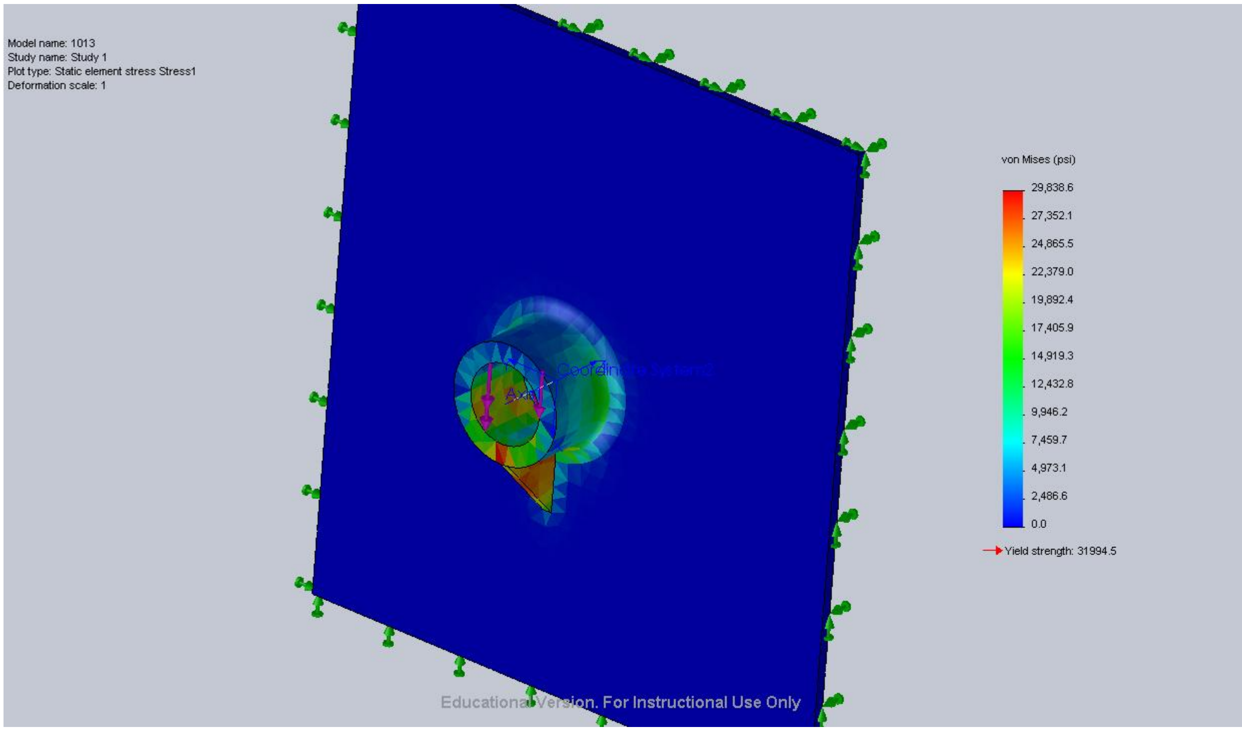


Figure 7: Box Mount Convergence 1

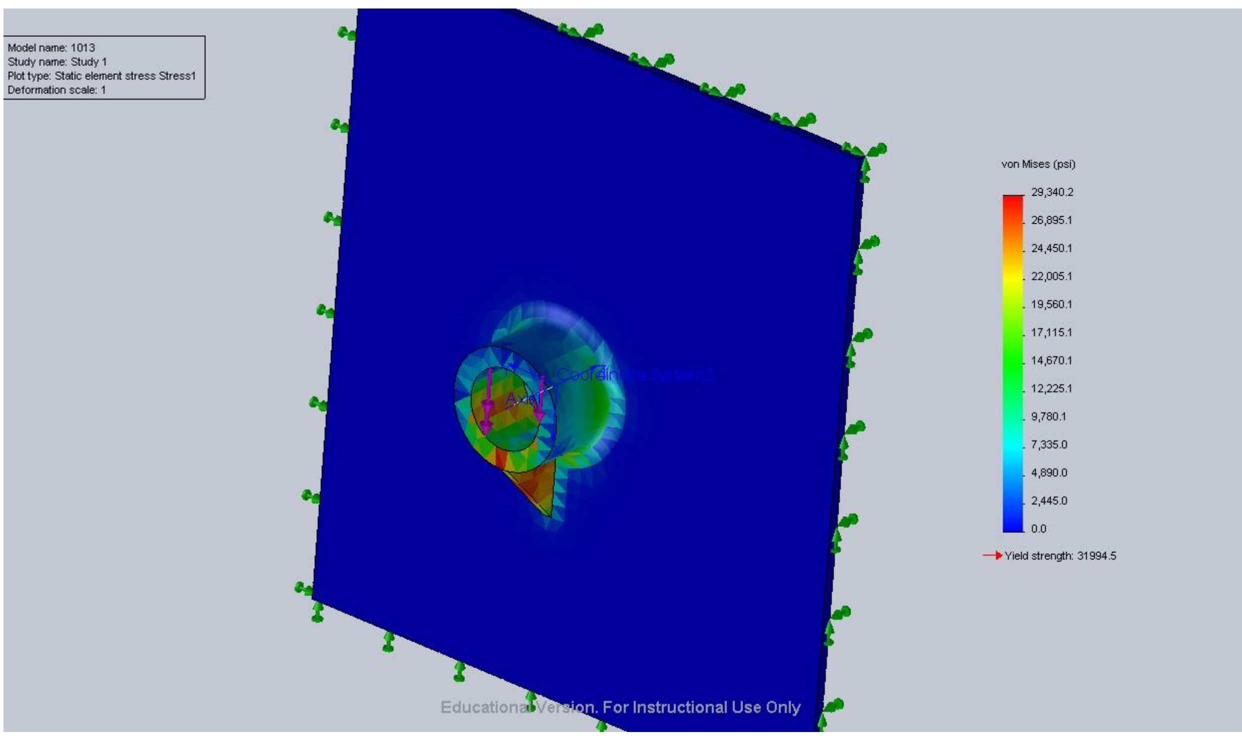


Figure 8: Box Mount Convergence 2

The maximum stress before the increase in mesh density was 29,836psi while afterwards it was 29,340psi. This gives a 1.7% difference which means that these results are valid as well.

## C-2 Hoist Exploded View and Bill of Materials

| ITEM NO. | PART NUMBER | DESCRIPTION | QTY. |
|---|---|---|---|
| 1 | | 6" Hydraulic Cylinder | 2 |
| 2 | 2003 | Box Mount | 2 |
| 3 | 2004 | Frame Mount | 1 |
| 4 | 2001 | Lower Hoist Member | 1 |
| 5 | 2002 | Upper Hoist Member | 2 |
| 6 | 1009 | 2" x 17" Round Bar | 1 |
| 7 | 1011 | 2" x 25" Round Bar | 1 |
| 8 | 1010 | 2" x 28 1/2" Round Bar | 1 |
| 9 | 1012 | 2" x 26 1/2" Round Bar | 1 |

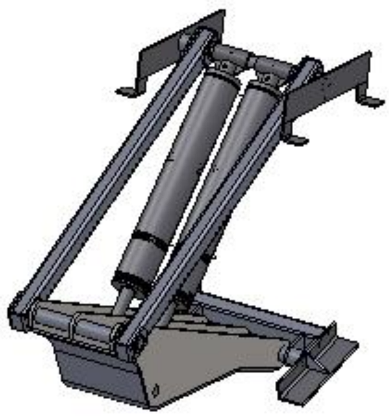

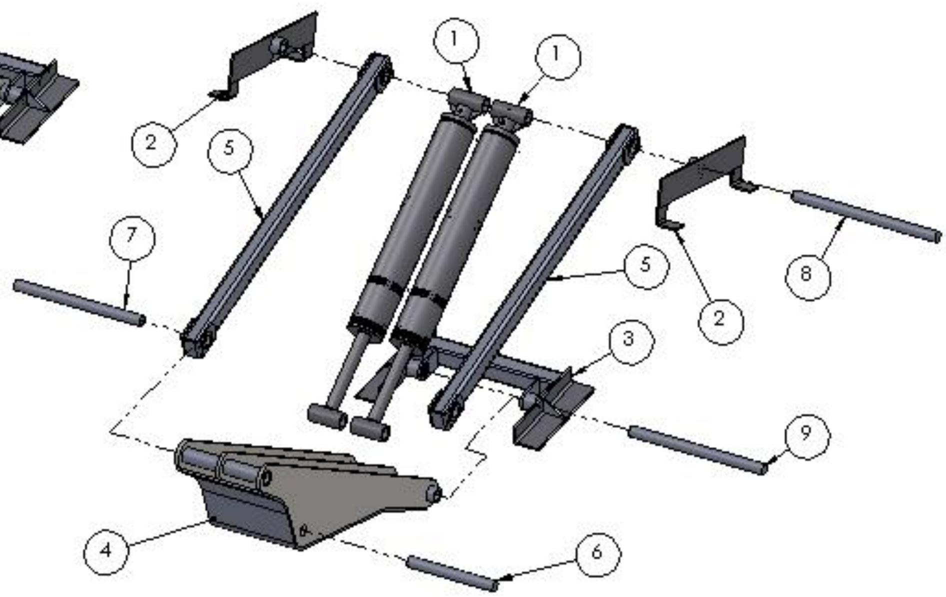

| ITEM NO. | PART NUMBER | DESCRIPTION | QTY. |
|---|---|---|---|
| 1 | 3349114 | 5" x 3 1/2" x 3/8" Angle Iron | 2 |
| 2 | 1014 | 3 1/4" OD x 2" ID Round Tube | 2 |
| 3 | 1016 | 3 1/2" x 3 1/2" x 0.188 wall Tube | 1 |
| 4 | 1017 | 1/2" Plate | 4 |
| 5 | 1018 | 1/2" Plate | 2 |

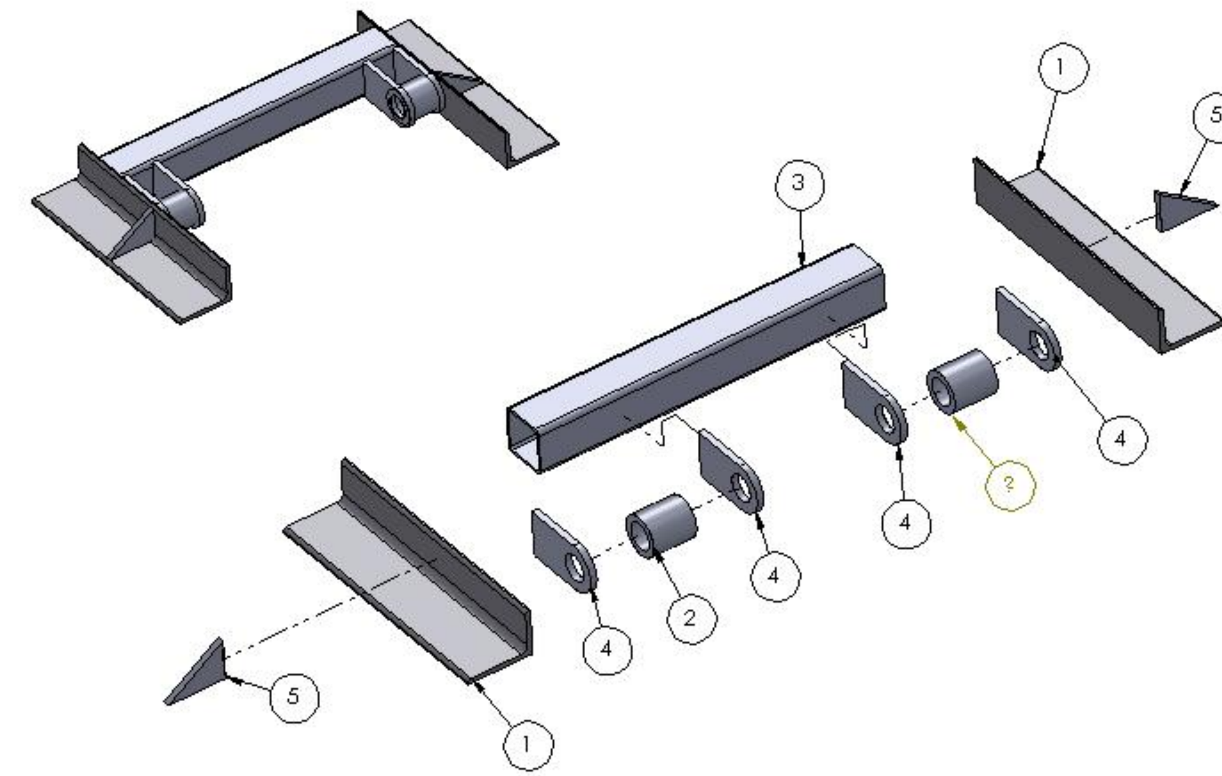

| ITEM NO. | PART NUMBER | DESCRIPTION | QTY. |
|---|---|---|---|
| 1 | 3069871 | 3/8" Plate | 1 |
| 2 | T013 | 3" OD x 2" ID Round Tube | 1 |
| 3 | 3069872 | 3/8" Plate | 2 |
| 4 | T015 | 1/4" Plate | 1 |

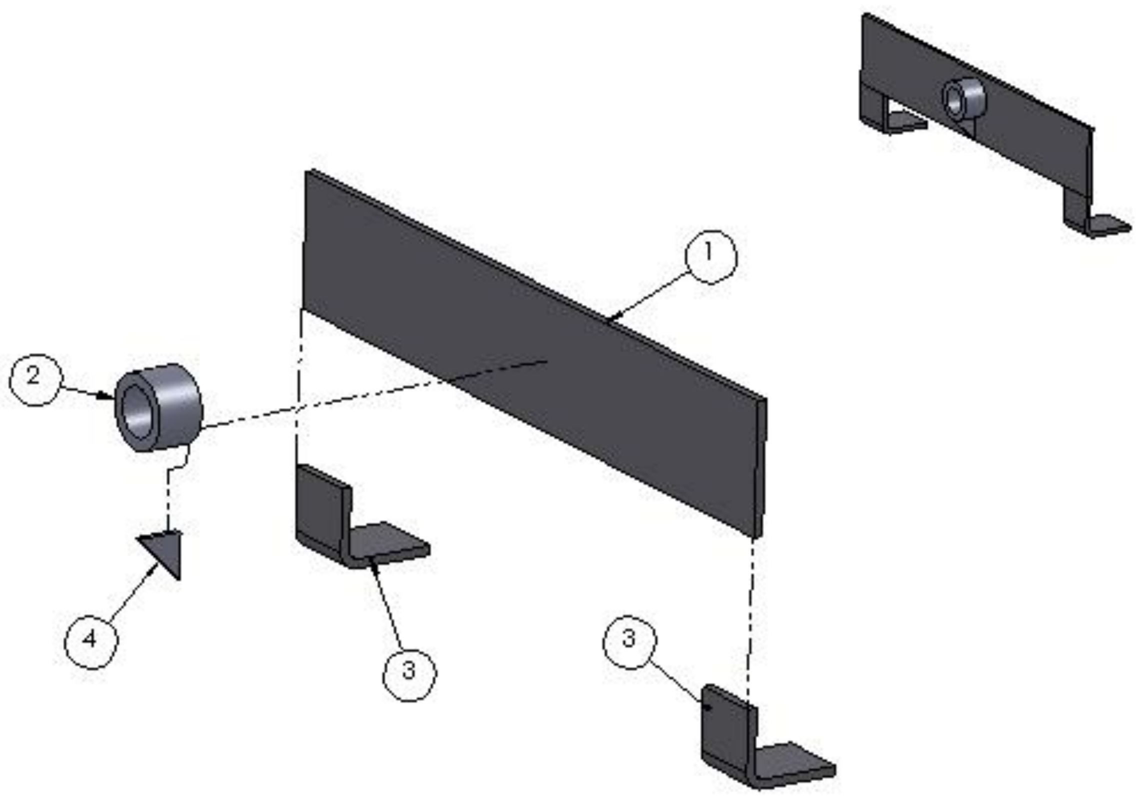

| ITEM NO. | PART NUMBER | DESCRIPTION | QTY. |
|---|---|---|---|
| 1 | 1101 | 3x4x0.375Wall Rectangular Tube, 71" Long | 1 |
| 2 | 1007 | 3/8" Plate | 2 |
| 3 | 1006 | 3 1/4" OD x 2"ID Round Tube, 4" Long | 2 |

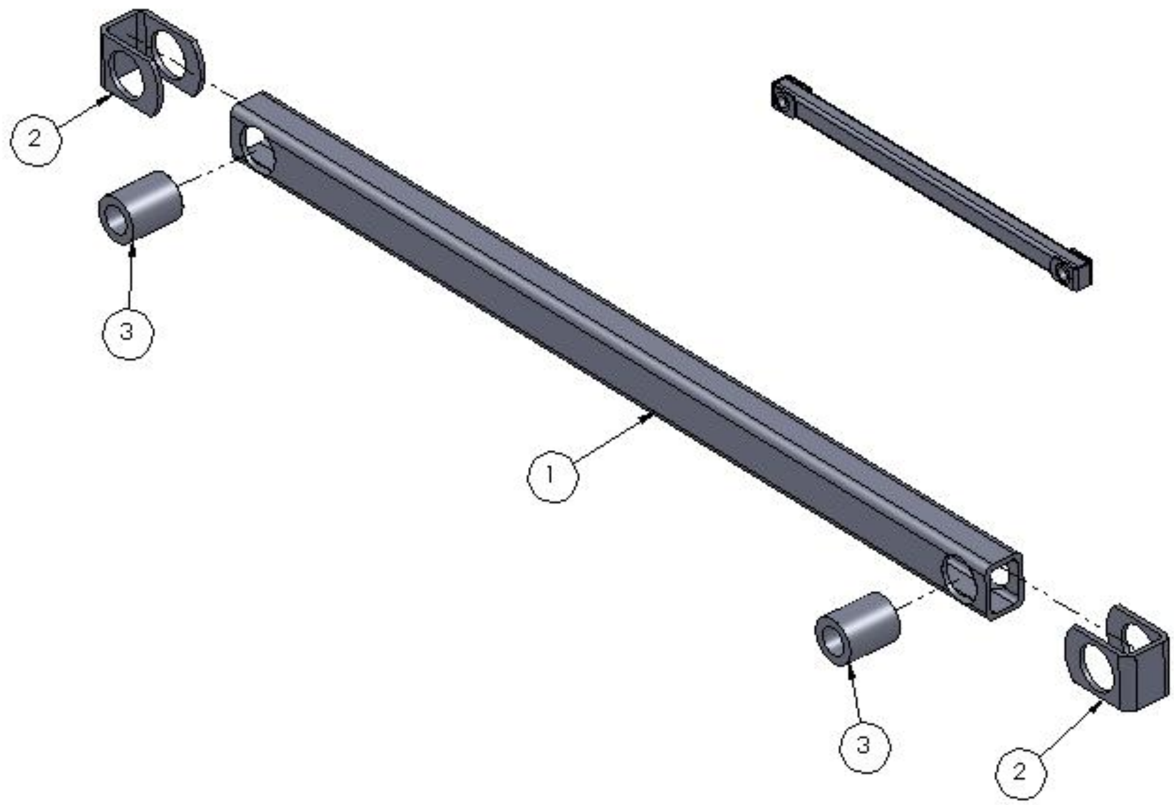

| ITEM NO. | PART NUMBER | DESCRIPTION | QTY. |
|---|---|---|---|
| 1 | 1002 | 3/4" Plate | 3 |
| 2 | 1004 | 2 3/4" OD x 2" ID Round Tube, 20" Long | 1 |
| 3 | 1003 | 2 3/4" OD x 2" ID Round Tube, 17" Long | 1 |
| 4 | 1005 | 1/2" Plate | 1 |
| 5 | 1008 | 1/2" Plate | 4 |

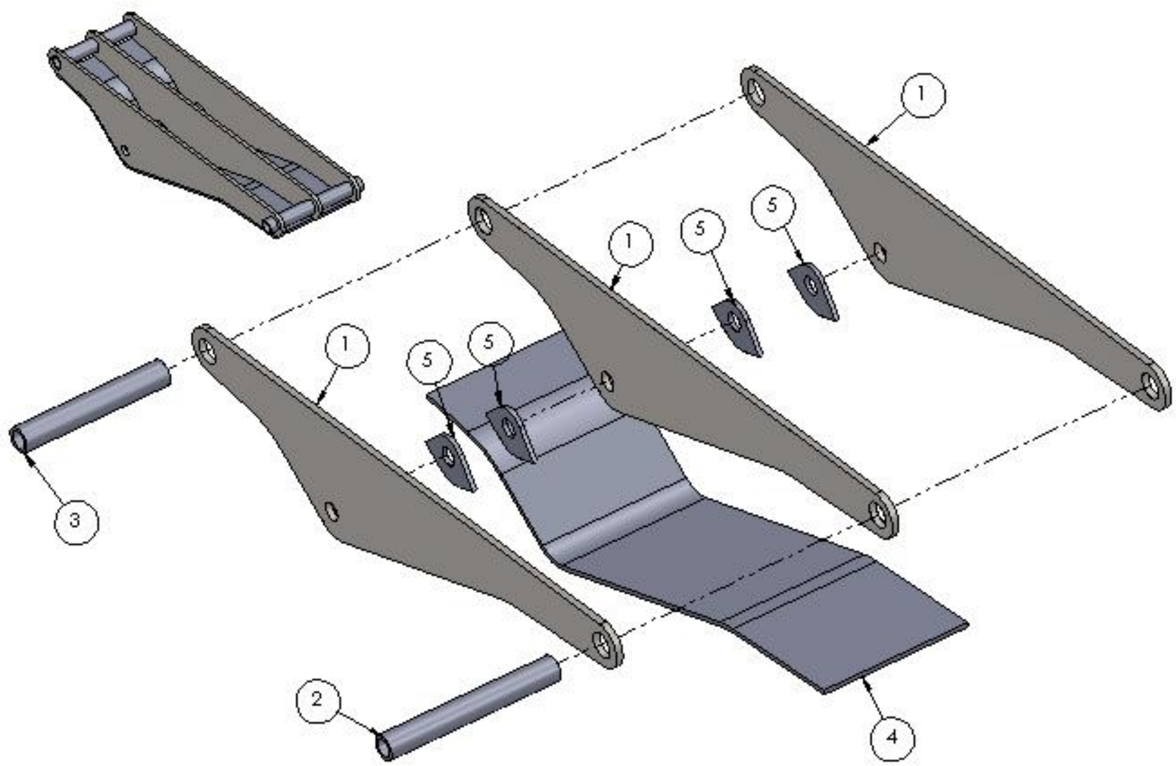

# Appendix D –

# Details of Design 2

## List of Figures

## D-1 Convergence Analysis

The first part of the Finite Element Analysis (FEA) is the lower member. From Figure 1 and Figure 2, the FEA shows that the lower members will be strong enough to withstand the maximum force of the cylinders at point of lift. The coarse and fine analysis showed differences of approximately 18.3%. This shows that the FEA is not converging; this is expected because of the sharp corners that had to be made in the lower pin hole in order to apply the force in the proper direction.

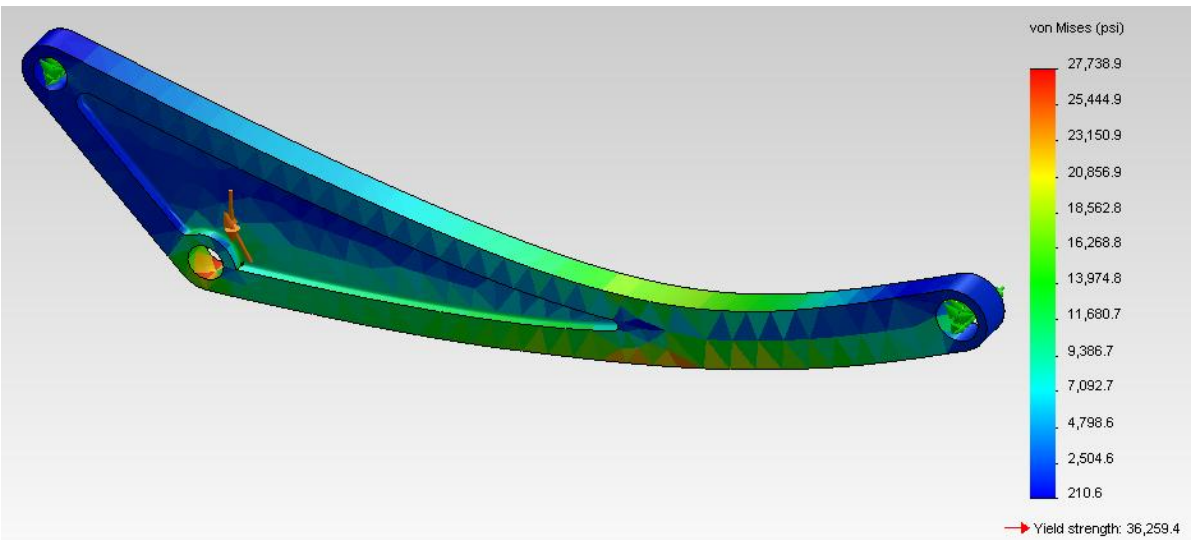


Figure 1: Lower member convergence 1

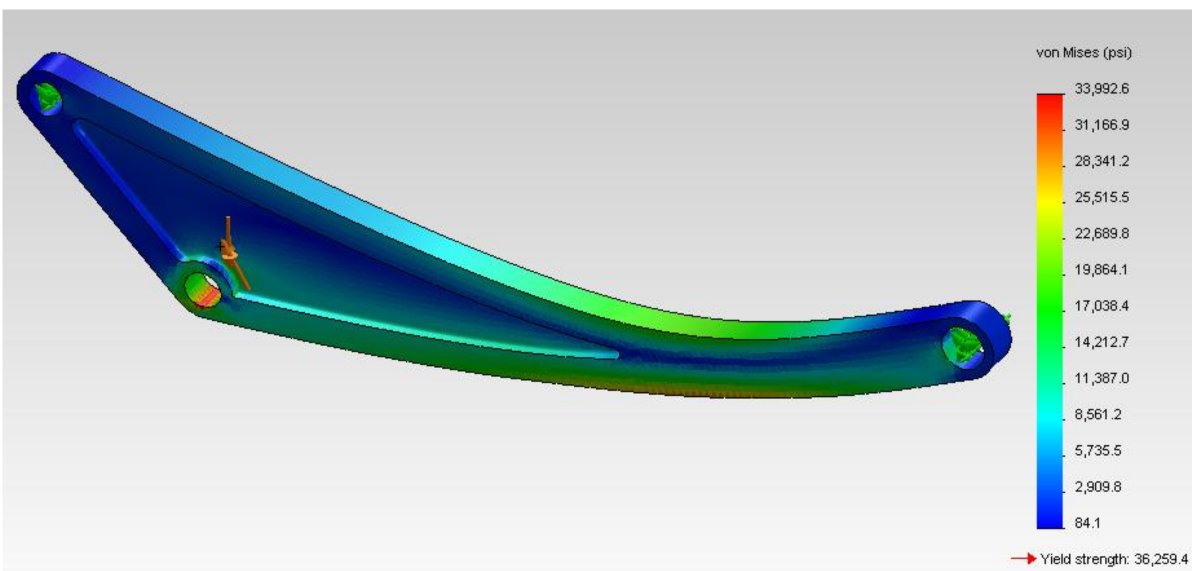


Figure 2: Lower member convergence 2

The second part of the hoist is the upper member shown in Figure 3 and Figure 4. The FEA on this part shows a variance of approximately 38.7%. The variance is due to the sharp inside and outside corners. The main areas where we would expect the part to fail are still below the yield stress and we can assume that the areas where there is stress concentration will be filled by the welds which will relieve the stress concentration.

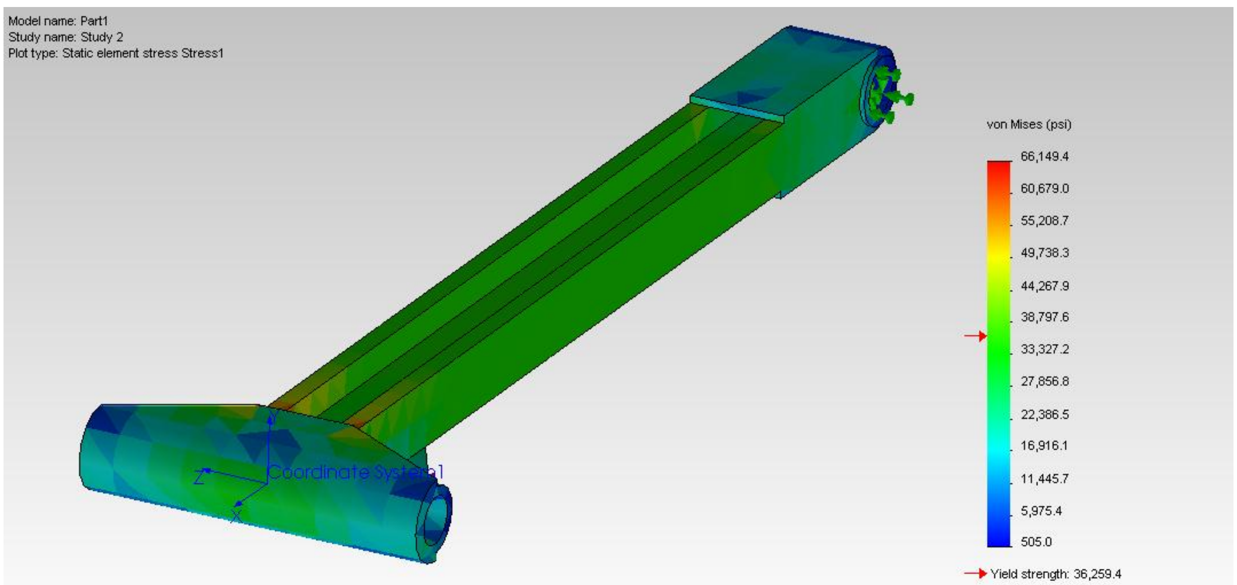


**Figure 3: Upper member convergence 1**

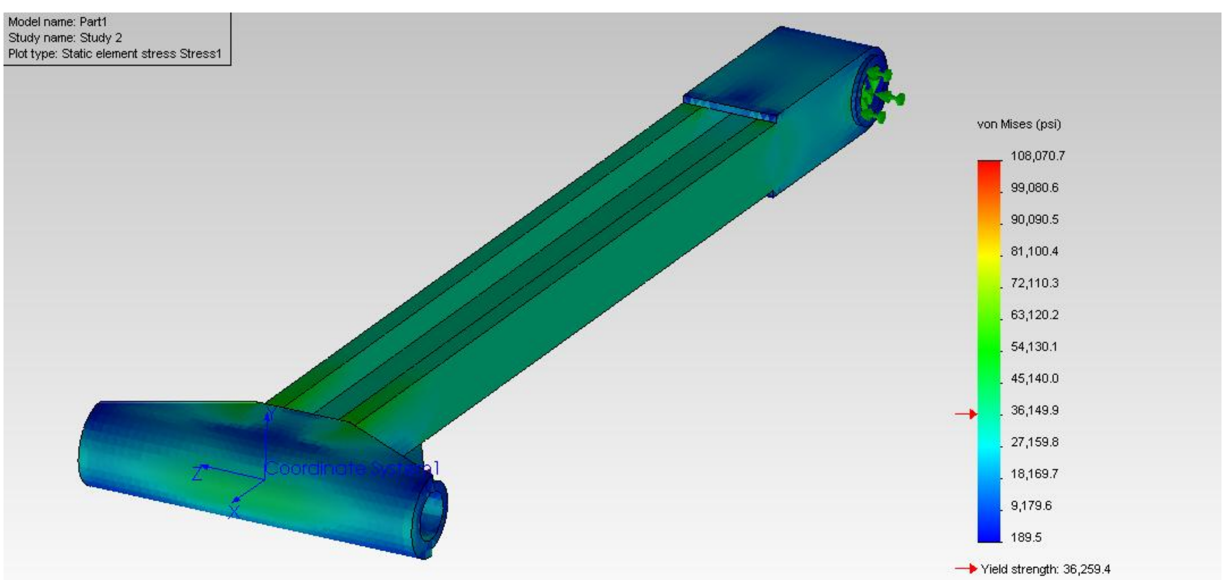


**Figure 4: Upper member convergence 2**

Figure 5 and Figure 6 show the FEA of the upper box mount where the hoist mounts to the frame of the box. The two analyses show a variance of 26.4%, showing that the FEA is not converging due to the sharp corners in the design. The maximum stress concentration still show to be less than the yield stress of the A36 steel.

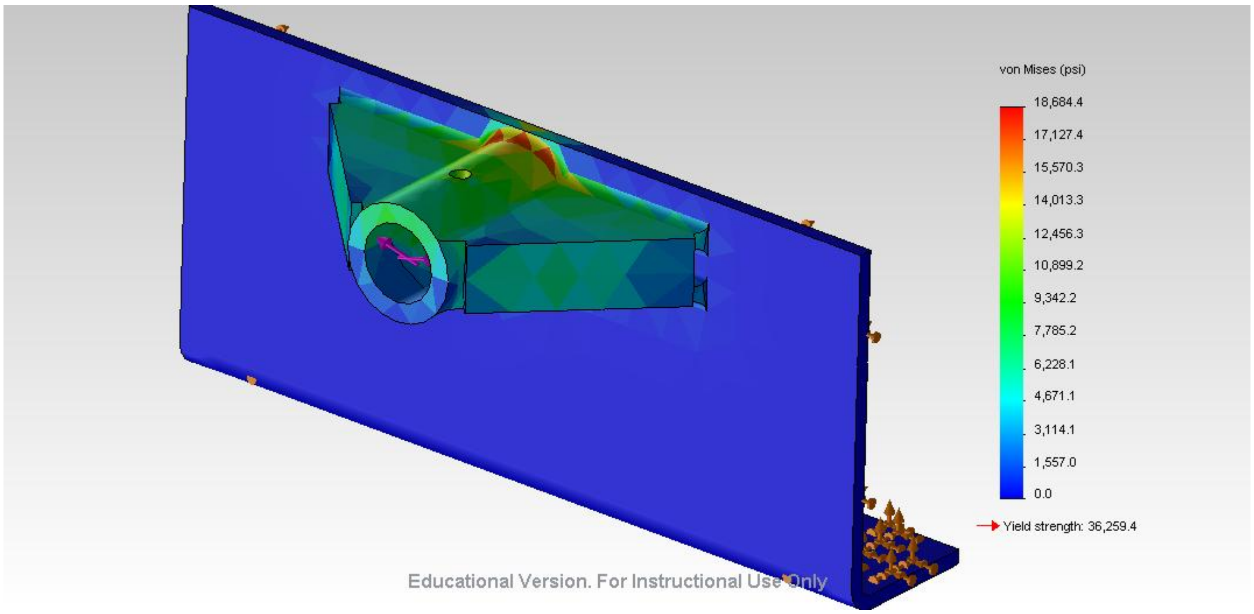


Figure 5: Box-mount convergence 1

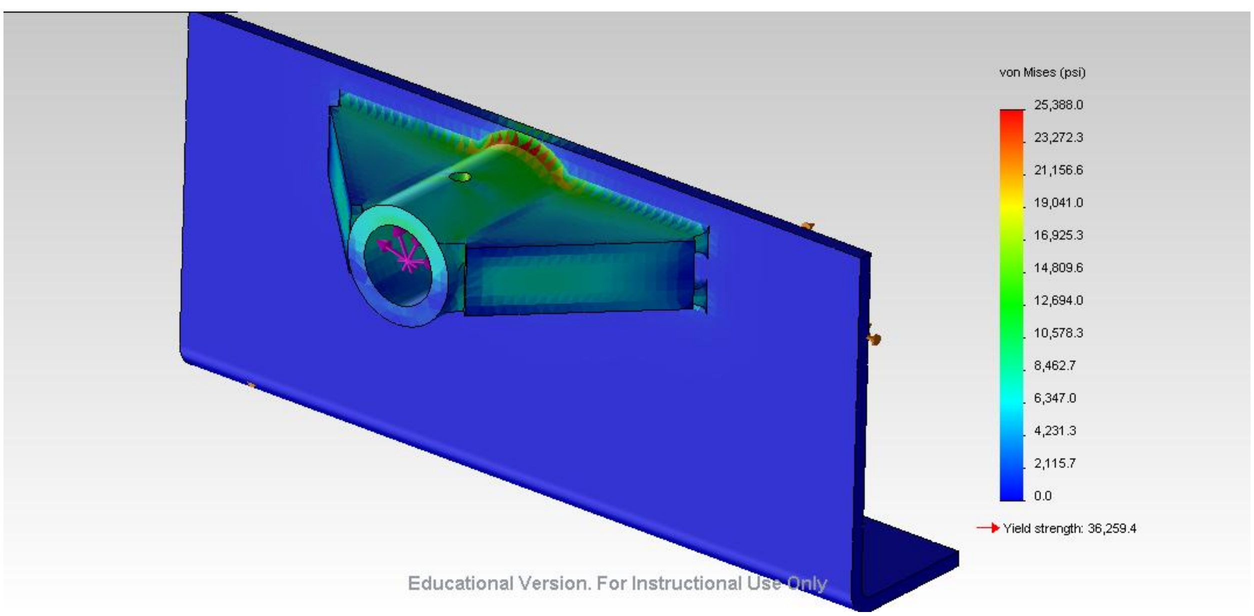


Figure 6: Box-mount convergence 2

The lower box-mount, shown in Figure 7 and Figure 8, connects the lower member to the frame of the truck. This part has many sharp corners which show high levels of stress concentration. These areas will be filled with welds which will relieve these stress concentrations. Because of the stress concentrations, the FEA does not show convergence as there is a variance of approximately 16.4%.

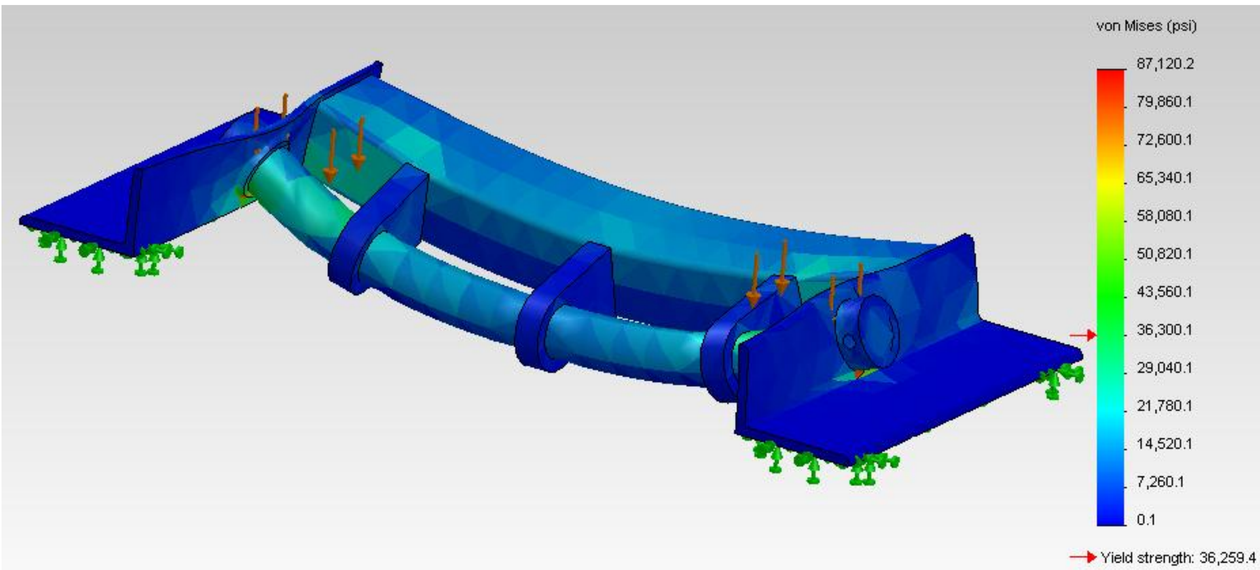


Figure 7: Frame-mount convergence 1

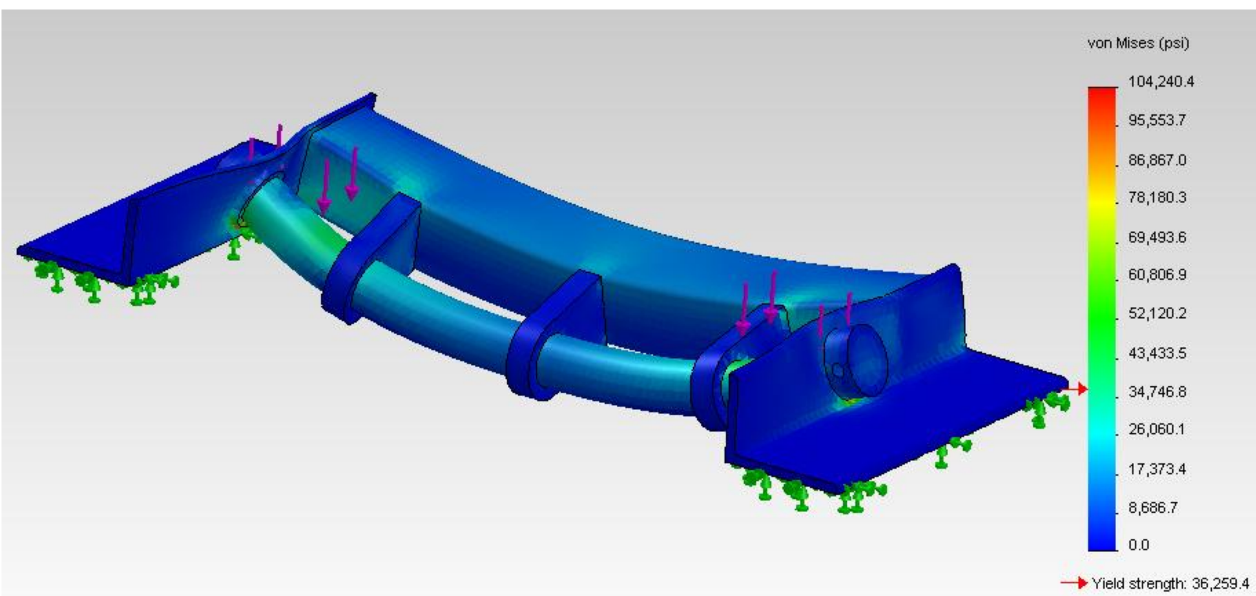


Figure 8: Frame-mount convergence 2

## D -2 Assembly

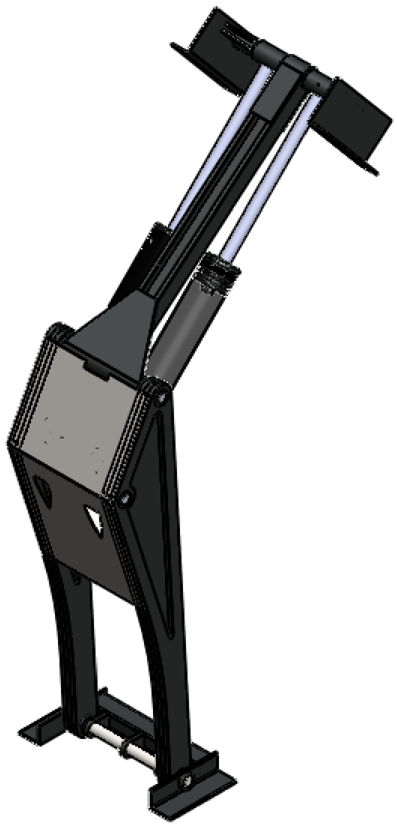

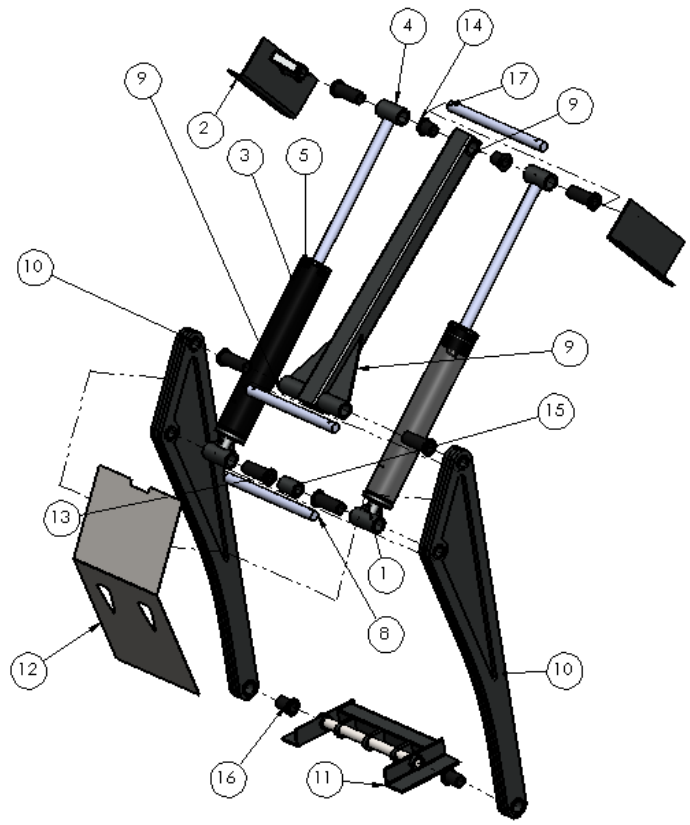


| ITEM NO. | PART NUMBER | DESCRIPTION | QTY. |
|---|---|---|---|
| 1 | 3347104 | cylinder part | 2 |
| 2 | upper box mount | see assembly drawing | 2 |
| 3 | 3117151 | cylinder part | 2 |
| 4 | 3117152 | cylinder part | 2 |
| 5 | 3119157 | cylinder part | 2 |
| 6 | 3119171 | cylinder part | 2 |
| 7 | NormalHexNut 1-1_4-12 UNF | cylinderpart | 2 |
| 8 | mid point pin | 2" bar stock | 2 |
| 9 | upper member | see assembly drawing | 1 |
| 10 | lower member | see assembly drawing | 2 |
| 11 | lower frame mount | see assembly drawing | 1 |
| 12 | Skid Plate | 1/4" chrome tread plate | 1 |
| 13 | greaseless cylinder bushing | polymer bushing | 6 |
| 14 | greaseless upper member bushing | polymer bushing | 2 |
| 15 | lower bushing spacer | 3.5" tubing 1/2" thick | 1 |
| 16 | greaseless lower member bushing | polymer bushing | 2 |
| 17 | mounting pin | 2" bar stock | 1 |

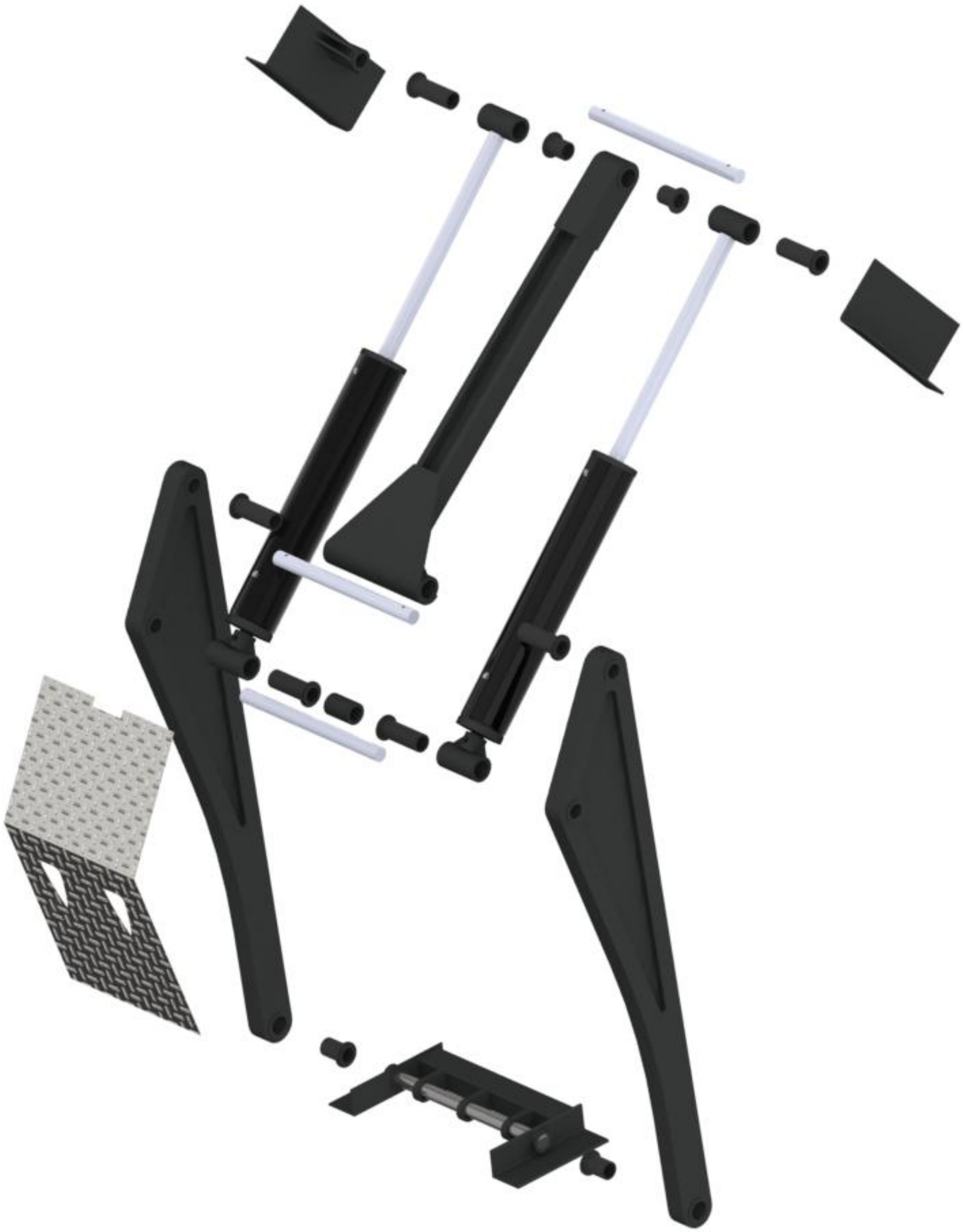

| ITEM NO. | PART NUMBER | DESCRIPTION | QTY. |
|---|---|---|---|
| 1 | lower member main | 1" plate | 1 |
| 2 | lower member material removed | 1" plate | 2 |
| 3 | lower member pin mount | 3" tubing 1/2" thick | 2 |
| 4 | lower member bushing mount | 3.5" tubing 1/2" thick | 1 |

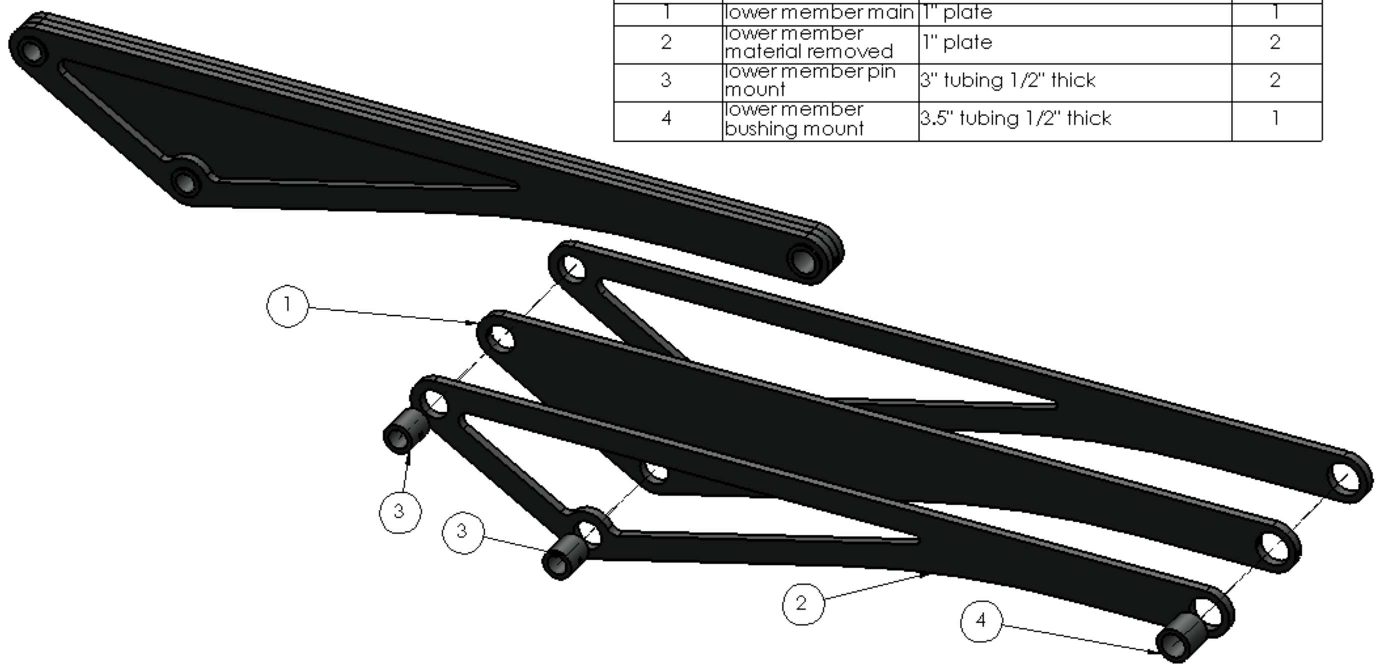


| ITEM NO. | PART NUMBER | DESCRIPTION | QTY. |
|---|---|---|---|
| 1 | upper mount L-bracket | 3/8" plate | 1 |
| 2 | upper mount pin brace | 2.5" tubing 1/2" thick | 1 |
| 3 | upper mount gusset brace | 1/4" plate | 2 |
| 4 | upper mount gusset | 3/8" plate | 4 |

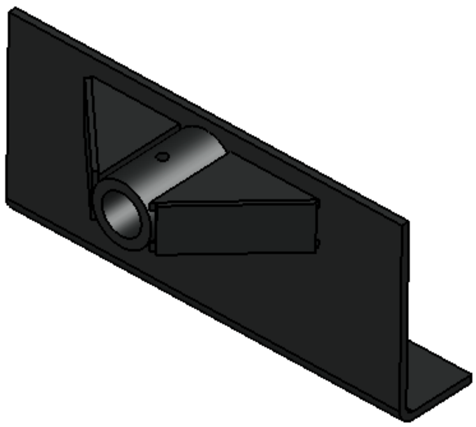

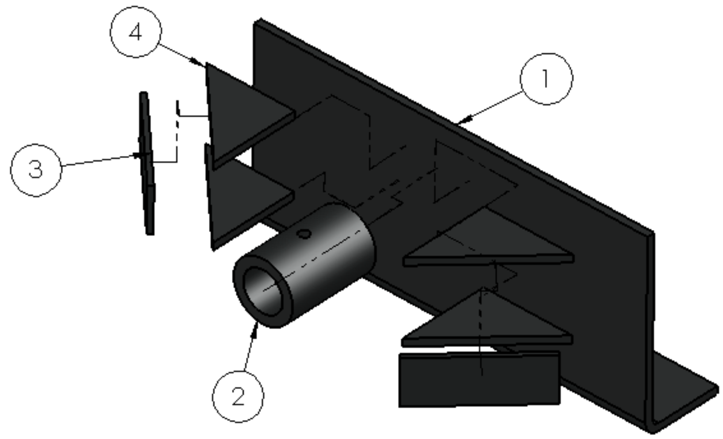


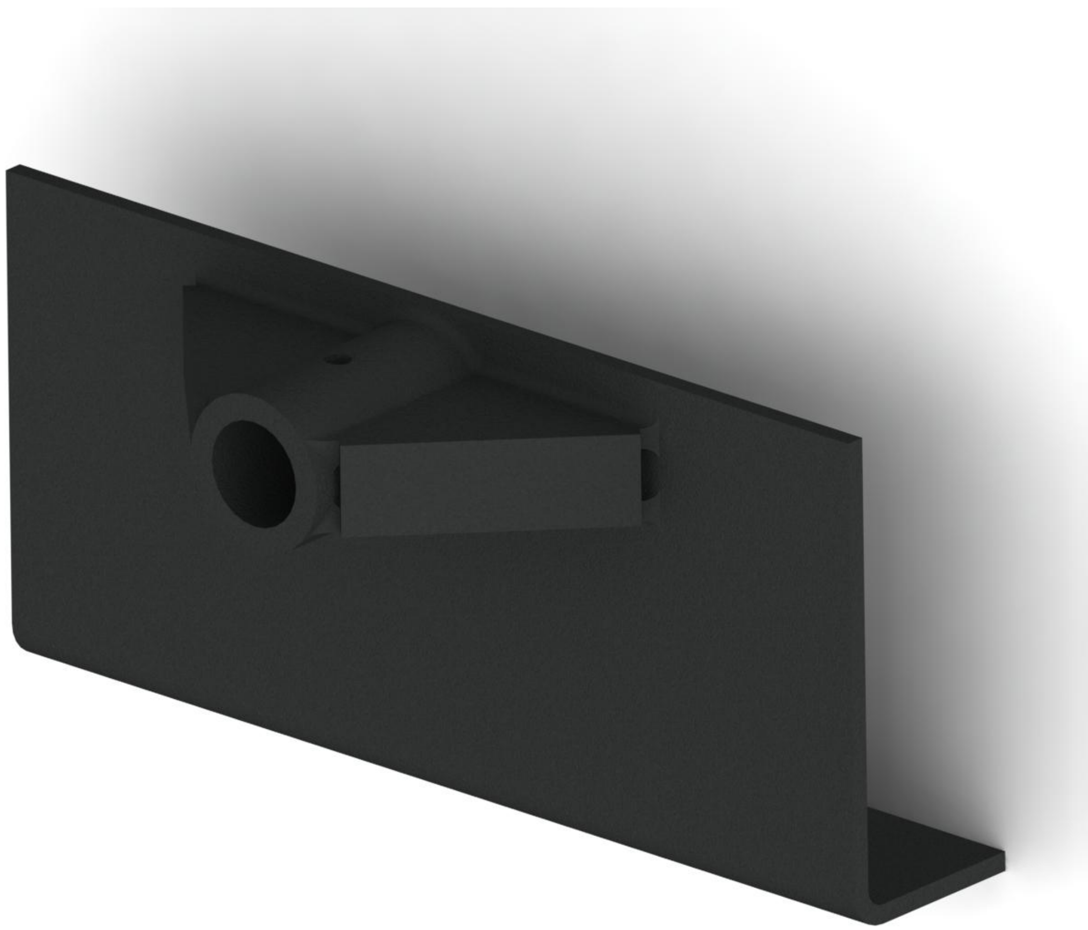

| ITEM NO. | PART NUMBER | DESCRIPTION | QTY. |
|---|---|---|---|
| 1 | lower frame mount cross brace | 3"x4" rect. tubing 3/8" thick | 1 |
| 2 | lower frame mount l-bracket | 4"x5" L-bracket 3/8" thick | 2 |
| 3 | lower frame mount pin brace | 3" tubing 1/2" thick | 3 |
| 4 | lower frame mount pin flange | 1" plate | 2 |
| 5 | lower frame mount pin | 2" rod | 1 |

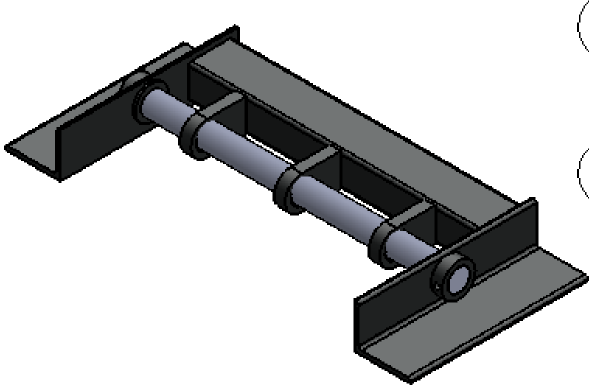

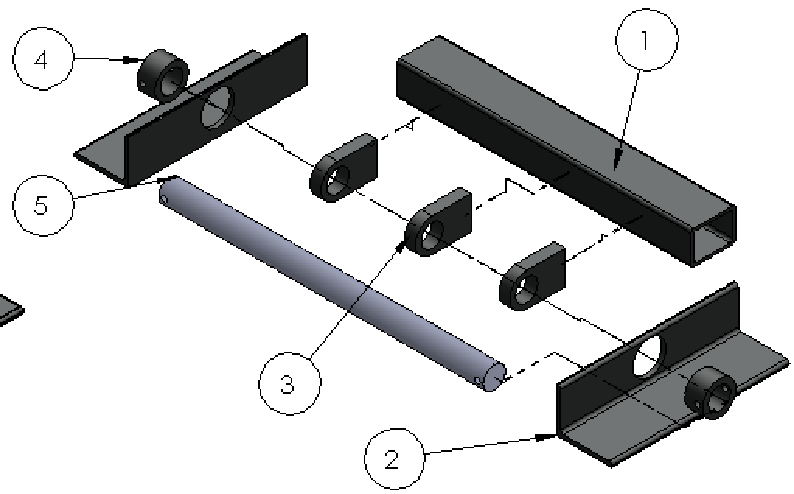


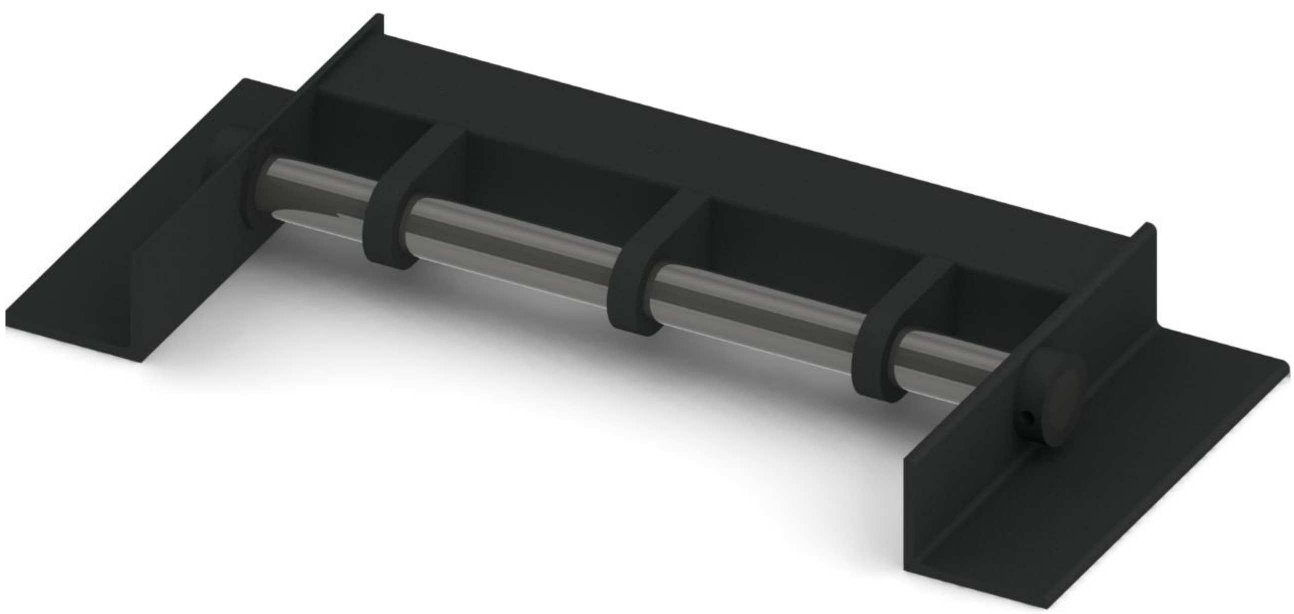

# Appendix E –

# Detailed Material Cost Analysis

## List of Tables

## E-1 Details of Material Cost Analysis

Quattro Consulting used a list of material pricing for the material cost analysis shown in TABLE I: LIST OF PRICING FOR A36 STEEL. The team contacted three local steel suppliers to obtain quoted pricing for A36 steel utilized in all the hoist designs. The suppliers were Castle Metal, Brunswick Steel and Russel Metals. Online Metal Store was also contacted; however, their price is not as competitive as the local counterparts. Quotes for material price were obtained between the periods of November 23rd to November 30th, 2011. To construct this analysis, Quattro Consulting created assumptions as follow:

- If price per unit, such as \$/ft or \$/ft$^2$, is not available the following assumptions apply:
  - Sheet material are ordered in dimensions of 5' x 10'. Material price is obtained from dividing final price by total area square footage
  - Square tubing, round tubing, bar, and angle iron are ordered per available minimum length. Material price is obtained from dividing final price by the length in feet
- Quattro Consulting assumes no guarantee of the availability of material other than at the time the quote is obtained
- Quattro Consulting assumes no guarantee of the stability of the material prices.

The table below contains the list of price for different type of A36 steel uses in all three designs.

TABLE I: LIST OF PRICING FOR A36 STEEL [1] [2] [3]

| | Type | Price | Unit | Source |
|---|---|---|---|---|
| **Plate** | Gage 14 | $0.02 | ft^2 | Russel Metals |
| | .25" Thick | $5.75 | ft^2 | Russel Metals |
| | .375" Thick | $8.65 | ft^2 | Russel Metals |
| | .5" Thick | $11.55 | ft^2 | Russel Metals |
| | .75" Thick | $15.74 | ft^2 | Brunswick |
| | 1" Thick | $29.00 | ft^2 | Russel Metals |
| | 1.25" Thick | $37.20 | ft^2 | Russel Metals |
| **Square Tubing** | 3" x 4" x. 25" Thick | $8.18 | ft | Russel Metals |
| | 3" x 3" x .375" Thick | $9.74 | ft | Brunswick |
| | 3" x 4" x .375" Thick | $11.76 | ft | Brunswick |
| **Round Tubing** | 2.5" OD x .25" Thick | $11.31 | ft | Castle Metal |
| | 3" OD x .25" Thick | $13.82 | ft | Castle Metal |
| | 4" OD x .25" Thick | $8.02 | ft | Brunswick |
| | 2.75" OD x .375" Thick | $17.91 | ft | Castle Metal |
| | 3.25"OD x .625" Thick | $24.35 | ft | Castle Metal |
| | 3" OD x .5" Thick | $25.60 | ft | Castle Metal |
| | 3.5" OD x .5" Thick | $30.70 | ft | Castle Metal |
| **Round Bar** | 2" Dia | $13.18 | ft | Online Metal Store |
| **Angle Iron** | 3" x 5" x .375 Thick | $7.62 | ft | Russel Metals |

## Works Cited

[1] L. Jones, Interviewee, *Inside Sales. Brunswick Steel.* [Interview]. 23 November 2011.

[2] J. Anderson, Interviewee, *Sales. Castle Metal.* [Interview]. 23-28 November 2011.

[3] Online Metal Store, "Online Metal Store - 1018 Cold Rolled Steel," 2011. [Online]. Available: http://www.onlinemetalstore.com/items/1018_Cold_Rolled_Steel_Round_Bar.cfm?item_id=161&size_no=32&pieceLength=full&sku_no=122&len_ft=0&len_in=0&len_fraction=0&itemComments=&qty=1. [Accessed 27 November 2011].